

INFORMATION TO USERS

This manuscript has been reproduced from the microfilm master. UMI films the text directly from the original or copy submitted. Thus, some thesis and dissertation copies are in typewriter face, while others may be from any type of computer printer.

The quality of this reproduction is dependent upon the quality of the copy submitted. Broken or indistinct print, colored or poor quality illustrations and photographs, print bleedthrough, substandard margins, and improper alignment can adversely affect reproduction.

In the unlikely event that the author did not send UMI a complete manuscript and there are missing pages, these will be noted. Also, if unauthorized copyright material had to be removed, a note will indicate the deletion.

Oversize materials (e.g., maps, drawings, charts) are reproduced by sectioning the original, beginning at the upper left-hand corner and continuing from left to right in equal sections with small overlaps.

ProQuest Information and Learning
300 North Zeeb Road, Ann Arbor, MI 48106-1346 USA
800-521-0600

UMI[®]

Sedimentology, Stratigraphy and Depositional History of the Falher F Conglomerate Trend, Alberta, Canada

By

Byron J. Nodwell

Department of Earth and Planetary Sciences

McGill University

Montreal, Quebec, Canada

August 2004

A thesis submitted to the Faculty of Graduate Studies and Research in partial

fulfillment of the requirements of the degree of

Master of Science

© B.J. Nodwell 2004



Library and
Archives Canada

Bibliothèque et
Archives Canada

0-494-06431-5

Published Heritage
Branch

Direction du
Patrimoine de l'édition

395 Wellington Street
Ottawa ON K1A 0N4
Canada

395, rue Wellington
Ottawa ON K1A 0N4
Canada

Your file Votre référence

ISBN: 0-596-00283-1

Our file Notre référence

ISBN: 0-596-00283-1

NOTICE:

The author has granted a non-exclusive license allowing Library and Archives Canada to reproduce, publish, archive, preserve, conserve, communicate to the public by telecommunication or on the Internet, loan, distribute and sell theses worldwide, for commercial or non-commercial purposes, in microform, paper, electronic and/or any other formats.

The author retains copyright ownership and moral rights in this thesis. Neither the thesis nor substantial extracts from it may be printed or otherwise reproduced without the author's permission.

AVIS:

L'auteur a accordé une licence non exclusive permettant à la Bibliothèque et Archives Canada de reproduire, publier, archiver, sauvegarder, conserver, transmettre au public par télécommunication ou par l'Internet, prêter, distribuer et vendre des thèses partout dans le monde, à des fins commerciales ou autres, sur support microforme, papier, électronique et/ou autres formats.

L'auteur conserve la propriété du droit d'auteur et des droits moraux qui protège cette thèse. Ni la thèse ni des extraits substantiels de celle-ci ne doivent être imprimés ou autrement reproduits sans son autorisation.

In compliance with the Canadian Privacy Act some supporting forms may have been removed from this thesis.

Conformément à la loi canadienne sur la protection de la vie privée, quelques formulaires secondaires ont été enlevés de cette thèse.

While these forms may be included in the document page count, their removal does not represent any loss of content from the thesis.

Bien que ces formulaires aient inclus dans la pagination, il n'y aura aucun contenu manquant.


Canada

Abstract

Detailed sequence stratigraphic analyses indicate that the lower Cretaceous Falher F unit is made up of 4 sandy/pebbly prograding parasequences labeled F1, F2, F3, and F4. Of the parasequences only F3 has a significant (>2m) thickness of conglomerate. Vertical lithological successions through a conglomeratic section suggest that the F3 pebbles were deposited on the upper shoreface and foreshore as part of a conformable, shoaling-upwards package of rocks. Detailed mapping, using core, well logs, production data and 3-D seismic, show that the conglomerates form a 4 km wide linear body deposited along a linear topographic trend. This topographic trend coincides with the northern edge of the underlying upper Devonian Gold Creek (Smokey) reef trend. Furthermore, the longshore termination of the conglomerate is located at a NW-SE trending structural feature that was active during Falher F deposition.

Two models could explain the development of a thick conglomerate buildup along a linear topographic step. The first suggests that southward (transgressive) movement of a pebbly barrier was halted at the topographic feature. Pebbles were sourced, by erosion, from the underlying (F2) parasequence and subsequent highstand reworking resulted in the progradational configuration of the conglomerate body as shown in cores and cross-sections. The second suggests that when the F3 parasequence shoreline arrived at the topographic step progradation rates slowed significantly. During this slowdown, shore-normal processes concentrated pebbles on the upper shoreface. We believe that the latter model best explains the available data.

The hypothesis, that underlying structure could control the deposition of shoreface conglomerates, was tested in two other map areas that contain productive, linear conglomerate reservoirs. Within the Deep Basin map area two indistinct linear structural features suggest that similar depositional processes were in effect during deposition of the Falher A and B reservoir trends. In the Carrot Creek field, clear, linear structural lows underlie two productive Cardium conglomerate trends.

Résumé

Des analyses détaillées de stratigraphie séquentielle indiquent que l'unité Falher F du Crétacé inférieur consiste de 4 paraséquences progradantes acérées/caillouteuses identifiées F1, F2, F3 et F4. De toutes ces paraséquences, seulement F3 contient une épaisseur significative (>2 m) de conglomérat. Des successions lithologiques verticales coupant une section conglomératique suggèrent que les cailloux de F3 ont été déposés près du rivage faisant partie d'un ensemble de roches conformable montrant une réduction systématique de la profondeur vers le haut. Une cartographie détaillée à l'aide de carottes, de diagraphies de forage, des données de production et des données sismiques 3-D, montre que les conglomérats forment une entité linéaire d'une largeur de 4 km déposée le long d'une topographie linéaire. Cet obstacle topographique coïncide avec l'extrémité nord du récif sousjacent Gold Creek (Smokey) du Dévonien supérieur. De plus, l'extrémité le long du rivage du conglomérat est située à l'emplacement d'un élément structural pointant NO-SE, actif durant la dépôt de Falher F.

Deux modèles peuvent expliquer le développement d'une épaisse accumulation de conglomérat le long d'un obstacle topographique linéaire. Le premier suggère le mouvement vers le sud (transgressif) d'une barrière caillouteuse arrêtée à l'encontre de la topographie. Les cailloux sont provenus de l'érosion de la paraséquence sousjacente (F2) et le réemplacemement subséquent a résulté en la configuration progradationale de l'entité conglomératique vue dans les carottes et les diagraphies de forage. Le second modèle suggère que le rythme de progradation ait ralenti de façon significative lorsque la côte de la paraséquence F3 est arrivée à l'élément topographique. Durant ce ralentissement, des procédés agissant perpendiculairement au rivage ont concentré les cailloux sur la partie supérieure du rivage. Nous croyons que ce dernier modèle explique de meilleure façon les données disponibles.

L'hypothèse, selon laquelle une structure sousjacente pourrait contrôler le dépôt de conglomérats de rivage, a été testée pour deux autres régions

cartographiques contenant des réservoirs de conglomérat linéaires et productifs. Deux structures linéaires non-distinctes, incluses dans la région cartographique de Deep Basin, suggèrent que de procédés sédimentaires similaires prévalaient durant le dépôt des réservoirs Falher A et B. Dans la région de Carrot Creek, d'évidentes dépressions linéaires sont situées sous deux entités conglomératiques de Cardium productives.

Preface

This thesis consists of 4 chapters. The third chapter is intended for submission to the Bulletin of Canadian Petroleum Geology published in Calgary, Alberta. The manuscript has been integrated as a chapter formatted to the general layout of the thesis.

The following is excerpted from Guidelines for Thesis Preparation, Faculty of Graduate Studies and Research, McGill University:

"Candidates have the option of including, as part of the thesis, the text of one or more papers submitted, or to be submitted, for publication, or the clearly-duplicated (not the reprints) of one or more published papers. These texts must conform to the "Guidelines for Thesis Preparation" with respect to font size, line spacing and margins and must be bound together as an integral part of the thesis.

The thesis must be more than a collection of manuscripts. All components must be integrated into a cohesive unit with a logical progression from one chapter to the next. In order to ensure that the thesis has continuity, connecting texts that provide logical bridges preceding and following each manuscript are mandatory.

The thesis must conform to all other requirements of the "Guidelines for Thesis Preparation" in addition to the manuscripts.

The thesis must include the following: a table of contents, a brief abstract in both English and French, an introduction which clearly states the rational and objectives of the research, a comprehensive review of the literature (in addition to that covered in the introduction to each paper), a final conclusion and summary, a thorough bibliography.

As manuscripts for publication are frequently very concise documents, where appropriate, additional material must be provided (e.g., in appendices) in sufficient detail to allow a clear and precise judgment to be made of the importance and originality of the research reported in the thesis.

In general, when co-authored papers are included in a thesis the candidate must have made a substantial contribution to all papers included in the thesis. In addition, the candidate is required to make an explicit statement in the thesis as to who contributed to such work and to what extent. This statement should appear in a single section entitled "Contributions of Authors" as a preface to the thesis. The supervisor must attest to the accuracy of this statement at the doctoral oral defense. Since the task of the examiners is made more difficult in these cases, it is in the candidate's interest to clearly specify the responsibilities of all the authors of the co-authored papers."

Contributions of Authors

I hereby declare that all practical and analytical aspects of the studies described in this thesis were carried out by me. Dr. Bruce Hart supervised the investigational work and ensured that a critical and coherent scientific approach was maintained throughout the study.

Acknowledgements

I would like to thank the collaborative partners on this project who provided financial and/or technical support: EOG Resources Inc., BP Canada, Devon Energy Corporation and Talisman Energy Inc. These companies provided well log data as well as constructive discussions about our ideas. Millennium Seismic donated the 3-D seismic volume without which this studies result would have been very much diminished.

I would like to thank Ivan Marroquin for his assistance in interpreting the 3-D seismic volume as well as Conor Byrne, Juliana Tebo, Sabrina Sarzelejo, and Justine Sagan for tolerantly listening to my ideas through the past year and a half. All have had such a thorough education in the Falher F that I think they could have written this thesis.

Immediately prior to writing, critical discussions with Bob Dalrymple, Bill Arnott, Mike Johnson, Dave O'Neill and Shona Ness helped to solidify some of the concepts discussed below as well as opening my eyes to what I was missing.

Special thanks go out to Lucy who listened to my original Falher talk and still thinks that the pebbles are in the F2 parasequence. She has been patient and supportive throughout the past two years, and even became government certified bilingual in order to support my time in school.

Bruce, your enthusiasm for the science, despite being misdirected into the world of seismic, has helped me to become a better geologist. For that I am very grateful.

Table of Contents

Abstract	ii
Resume	iii
Preface	v
Contributions of Authors	vii
Acknowledgements	viii
Table of Contents	ix
List of Figures	xii
List of Appendices	xviii

Chapter 1 **General Introduction**

Preamble	1
Previous Work	3
Objectives	4
Methods	5
Thesis Format	7

Chapter 2 **Lithofacies**

Introduction	8
Facies Descriptions and Interpretations	8
<u>Facies 1</u>	8
<i>Interpretation</i>	9
<u>Facies 2</u>	9
<i>Interpretation</i>	10
<u>Facies 3</u>	10

<i>Interpretation</i>	10
<u>Facies 4A</u>	11
<i>Interpretation</i>	11
<u>Facies 4B</u>	12
<i>Interpretation</i>	13
<u>Facies 5</u>	13
<i>Interpretation</i>	13
<u>Facies 6</u>	14
<i>Interpretation</i>	14
<u>Facies 7</u>	14
<i>Interpretation</i>	15
<u>Facies 8</u>	15
<i>Interpretation</i>	15
Core to Well Log Comparisons	16

Chapter 3

Deeply-Rooted Topographic Control on the Deposition of the Falher F Conglomerate Trend, Wapiti Field, Deep Basin, Alberta

Abstract	18
Introduction	20
Database and Methods	24
Results	25
<u>Falher F Lithofacies Descriptions and Interpretations</u>	25
<u>Falher F Lithological Successions from Core</u>	28
<i>Sandy Succession Description</i>	28
<i>Sandy Succession Interpretation</i>	30
<i>Pebbly Succession Description</i>	30
<i>Pebbly Succession Interpretation</i>	32
<i>Fining-Upwards Succession Description</i>	34
<i>Fining-Upwards Succession Interpretation</i>	34
<u>Stratigraphy and Depositional History</u>	34

<u>Mapping</u>	38
<i>Reservoir Mapping</i>	38
<i>Isopach and Isochron Mapping</i>	39
<i>Structural Residual Mapping</i>	43
Discussion	45
<u>Depositional Models for Falher F Conglomerates</u>	45
<i>Basin Configuration</i>	46
<i>Geomorphologic Considerations</i>	46
Null Point Theory.....	46
Coastal Profile Equilibrium.....	48
<i>Transgressive Concentration</i>	51
<i>Regressive Concentration</i>	55
<u>Regional Applicability</u>	58
Conclusions	62
Acknowledgements	64
 Chapter 4	
Conclusions	65
 Bibliography	67
Appendices	75

List of Figures

Figure 1.1: Province of Alberta showing the location of the Deep Basin (after Masters, 1984) and the three study areas. The south-western edge of the Deep Basin is the edge of the deformed belt.....	2
Figure 1.2: Map of study area showing location of correlation cross-sections. There are 24 north-south and 3 east-west cross-sections that include all wells that intersected the Falher F interval.....	6
Figure 3.1: a) General stratigraphic column showing key stratigraphic units discussed in this study; detailed stratigraphic column of the lower Cretaceous section in study area. Modified from Smith (1984) and Cant (1988). b) Seismic transect through study area showing key horizons.....	21
Figure 3.2: a) Province of Alberta with our three mapping areas: Wapiti (Stippled), Deep Basin and Carrot Creek (cross-hatched). Note the location of the southern edge of the Peace River Arch within the Deep Basin study area and the northern edge of the Gold Creek reef within the Wapiti study area. The edge of the deformed belt is indicated. Modified from Moore (1989) and Casas and Walker (1997). Detailed work on the Falher F was carried out in the Wapiti map area and other mapping was carried out in the Deep Basin and Carrot Creek areas. b) Map of the Wapiti study area showing Falher F well log coverage (small circles), core coverage (large circles), approximate location of the 3-D seismic survey (circle) and the location of cross-sections A-A' (Fig. 3.6a), B-B' (Fig. 3.6b) and C-C' (Fig. 3.8).....	22

Figure 3.3: Map of the Deep Basin area showing well log coverage (small circles) and cumulative gas production bubbles (large bubbles $> 8.5 \times 10^5 \text{ m}^3$ (30 Bcf), small bubbles $> 1.4 \times 10^6 \text{ m}^3$ (5 Bcf)). Cumulative production is used as a proxy for conglomerate distribution. The location of the Wapiti study area is indicated by the heavily outlined area in the southeast of the map and linear trends of the Falher A, B, C, D and F are indicated.....26

Figure 3.4: Map of the Carrot Creek area showing well log coverage (small circles) and cumulative oil production bubbles (large bubbles $> 40 \times 10^3 \text{ m}^3$, small bubbles $> 8 \times 10^3 \text{ m}^3$). Cumulative production is used as a proxy for conglomerate distribution and the linear trends of productive Cardium conglomerates are indicated.....27

Figure 3.5: Summary of Falher lithofacies including photographs of representative samples from Falher F cores.....29

Figure 3.6: a) Idealized dip-oriented cross-section (A-A') through cored wells. Note that the F3 parasequence is sandy both landward and seaward from the conglomerate. Thin pebble beds are interbedded within lower and upper shoreface sandstones in core 3-33-65-9. Both sandy and pebbly successions are immediately overlain by coastal plain shales and coals. The F3 conglomerate body is shown in stipple pattern. b) Well log dip-oriented cross-section (B-B') through conglomerate body. Note that the conglomerate bed is over 3 km wide at this location. A thick package of sandstones is shown at well 8-22-66-8W6. The F3 conglomerate body is shown in stipple pattern. See Figure 3.2b for location of cross-sections.....31

Figure 3.7: a) Photograph (2651 - 2652.4m, core 10-36-65-9W6) showing conglomerates immediately overlain by Facies 6 (carbonaceous shales) and Facies 8 (coal). Stratigraphic top is to the right. b) Close-up photograph of the top of the conglomerate succession in core 10-36-65-9W6. The intermixing of carbonaceous material suggests that the overlying carbonaceous shales were deposited immediately after deposition of the underlying conglomerates.....33

Figure 3.8: Dip-oriented cross-section (C-C') crossing the study area. Note the progradational geometry of the Falher F parasequences. The F3 conglomerate body is shown in stipple pattern. See Figure 3.2b for location of cross-section. Additional cross-sections illustrating Falher F stratigraphy are included in Appendix 3.....36

Figure 3.9: Isopach map of the four parasequences F1 (a), F2 (b), F3 (c) and F4 (d). Shifting depocenters towards the north indicates northward progradation of the Falher F shoreline. The thick linear trend in F3 parasequence (arrows; Fig. 3.9c) is due to differential compaction of the conglomerate body.....37

Figure 3.10: a) Map of net thickness of facies 4a and 4b conglomerate. Large circles indicate pressure control points used in Figure 3.10b. Note the thin NW-SE incised channel trends and 4 km width of conglomerate body (arrows). b) Pressure versus time plot for six productive wells in the trend. Note the three different pressure gradients indicating reservoir compartmentalization. This resulted from incision and shale infilling of the channels shown in Figure 3.10a. c) Strike-oriented cross-section (D-D')

showing channel incision into the conglomerate body. The shaded area indicates the conglomerate. The location of the cross-section is indicated in Figure 3.10a.....40

Figure 3.11: a) Isopach of interval from Coal E to the top of the Wilrich Member. Note that the isopach thickens abruptly to the southwest along a NW-SE trend (arrows). b) Isochron of the interval from Coal E to the top of the Bluesky Formation. Note that the isochron changes abruptly along a NW-SE trend. These trends are thought to be related to basement fault movement. c) Seismic transect showing flexural deformation within the basement and Paleozoic rocks underlying the study area (arrows).....42

Figure 3.12: a) Structural residual of Wilrich from well data (restored for depositional dip). Note NNW-SSE trending structural “step” running through the study area (arrows). b) Time-structural residual map of Wabumun horizon from seismic data showing linear reef-rim trend (arrows). Colour indicates dip curvature with positive dip curvature in red and negative dip curvature in blue (Roberts, 1998). c) Net conglomerate overlying Wabumun trend (line). Contours are net conglomerate thickness. d) Dip-oriented seismic transect showing the Wabumun horizon and a well which intersected a thick buildup of carbonate in the Leduc and Wabumun. The well intersects the reef-rim. The reef flat is to the left and basinal shales are to the right.....44

Figure 3.13: Block diagram of pre-F3 depositional basin topography inferred from structural residual and isopach maps.....47

Figure 3.14: a) Null point theory. Wave force asymmetries drive larger particles to the upper shoreface and smaller particle to the lower shoreface. Modified from Cowell et al. (1999). b) Landward translation of a shoreface during transgression. The invariant nature of the profile indicates that erosion will occur in the upper shoreface while aggradation will occur in the lower shoreface during transgression. Modified from Swift (1975). c) Seaward translation of a shoreface due to sediment input at the upper shoreface. The upper shoreface oversteepens becoming unstable. Sediment is driven from the upper to lower shoreface in an attempt to establish an equilibrium profile.

.....49

Figure 3.15: Transgressive model. Transgressive erosion and concentration of pebbles at upper shoreface and foreshore creates a pebbly barrier. The barrier's landward (southward) progress is stopped by topography. Stillstand wave re-working of the barrier yields final "progradational" configuration of the conglomerate body.....52

Figure 3.16: Regressive model. Rapid sandy progradation is slowed by topography. Shore-normal sorting traps pebbles at the upper shoreface and foreshore while driving sand to lower shoreface. As the shoreface profile re-establishes equilibrium the progradation rate increases and the pebble concentration diminishes until sandy progradation resumes.....56

Figure 3.17: Deep Basin base of Fish Scale zone structural residual map. Note the clear linear trend of Gold Creek reef underlying the Falher F production trend. No apparent linear trend exists below the Falher A and C production

trend. Two faint linear trends are indicated below the Falher A and B
production trend. Production bubbles as in Figure 3.3.....59

Figure 3.18: Carrot Creek base of Fish Scale zone structural residual map. Note
the two linear low trends underlying two productive Cardium conglomerate
trends. Production bubbles as in Figure 3.4.....61

List of Appendices

Appendix 1: Representative photographs of lithofacies discussed in Chapter 2. Refer to text for further discussion of sedimentological features in each facies	75
Appendix 2: Core logs alongside their respective logged interval. Well logs included are: Gamma-ray, resistivity, and neutron porosity.....	76
Appendix 3: Two dip-oriented cross-sections illustrating the progradational nature of the Falher F interval within the study area. One strike-oriented cross-section is included to illustrate consistency of picks across the study area. Note that the regional cross-section C-C' is located in Figure 3.8.....	77
Appendix 4: Volumetric calculation of the reserves of the mapped Falher F pool. This is compared to the actual recovered reserves of the pool in order to assess the accuracy of the mapping. The close correspondence of the reserve calculation to the actual cumulative production of the pool suggests that the mapping is accurate.....	78

Chapter 1 Introduction

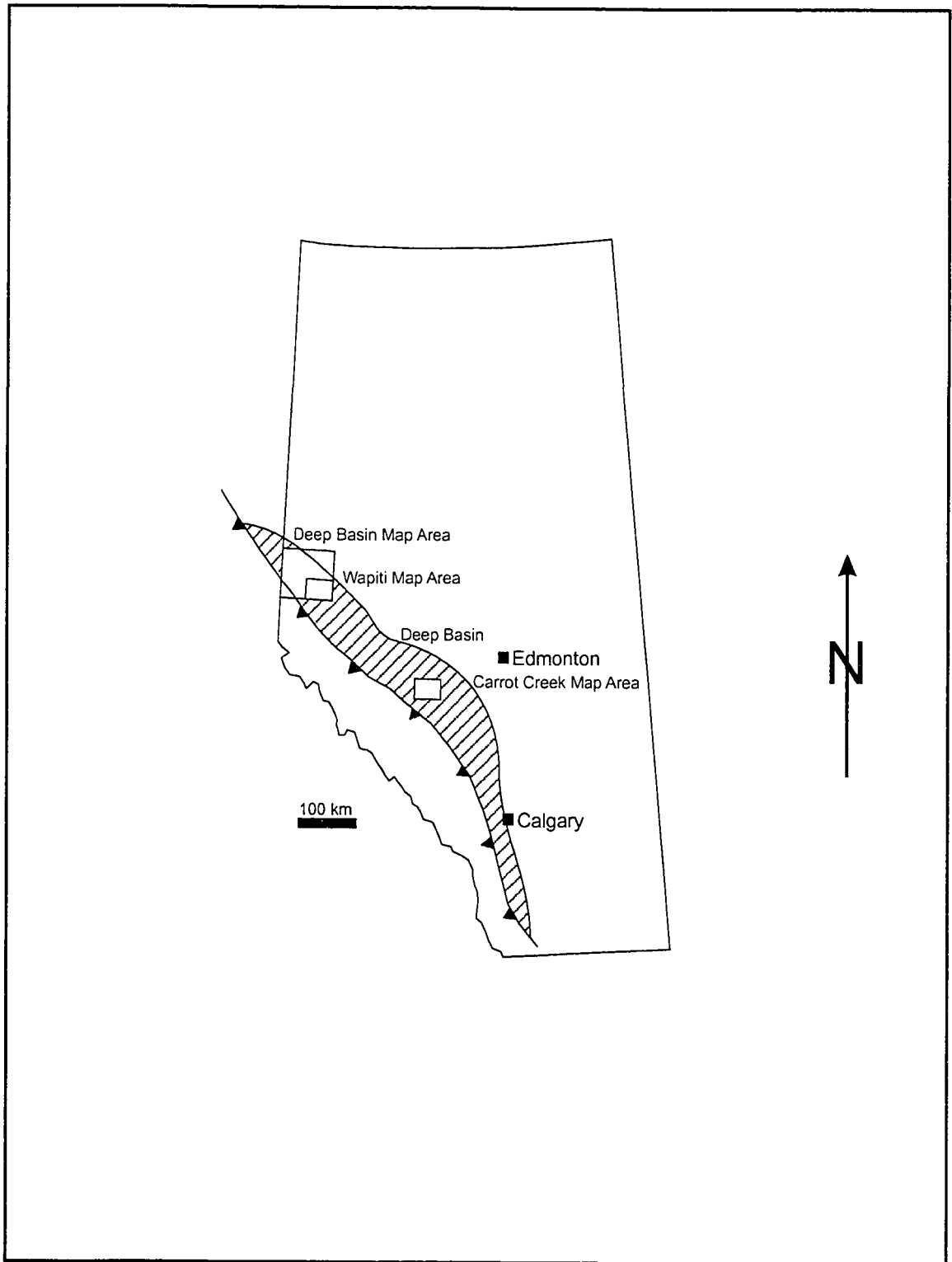
Preamble

The Deep Basin of western Alberta and northeastern British Columbia (Fig. 1.1) is a unique portion of the overall WCSB in that it is fully charged with natural gas under a hydrodynamic trap (Masters, 1984). Bound water in poor quality reservoir rock, at the up-dip edge of the Deep Basin acts as a permeability seal creating a trap in which water overlies gas (Masters 1984). Due to these characteristics most rocks in the Deep Basin with reservoir quality permeability and porosity produce natural gas.

The lower Cretaceous Falher Member of the Spirit River Formation forms a package of marginal-marine to non-marine rocks within the Deep Basin. In spite of the large quantities of clean shoreface sandstones making up the Falher Member almost no production is attributed to these sandstones because they lack reservoir quality permeability. This is due to diagenetic effects such as quartz overgrowths, cementing and mechanical compaction (Cant, 1983; Cant and Ethier, 1984). Only linear chert conglomerate bodies found within Falher strata contain sufficient permeability to produce economic quantities of natural gas.

Within the Deep Basin production from the conglomerate bodies within the Falher has yielded over 30 billion cubic metres of natural gas since the discovery of the gas field in 1976. Individual pools have produced as much as 3 billion

Figure 1.1: Province of Alberta showing the location of the Deep Basin (after Masters, 1984) and the three study areas. The south-western edge of the Deep Basin is the edge of the deformed belt.



cubic metres. Such large production numbers has resulted in numerous studies into the origin and nature of these conglomerate bodies.

Previous Work

Falher conglomerates occur within eight broad marginal marine to non-marine packages labeled A to H (Jackson, 1984). Initial studies of Falher conglomerates involved a discussion of depositional environments from a single core through the Falher A production fairway (McLean, 1979; Armstrong, 1979) and an examination of strata from the exposures of the Falher in the Rocky Mountains of Alberta and B.C. adjacent to the Deep Basin (Leckie and Walker, 1982). Early interpretations suggested that Falher conglomerates formed part of a package of sandy-pebbly strata deposited along shorelines that were prograding northward into the lower Cretaceous Clearwater Sea (Leckie and Walker, 1982).

With the advent of sequence stratigraphy in the mid 1980's the significance of relative sea-level changes became apparent in the Falher. Early sequence stratigraphic studies suggested that each Falher package was made of multiple shoaling-upwards packages (parasequences) bounded by surfaces indicating changes in relative sea-level (Leckie, 1986a; Demarest and Kraft, 1987). More detailed sequence and allostratigraphic studies of various Falher units have shown that the conglomerates are bound within specific, mappable stratigraphic sub-units of the lettered Falher units A-D (Arnott, 1993; Casas and Walker, 1997; Rouble and Walker, 1997; Caddel, 2000).

Cant (1995) and Caddel (2000) gave explanations for why a conglomerate body would develop within a package of prograding sandy shorelines. Cant (1995) suggested that concentration of pebbles during erosive transgression led to the development of multiple pebbly barriers in the Falher A and B. Caddel (2000) proposed that rapidly falling sea-level induced in deeper fluvial incision resulting in larger quantities of pebbles being sourced to the prograding shorelines.

Objectives

While Cant's (1995) study proposes a method for creating linear conglomerate bodies within the Falher it does not agree with the conclusions of other stratigraphic studies of the Falher (Arnott, 1993; Casas and Walker, 1997; Rouble and Walker, 1997; Caddel, 2000) which suggest that the conglomerates formed in a progradational setting. Caddel's (2000) proposal explains abundant pebbles in a progradational setting but fails to explain why a fluvial source that is eroding through sandy/pebbly sediments would result in a concentrated pebbly shoreface body with little sand.

With these considerations in mind the principal objectives of this study are to:

- 1) Describe and interpret the rocks that make up the Falher F strata.
- 2) Create a sequence stratigraphic model for the Falher F within the study area with a specific focus on the stratigraphic placement of the conglomerates.

3) Create detailed isopach, isochron, structure and structural residual maps using well logs and 3-D seismic and aided by production data in order to better understand the depositional processes that affected the Falher F conglomerates

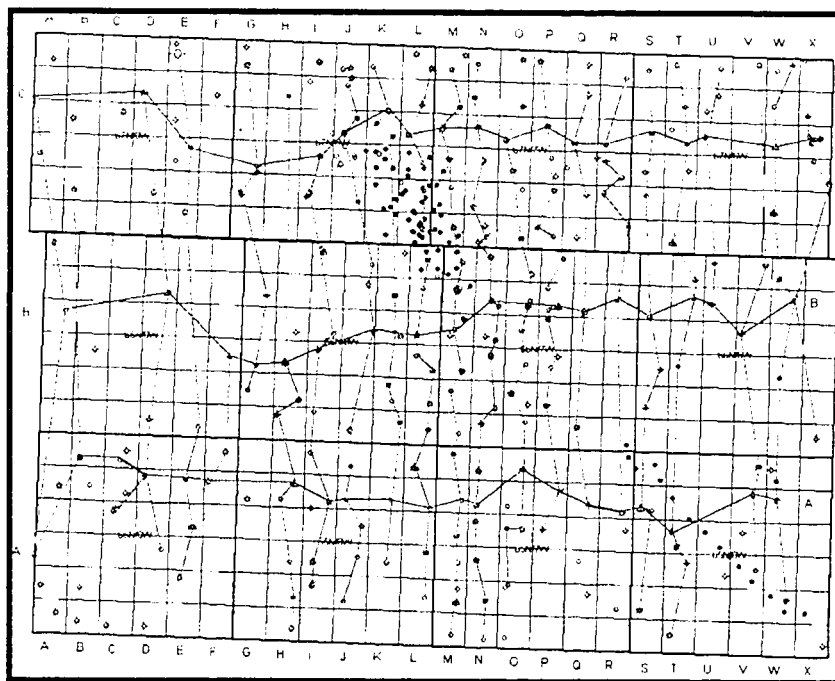
4) Identify the controls on the deposition of linear pebbly shorefaces in order to better predict conglomerate distribution in the subsurface.

Methods

Interpretations of Falher F lithologies were based on 305m of core taken from 18 wells in the study area that were measured and described in October 2002 and June 2003 at the Core Research Laboratory in Calgary, Alberta. Key stratigraphic surfaces were picked on geophysical well logs from 228 wells that intersected the Falher F interval with detailed correlations being carried out on a grid of 24 north-south and 3 east-west oriented cross-sections (Fig. 1.2). For the purpose of confirming our well-based interpretations several key regional horizons were picked in a 210 km² 3-D seismic survey that covered the central portion of the study area.

Most maps in this study were computer-generated using a Kriging gridding algorithm. It was felt that this best served the purposes of our study. Where more detailed mapping was needed, hand-contoured maps were generated. In particular reservoir mapping was carried out by hand. At the reservoir scale, production and pressure data, taken from the Alberta Energy and Utilities Board

Figure 1.2: Map of study area showing location of correlation cross-sections.
There are 24 north-south and 3 east-west cross-sections that include all wells that intersected the Falher F interval.



database using the Geoscout® database, were used to better define reservoir connectivity and therefore reservoir scale heterogeneity.

Further mapping was carried out in the Deep Basin and Carrot Creek map areas. Tops were picked by hand in 1850 wells in the Deep Basin map area and 350 wells in the Carrot Creek map area. Maps for both of these study areas were computer generated. This was judged to be sufficient for the purposes of this study.

Thesis Format

The thesis comprises four chapters. The first chapter gives a general introduction to past research efforts into linear shoreface conglomerate bodies in the Falher Member. The second chapter provides the detailed lithological descriptions and interpretations on which stratigraphic interpretations of chapter 3 are based. The third chapter offers the detailed stratigraphy, mapping and seismic interpretations produced for this project and a discussion of possible Falher F depositional models. The fourth chapter contains overall conclusions for the study. For ease of formatting, most figures were kept within chapter 3. References have been removed from each individual chapter and placed in a single bibliography at the end of the thesis.

Chapter 2 Lithofacies

Introduction

Within the Wapiti study area 228 wells intersect the Falher F member. Of these wells only 18 were cored in that interval. The 18 cores, totaling 305m, were measured and described in order to determine depositional processes affecting the Falher F strata, and to interpret depositional environments.

Within the Falher F interval, 8 lithofacies were defined in terms of lithology, sedimentary structures and trace fossil assemblage. Descriptions and interpretations are given below. Representative photographs of each facies are presented in both Figure 3.5 and Appendix 1. The log response of each facies was studied in order to better understand lithologies and depositional environments in wells without core.

Facies Descriptions and Interpretations

Facies 1

Black silty mudstone with minor ripple cross-laminated very fine-grained sandstone lenses grading upwards into flaser bedded very fine-grained sandstone characterizes facies 1. Bioturbation is common and consists of abundant *Chondrites*, *Thalassinoides* and *Palaeophycus*, minor *Helminthopsis*

and *Planolites* and rare *Rosselia*, *Cylindrichnus* and *Teichichnus*. Rare bivalve shell beds are observed.

Interpretation

This facies is interpreted as offshore sediments deposited below storm wave base. The predominance of a muddy substrate supports this interpretation (Walker and Plint, 1992). The trace fossil diversity as well as the presence of neritic burrowers such as *Helminthopsis* suggests that the sediment was deposited in the Nereites ichnofacies, which corresponds to the offshore (Eckdale et al., 1984; Walker and Plint, 1992; Pemberton et al., 2001).

Facies 2

Facies 2 can be subdivided into two sub-facies: 2A and 2B. Facies 2A consists of massive, dark grey, very fine- to lower fine-grained sandstones. Rarely, very faint hummocky cross-stratification is visible and no macro-traces were observed.

Facies 2B is composed of hummocky cross-stratified, lower fine- to upper fine-grained sandstones. Bioturbation is common with *Palaeophycus* being the predominant form; however *Ophiomorpha*, *Teichichnus*, *Thalassinoides* and rare *Skolithos* are also present. Pebbles occur as isolated clasts, single clast veneers on cross-stratification and 2-5 cm beds with pebble content typically increasing

upwards. Carbonaceous shale stringers and coaly particles are present in places. Rarely beds with abundant calcite cement were observed.

Interpretation

Hummocky cross-stratified sandstones are interpreted to be the result of storm reworking and deposition of shoreface sediments (Walker and Plint, 1992) and in particular lower shoreface sediments (Arnott, 1993). The trace fossil assemblage of facies 2B suggests deposition in the *Cruziana* ichnofacies, which corresponds to a lower-shoreface environment (Ekdale et al., 1984; Benton and Harper, 1997). The massive sandstones of facies 2A are interpreted to be sediments of facies 2B, which have been homogenized by meiofaunal bioturbation (Rouble and Walker, 1997; Pemberton et al., 2001).

Facies 3

Facies 3 overlies and can be interbedded with facies 2 and is characterized by trough cross-bedded, pebbly, medium-grained sandstones. The pebbly sandstones exhibit normal coarse-tail grading. *Palaeophycus*, *Macaronichnus* and *Teichichnus* are observed only rarely. Strata may contain disseminated carbonaceous material.

Interpretation

The cross-stratified sandstones of facies 3 are interpreted as upper shoreface deposits. Hydraulic conditions created by shoaling waves on the upper shoreface results in dune propagation (Arnott, 1993) that is preserved as cross-stratification. Coarse-tail grading is interpreted to result from the hydraulic segregation of particles during dune propagation (Swinchatt, 1967). The limited trace fossil assemblage is suggestive of a high-energy upper shoreface environment in which traces are poorly preserved (Benton and Harper, 1997).

Facies 4A

Facies 4A consists of very poorly sorted, bimodal, closed framework chert conglomerate with a medium-grained sandstone matrix. Bedding is characterized by centimeter to decimeter thick beds, which exhibit coarse-tail normal grading and scoured bases. Facies 4A strata may contain clasts up to 5 centimeters long, and can exhibit a planar, sub-horizontal fabric. Rarely, beds consisting of finer material may exhibit cross-bedding. No trace fossils were observed. Facies 4A pebbly material can also be interbedded with both facies 2 and facies 3 sandstones.

Interpretation

Strata of this nature could yield multiple interpretations ranging from fluvial to shoreface deposits. In the case of the Falher F, these rocks are interpreted as upper shoreface deposits due to their stratigraphic context. This facies overlies

and is interbedded with lower and upper shoreface deposits and underlies foreshore strata (discussed as facies 4B and 5). The poorly sorted nature of the strata suggests deposition and burial close to a fluvial source, before marine processes were able to effectively sort sand from pebbles (Hart and Plint, 1995). The coarse-grained nature of this facies has typically resulted in a fluvial or deltaic interpretation (McLean, 1979; Leckie and Walker, 1982; Cant, 1984; Arnott, 1993; Caddel, 2000). Cross-bedding in shoreface conglomerates is interpreted to represent shoreward, seaward and/or alongshore-migrating gravelly dunes (Hart and Plint, 1995). Cross-bedding may also be produced by progradation of the plunge step as has been observed on modern pebbly shorelines (Hart and Plint, 1989). Interbeds of facies 4A conglomerate in lower and upper shoreface facies 2 and 3 are interpreted as rip current deposits. This interpretation was also derived for similar strata in the upper Cretaceous Cardium Formation (Hart and Plint, 2003).

Facies 4B

This facies consists of moderately- to well-sorted conglomerate and very coarse-grained sandstones. Maximum observed bed thickness was 1.5 m. Low-angle planar lamination is common, but cross-bedding is present in places. Visual comparison of facies 4A and 4B pebbles indicate that facies 4B pebbles have a higher sphericity than those of the poorly sorted pebble beds in facies 4A. The rock is entirely clast supported, and only rarely is any sandy matrix material present.

Interpretation

This facies is interpreted as a beach deposit (Arnott, 1993). Foreshore wave reworking of facies 4A removed the medium sand matrix and sorted the grains (King, 1972; Kleinspehn et al. 1984, Arnott, 1993). The higher degree of clast sphericity results from constant swash and backwash rolling of pebbles which mechanically abraded non-spherical pebbles towards higher sphericity (King, 1972). Dune migration has been observed on modern pebbly beaches (Carter and Orford, 1984) and would produce cross-bedding if preserved in the rock record.

Facies 5

Facies 5 is composed of light grey, fine- to medium-grained sandstones. The sandstones are predominantly massive however faint horizontal to low-angle planar laminations are visible. *Macaronichnus* bioturbation is common and bioturbation can be sufficiently intense to result in a massive appearance.

Interpretation

The planar laminations of facies 5 are interpreted as beach laminations (Walker and Plint, 1992). The slight dip to the bedding is typical of foreshore deposits. Intense *Macaronichnus* bioturbation suggests that these rocks were

deposited in the Skolithos ichnofacies and are typical of a foreshore environment (Pemberton et al., 2001).

Facies 6

Black carbonaceous mudstones with very fine-grained sandstone asymmetrical ripples characterize this facies. Thin coal seams ranging from 3 mm to 1 cm are present. Slickensides are common in the mudstones. No trace fossils were observed however the mudstones may exhibit a mottled appearance.

Interpretation

These strata are interpreted as coastal plain swamp deposits. Preservation of thin coal seams within carbonaceous shaley strata suggests deposition in non-marine but wet conditions (Miall, 2000; Wadsworth et al., 2003). Slickensides are interpreted as pedogenic, formed by swell-shrink movements resulting from drying and wetting of a soil (Retallack, 1990). The lack of bioturbation suggests a non-marine depositional environment (Eckdale et al., 1984). The mottled appearance of some of the mudstones may be the result of biologic reworking of the sediment.

Facies 7

Facies 7 is identified in core as light grey, friable, massive, medium-grained sandstones. Facies 7 often overlies or is interbedded with facies 6 strata and beds often have scoured bases. Trace fossils were not observed. In drill cuttings facies 7 consists of unconsolidated medium-grained sand.

Interpretation

Due to its stratigraphic relationship with facies 6, facies 7 is interpreted as a fluvial channel fill deposit. A kaolinitic matrix is considered responsible for the pale appearance of Facies 7 as well as its unconsolidated nature. The lack of bioturbation suggests a non-marine depositional environment (Eckdale et al., 1984).

Facies 8

Facies 8 consists of black sub-anthracitic coal. The coal may consist of beds with 10 to 40 cm seams separated by Facies 6 (carbonaceous shales) or could be massive and up to 2m thick. Original plant material may be seen on bedding surfaces.

Interpretation

Clean coals result from accumulations of peat (Miall, 2000). Such accumulations normally occur distally from clastic sources. Interbedding with Facies 6 (carbonaceous shales) suggests that the depositional environment

shifted between swampy/shaley deposition and sub-aerial peat deposition (Wadsworth et al., 2003).

Core to Well Log Comparisons

All of the drafted core sections are presented in Appendix 1. Each core log has been placed beside its respective well log in order to illustrate the characteristic log response of each lithofacies. As expected, the shaley and finer-grained rocks have higher gamma-ray and neutron porosity responses than the more coarse-grained strata. However, no diagnostic set of log readings is unequivocally representative of any lithofacies. Therefore stratigraphic context as well as log response becomes important in determining the depositional environments represented in each logged well. The picking of key sequence stratigraphic surfaces in each well is discussed in more detail in Chapter 3.

**Chapter 3 Deeply-Rooted Topographic Control on the
Deposition of the Falher F Conglomerate Trend, Wapiti
Field, Deep Basin, Alberta**

Byron Nodwell and Bruce Hart

Department of Earth and Planetary Sciences

McGill University

Submitted for publication in: Bulletin of Canadian Petroleum Geology,
Canadian Society of Petroleum Geologists, Calgary, Canada.

Abstract

The lower Cretaceous Falher F unit of Alberta is subdivided into four prograding parasequences labeled F1 to F4. F1, F2, and F4 consist of shallowing-upwards successions typical of prograding sandy shorelines with minor amounts of pebbles. The F3 parasequence, however, contains an anomalously thick (12m) succession of prograding, upper-shoreface and foreshore conglomerate. The conglomerates within the F3 parasequence form a NE-SW trending linear body that terminates abruptly to the northeast. These conglomerates have produced over $9.0 \times 10^9 \text{m}^3$ (320 Bcf) of natural gas within the study area since 1979. Detailed mapping using log, core, and 3-D seismic data indicates that the conglomerates were deposited along a linear topographic feature that coincides with the northern edge of the underlying upper Devonian Gold Creek (Smoky) reef trend (Leduc, Nisku, and Wabumun Formations). Furthermore, the northeastern termination of the conglomerate trend is coincident with a NW-SE striking structural feature that influenced accommodation.

Two models, consistent with the currently available data, may explain the deposition of conglomerates. The first proposes that the landward movement of a pebbly barrier, formed during flooding at the end of F2 deposition, was halted at the reef-induced topographic high. The second proposes that an abrupt slowdown in progradation rate of the F3 parasequence and steepening of the shoreface profile at the topographic feature lead to concentration of pebbles by normal shoreface processes. Both models explain how the reef-induced

topography controlled the location and lithology of a conglomeratic shoreface and foreshore within the dominantly sandy Falher F, although we argue that the second model best explains the available data. In either case, syn-depositional patterns of accommodation development prevented longshore drift from carrying pebbles to the northeast portion of the study area.

Introduction

The Lower Cretaceous Falher Member of the Spirit River Formation (Fig. 3.1), in west-central Alberta, is an economically significant producer of hydrocarbons. Well over 30 billion cubic metres (1 Tcf) have been produced from the various units of the Falher, labeled A through H (Jackson, 1984). Within the study area (Fig. 3.2), three pools of the Falher F unit have produced over nine billion cubic metres (320 Bcf) of condensate-rich natural gas from nine wells, making it one of the most prolific production trends in the Deep Basin. In spite of these impressive production values most rocks of the Falher have very low effective permeability due to diagenetic effects such as quartz cementation, quartz overgrowths, and mechanical compaction (Cant, 1983; Cant and Ethier, 1984). Only chert conglomerate intervals within each Falher unit have any significant permeability, therefore most production comes from these conglomeratic intervals (Cant, 1983; Cant and Ethier, 1984; Rahmani, 1984). The Falher F conglomerate unit forms a linear trend, which is 38 km long and 4km wide (Fig. 3.3).

Due to the economic significance of the conglomeratic intervals within the Falher units they have been the subject of many studies carried out in order to determine Falher depositional environments (McLean, 1979; Armstrong, 1979; Leckie and Walker, 1982; Cant, 1984; Smith et al., 1984), marine stratigraphy (Leckie, 1986a; Demerest and Kraft, 1987; Arnott, 1993; Cant, 1995; Casas and Walker, 1997; Rouble and Walker, 1997; Caddel, 2000), non-marine stratigraphy

Figure 3.1: a) General stratigraphic column showing key stratigraphic units discussed in this study; detailed stratigraphic column of the lower Cretaceous section in study area. Modified from Smith (1984) and Cant (1988). b) Seismic transect through study area showing key horizons.

a)

Upper Cretaceous	Badheart	
	Cardium	
	Dunvegan	
	Fish Scales	
	Lower Cretaceous	
Spirit River		Notikewin
		Falher
		Wilrich
Bluesky		
Jurassic-Mississippian		
Upper Devonian	Wabumun	
	Nisku	
	Leduc	

Fort St. John Group	Peace River Fm	Shitsbry Fm.	Fish Scale Zone	
		Paddy Mbr.	Cadotte Mbr.	
			Harmon Mbr.	
	Notikewin Mbr.			
	Spirit River Formation	Falher Member	Falher A	
			Falher B	
			Falher C	
			Falher D	
			Coal E	
			Falher F	
		Wilrich Member		
	Bullhead Group	Bluesky Formation		
Gething Formation				
Cadomin Formation				

b)

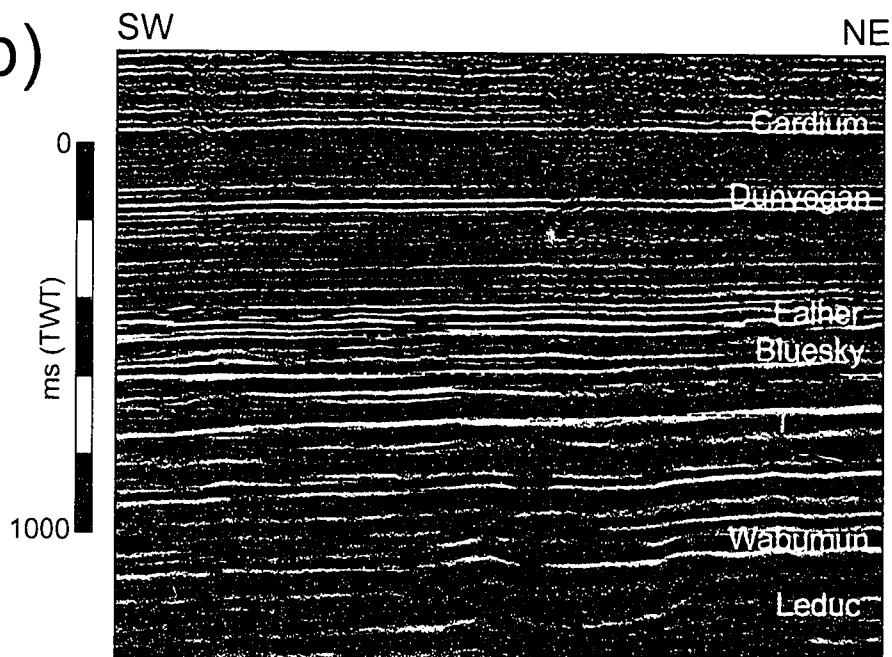
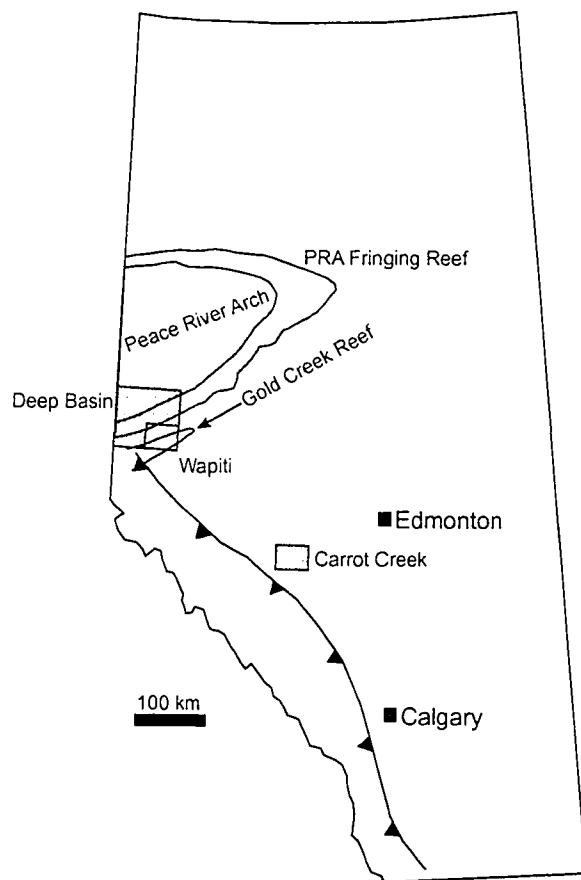
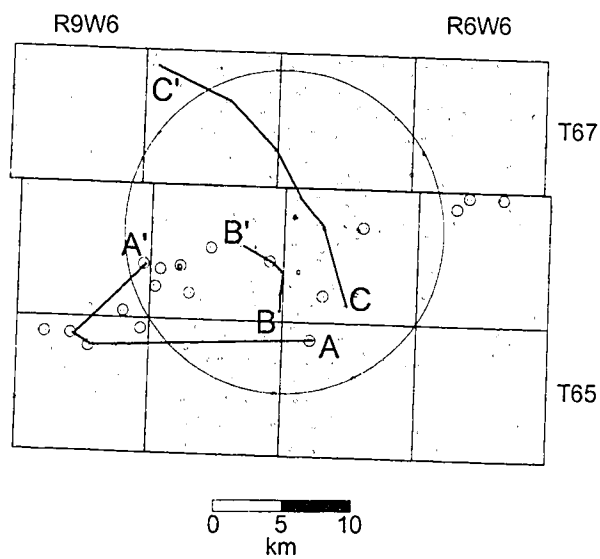


Figure 3.2: a) Province of Alberta with our three mapping areas: Wapiti (Stippled), Deep Basin and Carrot Creek (cross-hatched). Note the location of the southern edge of the Peace River Arch within the Deep Basin study area and the northern edge of the Gold Creek reef within the Wapiti study area. The edge of the deformed belt is indicated. Modified from Moore (1989) and Casas and Walker (1997). Detailed work on the Falher F was carried out in the Wapiti map area and other mapping was carried out in the Deep Basin and Carrot Creek areas. b) Map of the Wapiti study area showing Falher F well log coverage (small circles), core coverage (large circles), approximate location of the 3-D seismic survey (circle) and the location of cross-sections A-A' (Fig. 3.6a), B-B' (Fig. 3.6b) and C-C' (Fig. 3.8).

a)



b)



(Wadsworth et al., 2003), and petrology (Cant, 1983; Cant and Ethier, 1984; Leckie, 1986b).

Previous interpretations of the Falher concluded that each lettered unit was a single northward-prograding marginal-marine succession (Leckie and Walker, 1982; Cant, 1983, 1984; Cant and Ethier, 1984). More recent studies have used sequence stratigraphic and allostratigraphic principles to suggest that the Falher units from A to D are composite units made up of multiple, approximately E-W striking, northward prograding marginal-marine packages (Leckie, 1986a; Arnott, 1993; Cant, 1995; Casas and Walker, 1997; Rouble and Walker, 1997; Caddel, 2000). Each of these more recent studies showed that the conglomerates were located only within specific stratigraphic intervals thus emphasizing the importance of more detailed stratigraphy for locating conglomerates within each Falher unit. In spite of this agreement on the composite stratigraphic nature of the Falher intervals, debate continues on the exact stratigraphic placement of the conglomerates, with some authors arguing deposition during progradation (Cant, 1984; Leckie, 1986a; Arnott, 1993; Casas and Walker, 1997; Rouble and Walker, 1997; Caddel, 2000) and others arguing that the conglomerates were deposited as transgressive barriers (Cant, 1995).

Although the previous studies of the Falher established a stratigraphic framework for the producing conglomerates, they failed to determine the reason why, in a package of prograding, sandy shorelines, only selected stratigraphic intervals would develop anomalously thick sections of conglomerate. Thus while previous authors provided vital knowledge into the internal stratal architecture of

the various Falher units, they fell short of providing diagnostic tools for predicting conglomerate distribution. This paper seeks to provide not only a stratigraphic study of the Falher F unit, but also to determine the fundamental controls on the development of thick conglomerate intervals. The concepts developed here appear to help explain the distribution of some other linear shoreface conglomerates in Cretaceous rocks of the Western Interior Seaway.

Database and Methods

Results presented in this paper are derived from correlations of gamma-ray, density, neutron porosity, sonic, photoelectric and resistivity logs from the 228 wells that intersected the Falher F interval within the study area and were publicly available as of December 2002 (Fig. 3.2b). Sedimentological interpretations were derived from the measurement of 305m of core from 18 wells. Production and pressure data were taken from the Alberta Energy and Utilities Board database using the Geoscout® database. Finally, a 210 km² 3-D seismic survey was provided by Millennium Seismic in order to complete and compliment our well-based interpretations.

Key stratigraphic surfaces were picked throughout the study area using a grid of 24 North-South and 3 East-West cross-sections (Fig. 1.2). These correlations were used to construct isopach, structure and structural residual maps. Key regional horizons were picked in the 3-D survey and were used to construct isochron and time-structural residual maps. Computer-based contouring was

judged to be adequate for showing large-scale structural and stratigraphic trends, but in some cases hand-contoured maps were prepared to show more detail at the reservoir-scale.

A regional study was carried out to determine if the findings of our Falher F study were more broadly applicable to other linear conglomerate trends in the Falher and the upper Cretaceous Cardium Formation. Data for this regional study was derived from horizons picked on the logs for 1850 wells in the Elmworth to Wapiti region of the Deep Basin (Figs. 3.2a and 3.3) and 350 wells from the Carrot Creek field (Figs. 3.2a and 3.4).

Results

Falher F Lithofacies Descriptions and Interpretations

In order to better understand the depositional processes active during deposition of Falher F strata, detailed description and interpretation of 8 lithofacies were made from 18 cores that sampled strata from the Falher F interval. Multiple authors have made detailed facies descriptions and interpretations of Falher lithologies (Leckie and Walker, 1982; Arnott, 1993; Casas and Walker, 1997; Rouble and Walker, 1997; Caddel, 2000; Wadsworth et al., 2003). Our descriptions and interpretations are very similar to those of these previous authors and therefore, for the sake of brevity, a summary of the facies is

Figure 3.3: Map of the Deep Basin area showing well log coverage (small circles) and cumulative gas production bubbles (large bubbles $> 8.5 \times 10^5 \text{ m}^3$ (30 Bcf), small bubbles $> 1.4 \times 10^6 \text{ m}^3$ (5 Bcf)). Cumulative production is used as a proxy for conglomerate distribution. The location of the Wapiti Study area is indicated by the heavily outlined area in the southeast of the map and linear trends of the Falher A, B, C, D and F are indicated.

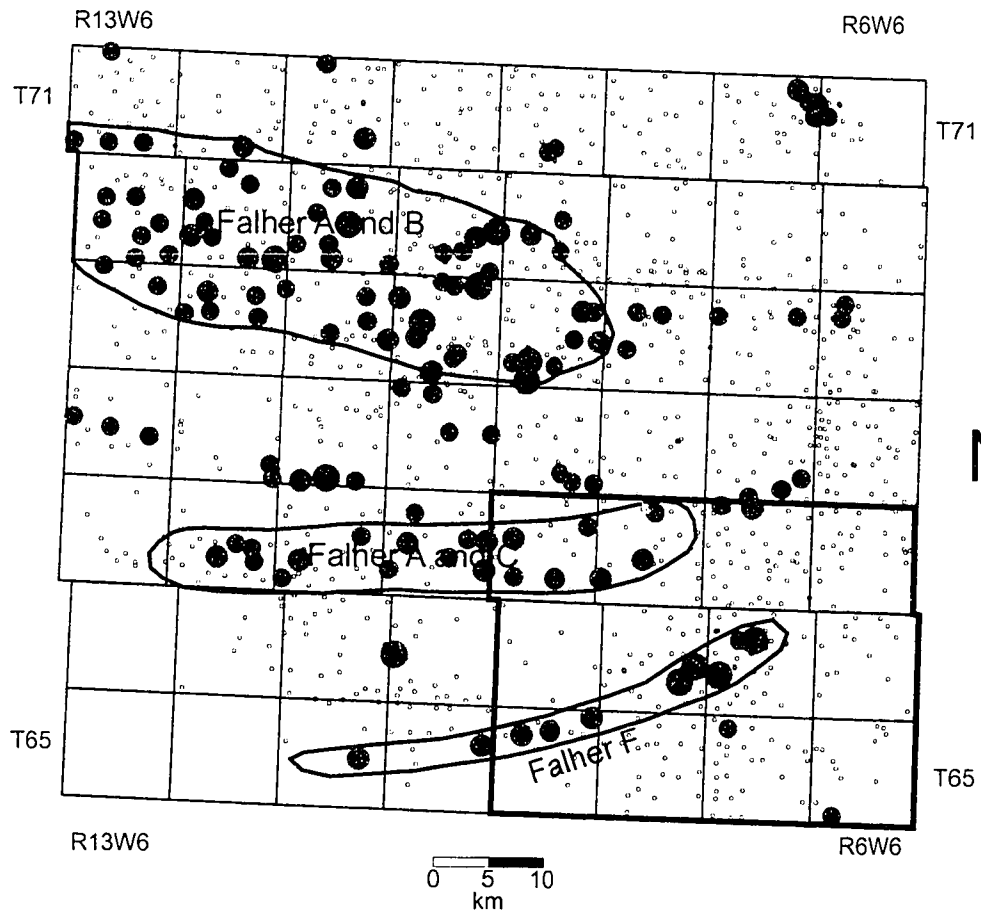
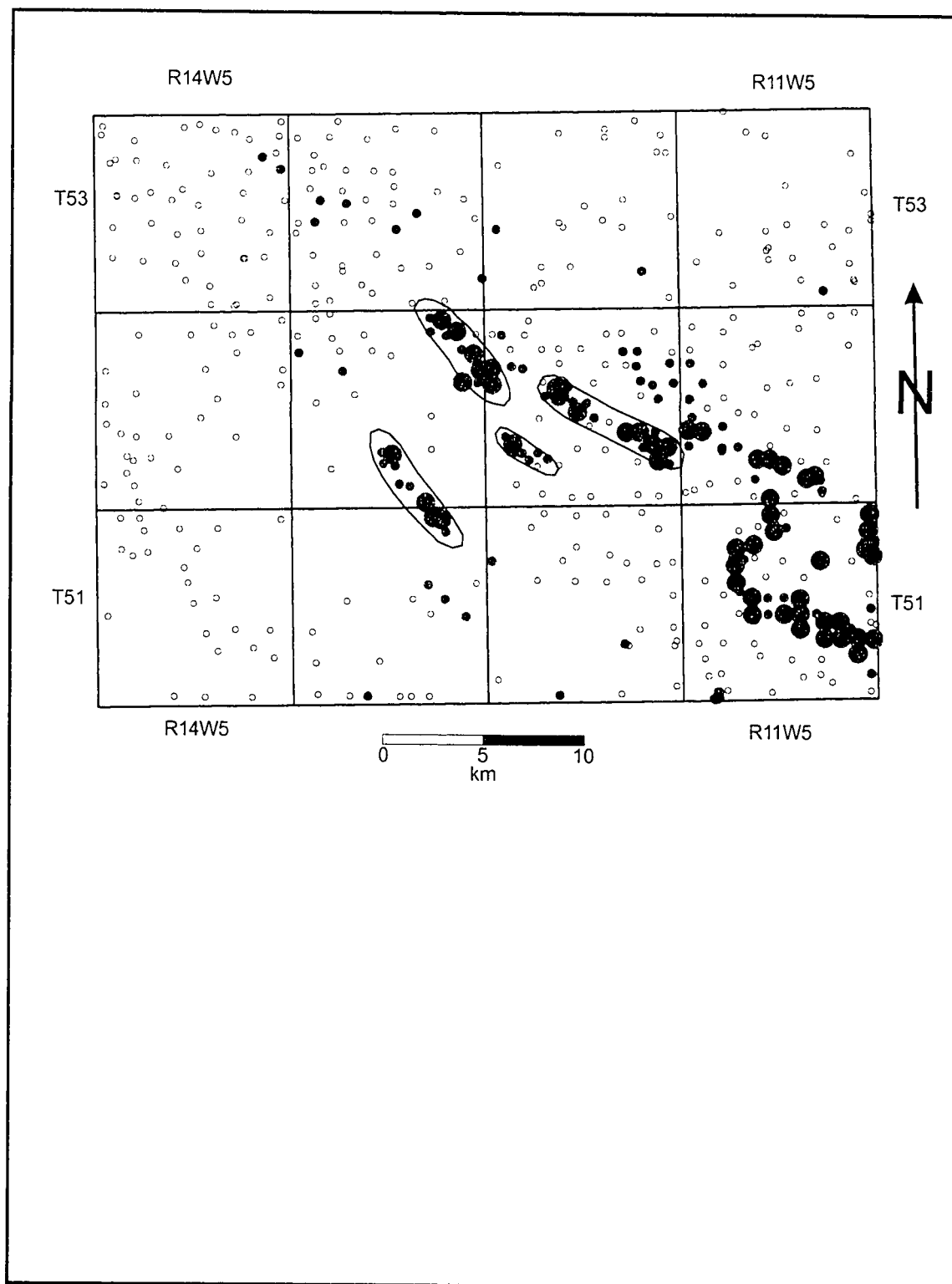


Figure 3.4: Map of the Carrot Creek area showing well log coverage (small circles) and cumulative oil production bubbles (large bubbles $> 40 \times 10^3 \text{ m}^3$, small bubbles $> 8 \times 10^3 \text{ m}^3$). Cumulative production is used as a proxy for conglomerate distribution and the linear trends of productive Cardium conglomerates are indicated.



presented in Figure 3.5. Interested readers are directed to Rouble and Walker (1997) for a more thorough discussion of Falher lithofacies interpretations.

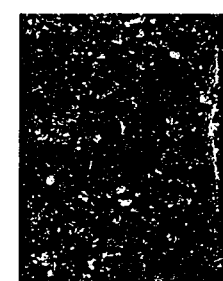
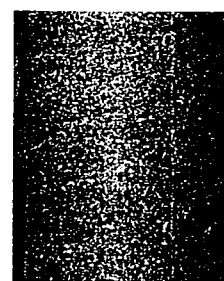
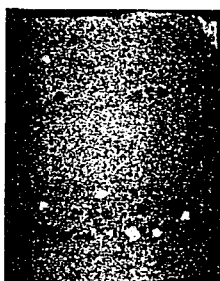
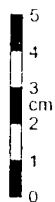
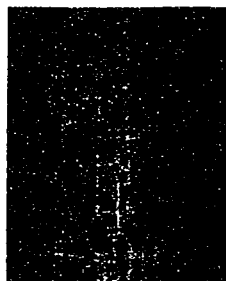
Falher F Lithological Successions from Core

Two thick coarsening-upwards successions and one thin fining-upwards succession are present within the Falher F. Of the coarsening-upwards successions one is pebble-rich and can contain as much as 12m of conglomerate while the other is pebble-poor. A comparison of the two successions offers insight into the depositional and stratigraphic context of the conglomerate body.

Sandy Succession: Description

A typical vertical succession through a sandy Falher F shoreline consists of a gradual vertical shift in lithology from Facies 1 (offshore mudstones) through to Facies 5 (foreshore sandstones); excluding Facies 4 conglomerates (e.g. core 7-13-66-9W6, Fig. 6a). Facies 5 beach sandstones may be rooted and overlain by carbonaceous shales of Facies 6 followed by Facies 8 coals (Fig. 3.6). Although some pebbles are present in the upper shoreface of most Falher F shoreline successions, thick (>2m) accumulations of facies 4A or 4B conglomerate are absent.

Figure 3.5: Summary of Falher lithofacies including photographs of representative samples from Falher F cores.

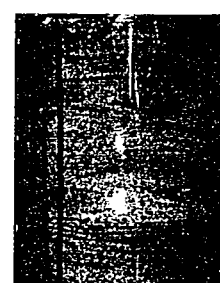
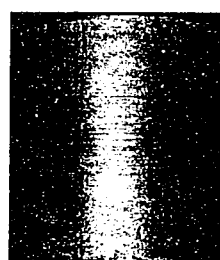
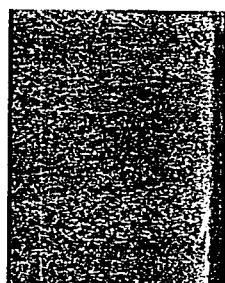
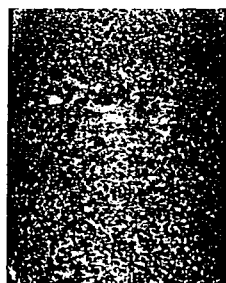


Facies 1
Sandy Shales
Nereites Ichnofacies
Offshore
2393m, core 7-27-66-7W6

Facies 2
HCS Sandstones
Cruziana Ichnofacies
Lower Shoreface
2908m, core 5-32-65-9W6

Facies 3
Cross-bedded Sandstones
Skolithos/Cruziana Ichnofacies
Upper Shoreface
2743m, core 3-33-65-9W6

Facies 4a
Poorly Sorted Conglomerate
Closed Framework
Upper Shoreface
2641m, core 13-27-65-9W6



Facies 4b
Well Sorted Conglomerate
Open Framework
Foreshore
2727m, core 3-33-65-9W6

Facies 5
Planar Bedded Sandstones
Skolithos Ichnofacies
(*Macaronichnus*)
Foreshore
2220m, core 9-34-66-6W6

Facies 6
Carbonaceous Shale
Abundant Plant Material
Coastal Plain
2901m, core 5-32-65-9W6

Facies 7
Current Rippled Sandstone
Carbonaceous Shale Partings
Coastal Plain Fluvial
2567m, core 8-2-66-9W6

Facies 8
Coal
Coastal Plain
2569m, core 8-2-66-9W6

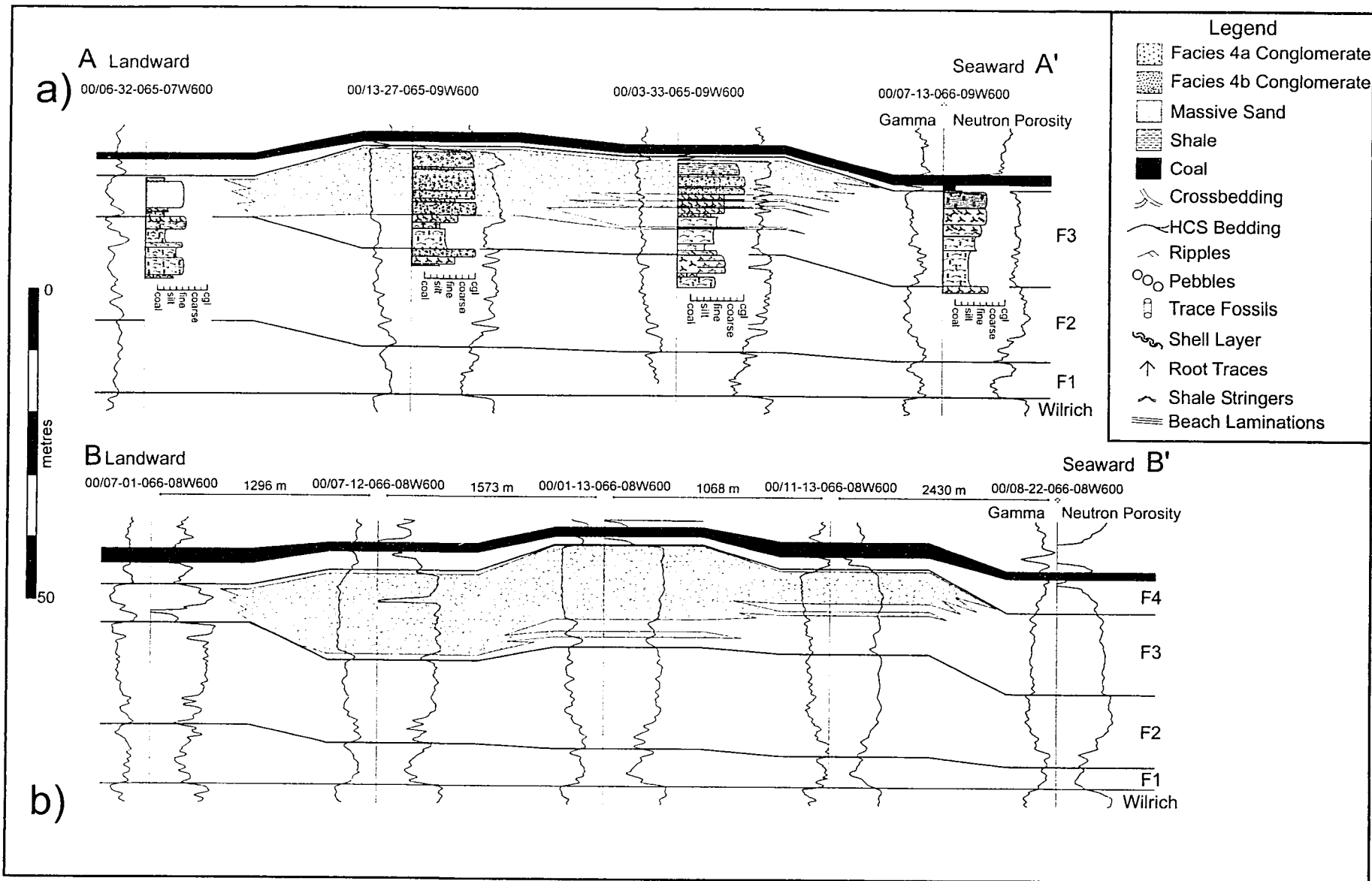
Sandy Succession: Interpretation

This succession of facies is typical of a prograding, sandy, wave- and storm-dominated shoreline (Walker and Plint, 1992). The abundance of hummocky cross-stratification and the lack of obvious tidal structures such as mud drapes and herringbone cross-stratification support this interpretation. This interpretation agrees with those of previous Falher studies (Leckie and Walker, 1982; Arnott, 1993; Casas and Walker, 1997; Rouble and Walker, 1997; Caddel, 2000). The non-marine succession, from carbonaceous shales through to coal, is interpreted as a drying-up succession (Wadsworth et al., 2003) suggesting that the coastal plain sediments formed part of a continuous shoaling-up/drying-up package with the underlying marine rocks. Logs and core suggest that this succession is repeated multiple times (Fig. 3.6) in the Falher F interval within the study area indicating that Falher F sedimentation is dominantly sand-rich with some pebbles.

Pebbly Succession: Description

When the Falher F succession becomes anomalously (>2m) conglomeratic, Facies 2, 3 and 5 are variably replaced by, and interbedded with, Facies 4a and 4b conglomerates (e.g. cores 13-27-65-9W6 and 3-33-65-9W6, Fig. 3.6a). Thin beds (2-10cm) of conglomerate often occur within Facies 2 and 3 shoreface sandstones underlying the main conglomerate body, and pebble content within the shoreface sandstones increases upwards. Facies 4b conglomerates, which

Figure 3.6: a) Idealized dip-oriented cross-section (A-A') through cored wells. Note that the F3 parasequence is sandy both landward and seaward from the conglomerate. Thin pebble beds are interbedded within lower and upper shoreface sandstones in core 3-33-65-9W6. Both sandy and pebbly successions are immediately overlain by coastal plain shales and coals. The F3 conglomerate body is shown in stipple pattern. b) Dip-oriented well log cross-section (B-B') through conglomerate body. Note that the conglomerate unit is over 3km wide at this location. A thick package of sandstones is shown at well 8-22-66-8W6. The F3 conglomerate body is shown in stipple pattern. See Figure 3.2b for location of cross-sections.



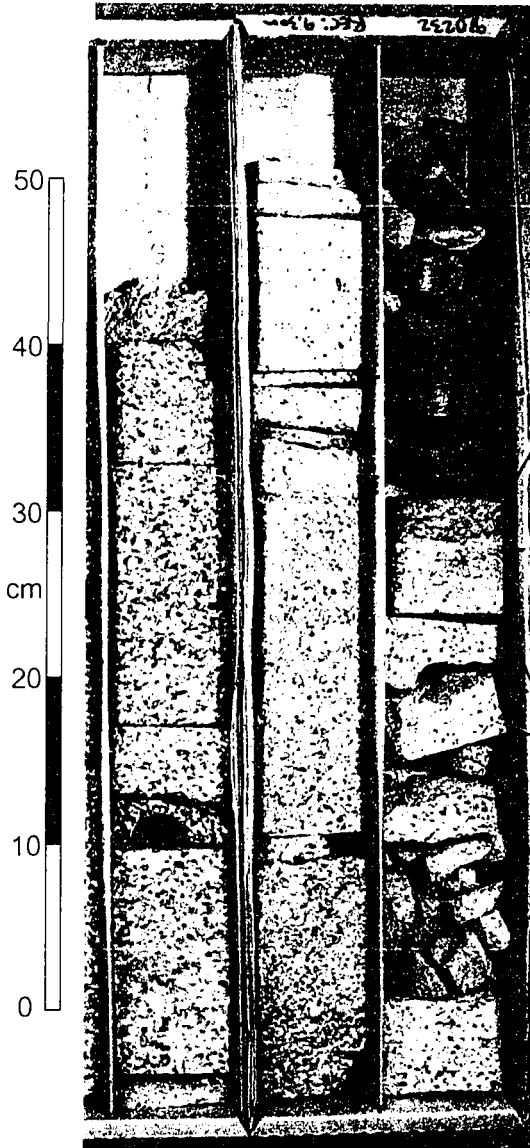
cap the marine succession, are immediately overlain by non-marine strata consisting of carbonaceous shales overlain by coals (Fig. 3.7).

Pebbly Succession: Interpretation

As with the sandy shoreface successions, the stratigraphic position of the conglomerate is indicative of shoaling water and the conglomerates are interpreted as having been deposited in a progradational setting. Upward-increasing pebble content and conglomerate interbeds in lower- and upper-shoreface sediments are seen as "heralding" the arrival of the overlying shoreface conglomerate bodies (Leckie and Walker, 1982). The vertical succession of facies and interbedding of conglomerate beds in lower- and upper-shoreface sandstones is similar to that seen in progradational conglomerate deposits described in the upper Cretaceous Cardium Formation of western Canada (Hart and Plint, 1989, 1995, 2003) and the Pliocene of western Italy (Massari and Parea, 1988). The overlying coastal plain strata at the top of the conglomerate suggest conformable deposition within an overall shoaling-up/drying-up succession as has been suggested in other non-marine Falher successions by Wadsworth et al. (2003). The conglomerate body gradationally overlies a shoaling-upwards succession suggesting that its base is not a transgressive surface of erosion (TSE) as has been suggested for other Falher conglomerate bodies (Cant, 1995). As discussed below, we believe that this

Figure 3.7: a) Photograph (2651 - 2652.4m, core 10-36-65-9W6) showing conglomerates immediately overlain by Facies 6 (carbonaceous shales) and Facies 8 (coal). Stratigraphic top is to the right. b) Close-up photograph of the top of the conglomerate succession in core 10-36-65-9W6. The intermixing of carbonaceous material suggests that the overlying carbonaceous shales were deposited immediately after deposition of the underlying conglomerates.

a)



b)



does not preclude a transgressive depositional model for the Falher F conglomerates.

Fining-Upwards Succession: Description

This succession, which is rarely more than 3m thick, is made up of Facies 2 (HCS sandstones) gradationally overlain by Facies 1 shales (e.g. core 13-27-65-9W6, Fig. 3.6a). This succession may contain thin (1-2cm) pebble beds.

Fining-Upwards Succession: Interpretation

These strata are interpreted as having been deposited during a relative rise in sea level. The fining-upwards nature reflects both an increase in water depth and distance from shoreline as transgression proceeded. The pebble beds are interpreted to be rip-current deposits derived from a nearby gravel body and deposited on the lower shoreface (Hart and Plint, 2003).

Stratigraphy and Depositional History

Multiple shallowing upward progradational successions, capped by flooding surfaces are preserved within the Falher F (Fig. 3.6). The flooding surfaces are recognized as an abrupt shift to deeper water facies and are parasequence boundaries (Van Wagoner et al., 1990; Kamola and Van Wagoner, 1995). In core, a flooding surface may be represented by Facies 2 HCS sandstones

overlying upper shoreface Facies 3 sandstones (e.g. core 7-13-66-9W6, Fig. 3.6a). In some cores a thin deepening-/fining-upwards succession, up to 3.5m thick, is preserved above the flooding surface (e.g. core 3-33-65-9W6, Fig. 3.6a).

Falher F flooding events have a distinctive expression in well logs. The gamma-ray log shifts towards higher radioactivity and the neutron porosity shifts towards higher values (Fig. 3.6), reflecting the change from cleaner strata to shalier lithologies. In wells where the parasequence boundary is a sand-on-sand contact with no clear gamma ray marker, the neutron porosity log allows identification of the flooding surface. This neutron shift may be indicative of a diagenetic difference between the two parasequences, as has been observed in analogous rocks of the upper Cretaceous Cardium Formation (Hart and Plint, 1993a). In the south of the study area non-marine strata may cap parasequences F2, F3 and F4. Although some non-marine sediments were probably deposited during transgression, the transgressive surface of marine erosion above the non-marine deposits was used to define the parasequences.

The characteristic log response of a flooding surface was used to pick parasequence boundaries in all of the wells within the study area. Four parasequences, labeled F1 through F4, form a progradational parasequence set in the Falher F interval within the study area (Fig. 3.8). The overall northward progradation of the Falher F unit over the Wilrich Member involved a stepwise northward deposition of each parasequence, with F1 being deposited in the south of the study area and F4 in the north (Figs. 3.9a-d).

Figure 3.8: Dip-oriented cross-section (C-C') crossing the study area. Note the progradational geometry of the Falher F parasequences. The F3 conglomerate body is shown in stipple pattern. See Figure 3.2b for location of cross-section. Additional cross-sections illustrating Falher F stratigraphy are included in Appendix 3.

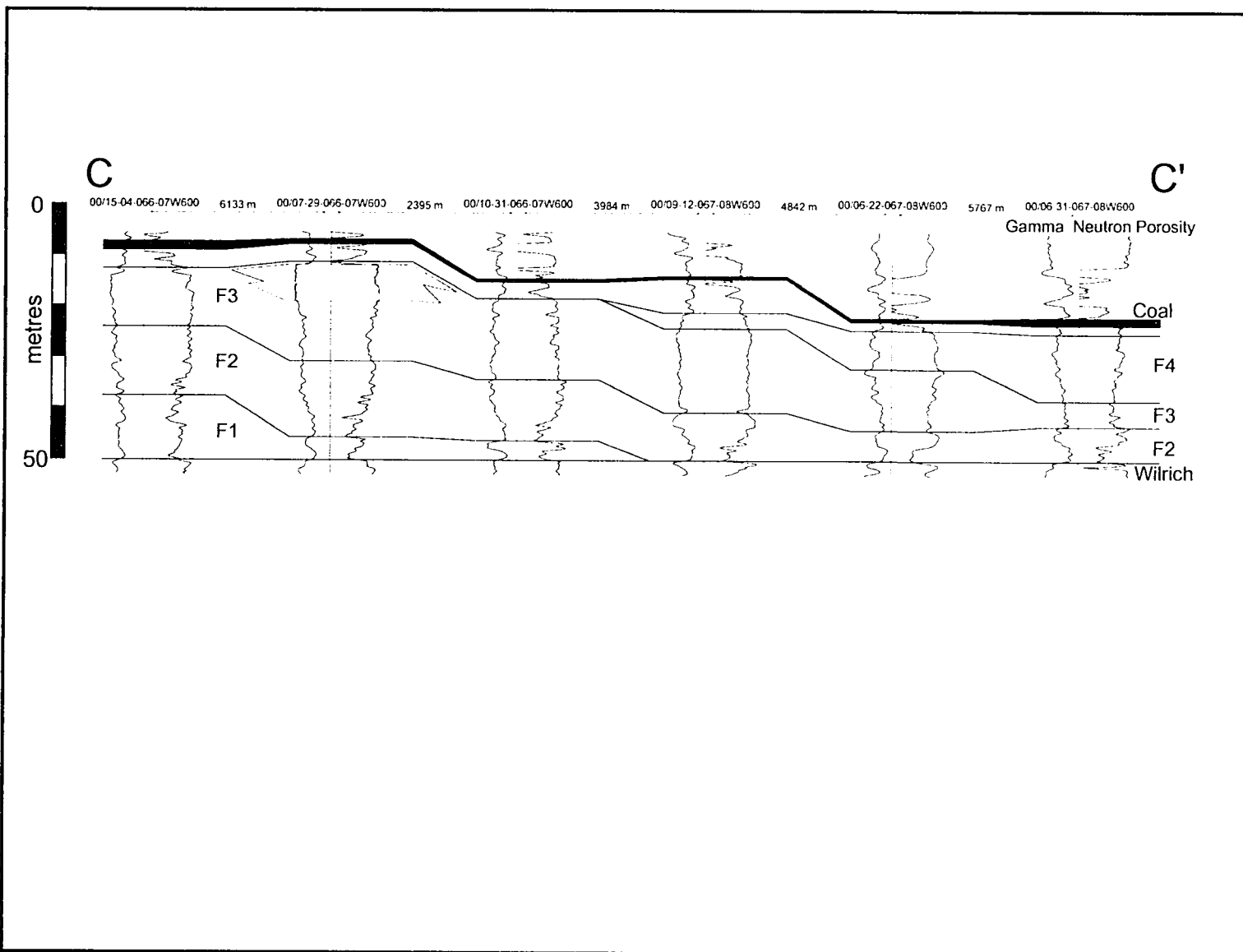
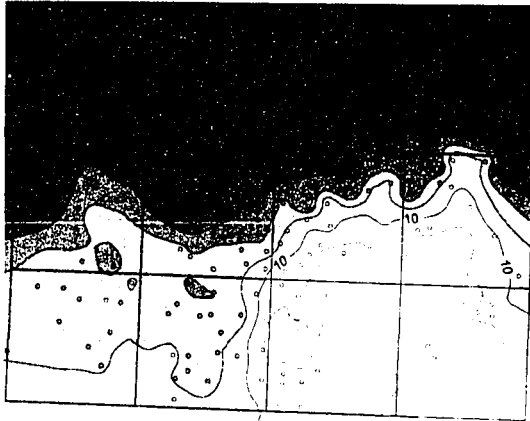
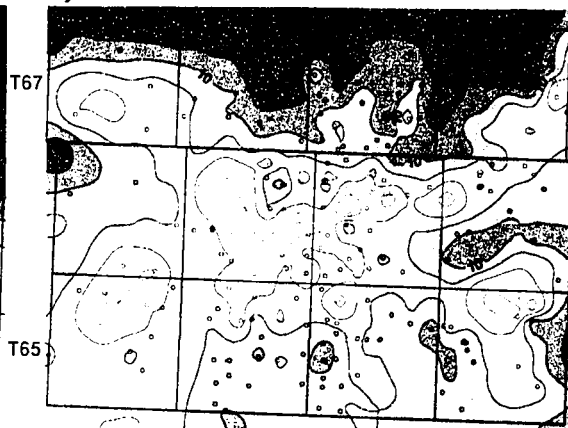


Figure 3.9: Isopach map of the four parasequences F1 (a), F2 (b), F3 (c) and F4 (d). Shifting depocenters towards the north indicates northward progradation of the Falher F shoreline. The thick linear trend in F3 parasequence (arrows; Fig. 3.9c) is due to differential compaction of the conglomerate body.

a)



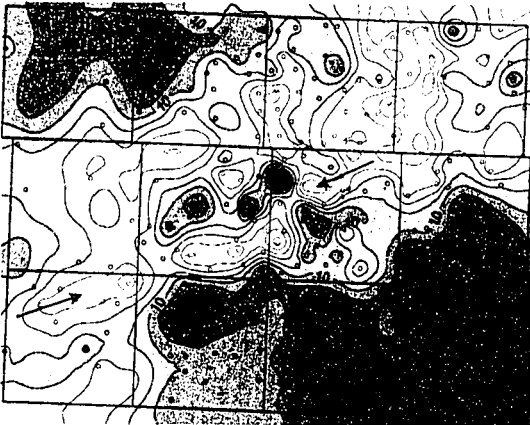
b)



c)

R9W6

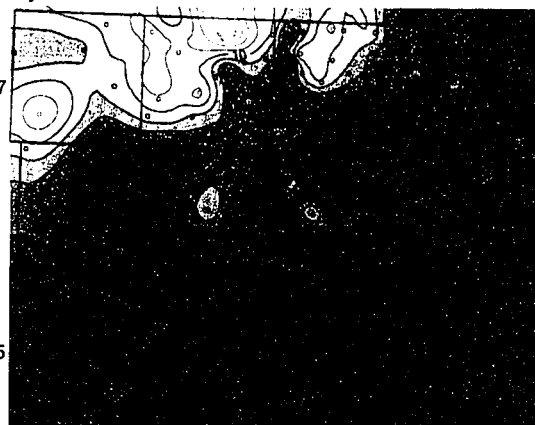
R6W6



d)

R9W6

R6W6



0 5 10
km

Contour Interval: 2m

○ Control Point

Isopach maps of the four parasequences show E-W trending shorelines with the locus of shoreline deposition shifting from the south to the north (Figs. 3.9a-d).

The Falher F conglomerate body is present only in the F3 parasequence. As with previous Falher studies, sequence stratigraphy has provided a stratigraphic context for the conglomerates. However, it has not explained why only F3 is conglomeratic and why an anomalously thick (10-12m) section of conglomerate formed in an environment where sediment input was dominantly sandy with some pebbles. For this reason additional detailed mapping was undertaken to identify additional controls on conglomerate deposition.

Mapping

Reservoir Mapping

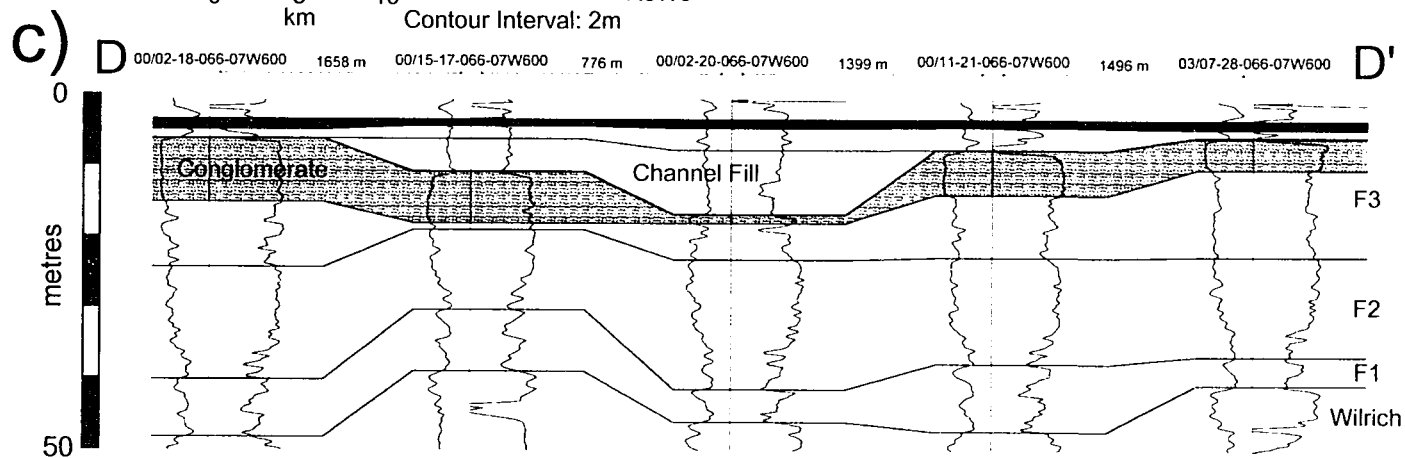
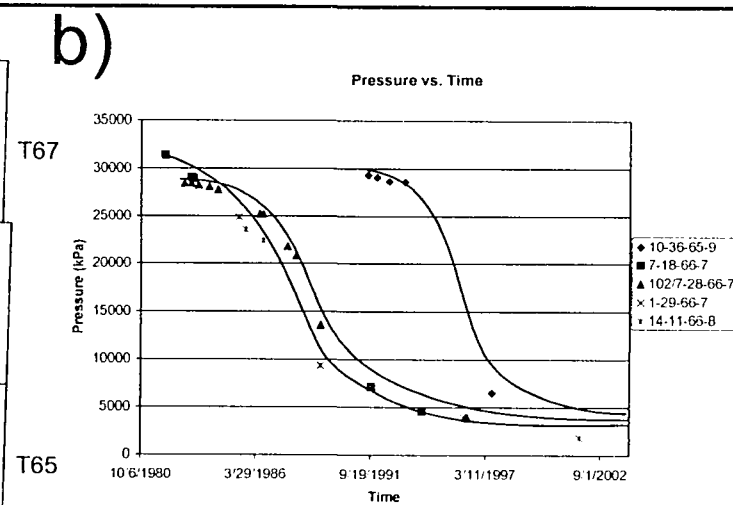
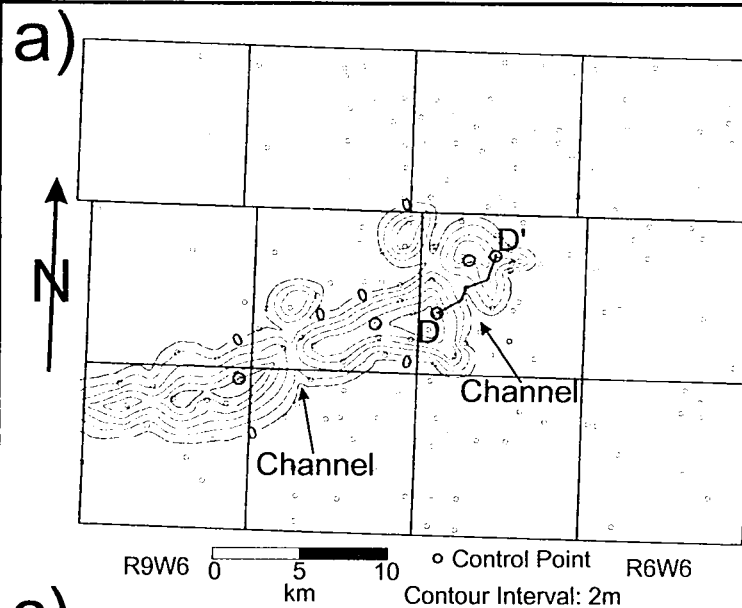
The net thickness of facies 4A and 4B conglomerate was derived from each well using direct core measurements where possible, or using log cutoffs derived from cored wells. In general a gamma ray volume-of-shale (Vshl) of less than 10% and a density-porosity of greater than 12% were used to identify these facies. These cutoffs were only used as guidelines for determining net conglomerate due to differential calibration of gamma ray and density-porosity logs by different logging companies and the abundance of wellbore washouts in the Wapiti Field area.

The Falher F conglomerate forms a linear body trending 65-245° that continues out of the study area to the southwest and ends abruptly to the northeast in a longshore direction (Fig. 3.10a). The trend has a maximum conglomerate thickness of 12 meters and is up to 4km wide. The size of the mapped conglomerate body was confirmed using a volumetric reserve calculation (Appendix 4). The conglomerate trend thins significantly at two places. North (seaward) of these two thin areas are two conglomerate lobes. Pressure data from the producing wells in the trend indicate three discrete reservoirs (Fig. 3.10b). Distinct pressure differences between the wells 10-36-65-9W6 and 1-8-66-8W6 and between the wells 2-18-66-7W6 and 7-28-66-7W6 define the approximate location of reservoir boundaries and correspond to the location of the two narrow breaks that cross the conglomerate trend.

The breaks defined by pressure data and suggested by the logs are interpreted to be channels that incised into the conglomerate trend. These channels may have been originally overwash channels during deposition of the conglomerate trend that were subsequently occupied by fluvial channels feeding sediment through the conglomerate trend onto the advancing shoreface. Overwash channels in gravel barriers are known to remain at one location through time unlike tidal channels on sandy barriers (Carter and Orford, 1981). Shale infill of these channels is interpreted as the likely cause of reservoir compartmentalization (Figs. 3.10b,c) within the conglomerate trend.

Isopach and Isochron Mapping

Figure 3.10: a) Map of net thickness of facies 4a and 4b conglomerate. Large circles indicate pressure control points used in Figure 10b. Note the thin NW-SE incised channel trends and 4 km width of conglomerate body (arrows). b) Pressure versus time plot for six productive wells in the trend. Note the three different pressure gradients indicating reservoir compartmentalization. This resulted from incision and shale infilling of the channels shown in Figure 10a. c) Strike-oriented cross-section (D-D') showing channel incision into the conglomerate body. The shaded area indicates the conglomerate. The location of the cross-section is indicated in Figure 3.10a.

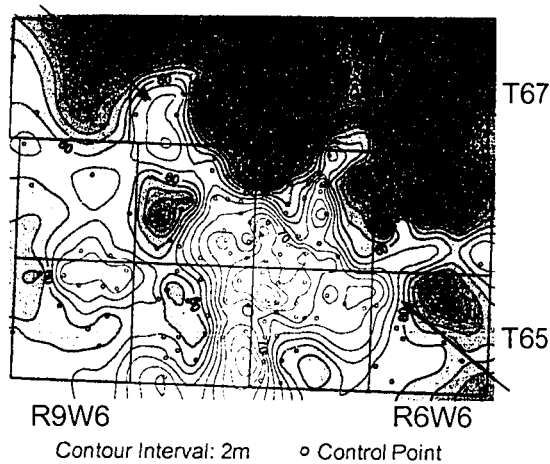


The possible effect of basement structures on Falher deposition was examined using various isopach and isochron maps of regional markers within the study area. Basement fault trends in the broader area that are known or suspected to have been active during the Cretaceous include NNE-SSW trending faults of the actively subsiding Peace River Arch (Cant, 1988; O'Connell, 1990) and NW-SE trending faults caused by tectonic flexure of the underlying crust during thrust loading (Hart and Plint, 1993b). Movement on these fault trends has been invoked to explain various depositional anomalies, including the location of incised Cardium shorelines (Hart and Plint, 1993b), stacking of multiple Falher shoreline trends (Cant, 1984; Leckie, 1986a) and the western limit of producing Falher wells (McLean, 1979).

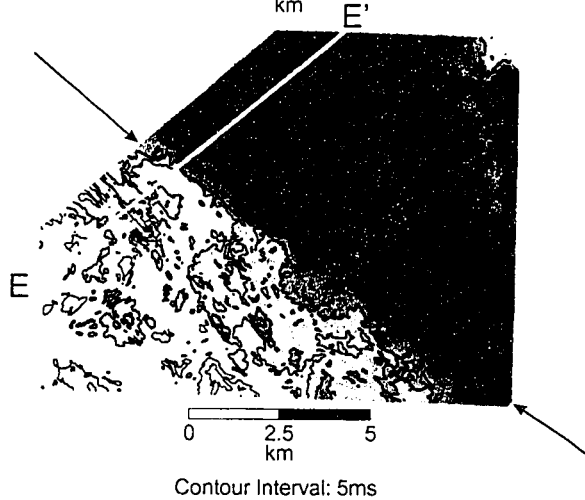
Both isopach and isochron maps show that there is an abrupt increase in thickness of the Falher F and overlying Falher E interval along a linear trend running NNW-SSE through the study area (Figs. 3.11a,b). Thickening of the Falher F interval suggests additional accommodation contemporaneous with the deposition of the Falher F parasequences. This linear accommodation trend is co-linear with a "bevel" trend in the Cardium that was interpreted by Hart and Plint (1993b) to have resulted from syn-depositional basement fault movement. Our data indicate that this basement feature was also active during Falher F time. In seismic data this trend appears to overly a flexural feature in the underlying Paleozoic and basement (Fig. 3.11c). The NW-SE structural feature corresponds to the abrupt northeastward truncation of the Falher F conglomerate trend, suggesting that it probably influenced deposition of the conglomerate.

Figure 3.11: a) Isopach of interval from Coal E to the top of the Wilrich Member. Note that the isopach thickens abruptly to the southwest along a NW-SE trend (arrows). b) Isochron of the interval from Coal E to the top of the Bluesky Formation. Note that the isochron changes abruptly along a NW-SE trend. These trends are thought to be related to basement fault movement. c) Seismic transect showing flexural deformation within the basement and Paleozoic rocks underlying the study area (arrows).

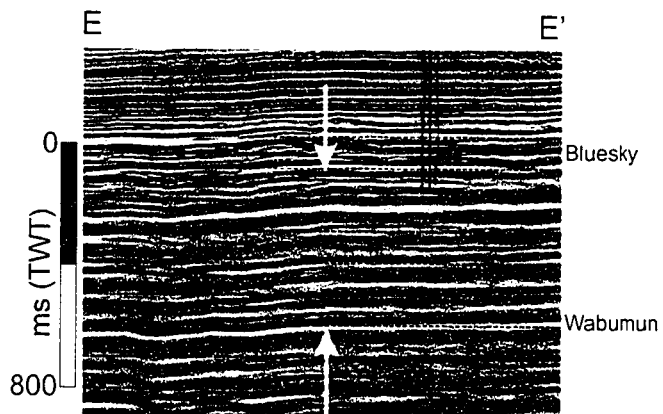
a)



b)



c)



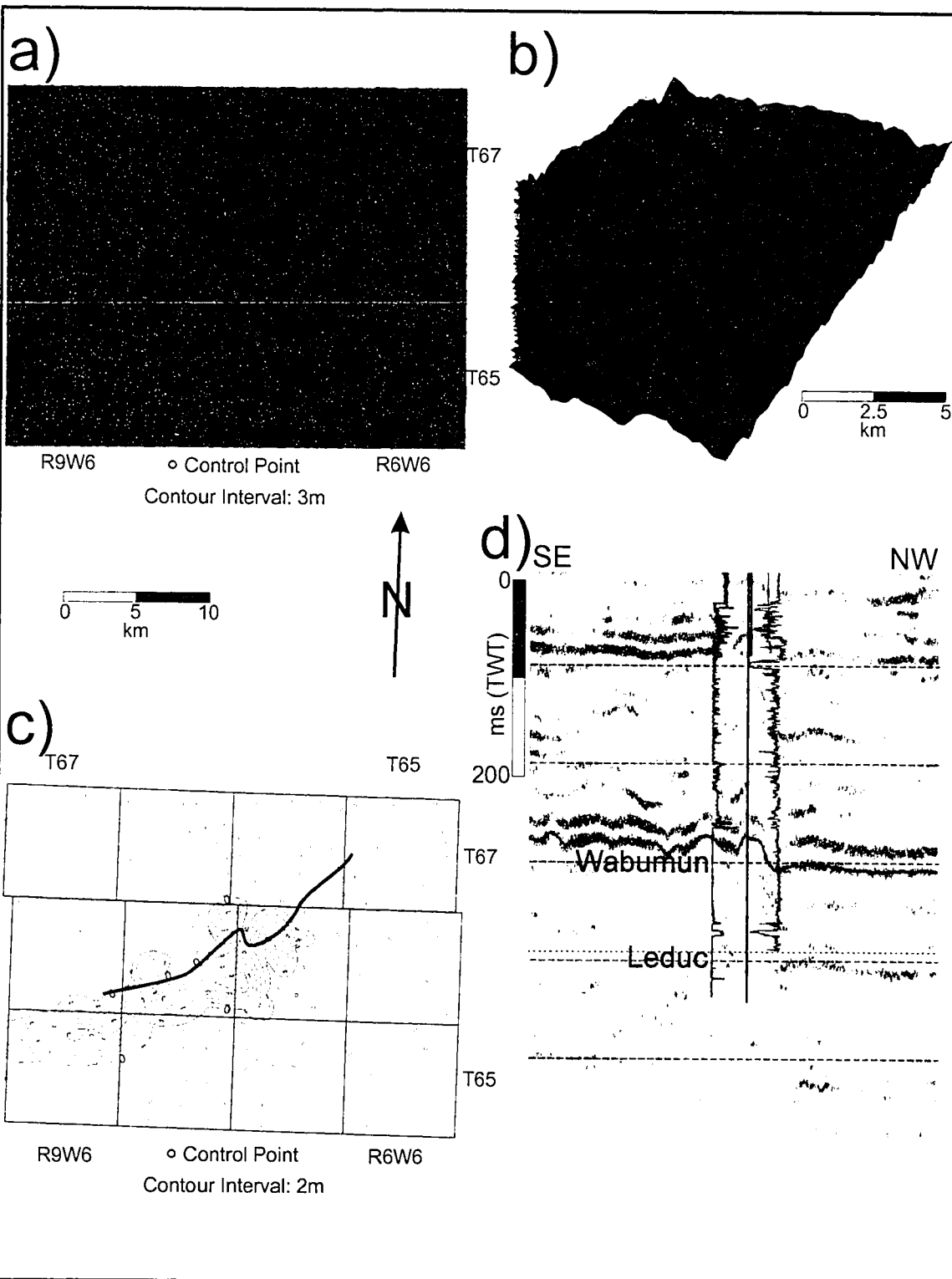
Structural Residual Mapping

Given the possible influence of deeper features on the deposition of the Falher F conglomerates, structural residual mapping was carried out on key regional surfaces in order to map subtle structural features within the study area. A planar surface, fitted to the structural data and approximating regional dip was generated and then removed from computer-contoured structure maps. This removes the over-printing of regional dip that obscures more subtle structural features. As a final step a planar surface dipping 0.1° towards the northwest (approximate depositional dip) was added to the structural residual map in order to image the topography as it may have looked during Falher F deposition.

A linear topographic step, approximately 30m in height and trending $65-245^{\circ}$ is present in the log-derived structural residual of the top of the Wilrich Member (Fig. 3.12a). This trend is co-linear with that of the F3 conglomerate trend (Fig. 3.10a). A similar linear trend is visible in the time-structural residual of the upper Devonian Wabumun horizon extracted from the 3-D seismic survey (Fig. 3.12b). This linear trend in the Wabumun corresponds to the northern edge the Gold Creek (Smoky) reef trend (Fig. 3.2) a rimmed carbonate buildup, formed during the upper Devonian.

We propose that this trend, which was present immediately prior to Falher F time is representative of the depositional topography across which the Falher F shorelines prograded. The edge of the underlying Gold Creek reef (1500m below the Falher F) trend caused the development of this linear topographic

Figure 3.12: a) Structural residual of Wilrich from well data (restored for depositional dip). Note NNW-SSE trending structural “step” running through the study area (arrows). b) Time-structural residual map of Wabumun horizon from seismic data showing linear reef-rim trend. Colour indicates dip curvature with positive dip curvature in red and negative dip curvature in blue (Roberts, 1998). c) Net conglomerate overlying Wabumun trend (line). Contours are net conglomerate. d) Dip-oriented seismic transect showing the Wabumun horizon and a well which intersected a thick buildup of carbonate in the Leduc and Wabumun. The well intersects the reef-rim. The reef flat is to the left and basinal shales are to the right.



feature. As discussed below we propose that the reef-induced topography influenced deposition of the Falher F conglomerate.

Discussion

Depositional Models for Falher F Conglomerates

Any depositional model generated for the Falher F must explain why only one parasequence is anomalously conglomeratic and why the deposition of this conglomerate is associated with the two deeply rooted structural trends within the study area. Core and well logs suggest that shoreface deposits of the F1, F2, and F4 shorelines are dominantly sandy with some pebbles (Fig. 3.6). Furthermore, the F3 parasequence is mostly sandy except for the 3.5 - 4km wide conglomerate trend. Arnott (1993) invoked the deposition of pebbly deltas to explain the anomalous buildup of conglomerate in the Falher D. We propose that the deposition of a series of pebbly deltas at a time when the F3 coastline overlay, and was parallel to, the northern edge of the Gold Creek reef trend is too coincidental. Instead we suggest that Falher F sediment input during parasequence F3 did not become increasingly pebbly but rather the particular basin configuration in the study area caused a concentration of pebbles along the reef-induced topographic trend.

Basin Configuration

Our mapping suggests that prior to deposition of the F3 parasequence, reef-induced topography and accommodation along a NW-SE trend resulted in a basin setup with three distinct topographic zones (Fig. 3.13). In the north-central portion of the study area there was a deep-water zone northwest of the reef-induced topographic step and on the down-thrown (southwest) side of the NW-SE striking structural hinge. In the south/southeast there was a region of shallow water on the updip portion of the reefal step but also on the down-thrown side of the structural hinge. Finally, in the east there was a shallow-water zone on the up-thrown side of the structural hinge. These three zones make up the pre-depositional topography that influenced the deposition of the Falher F parasequences.

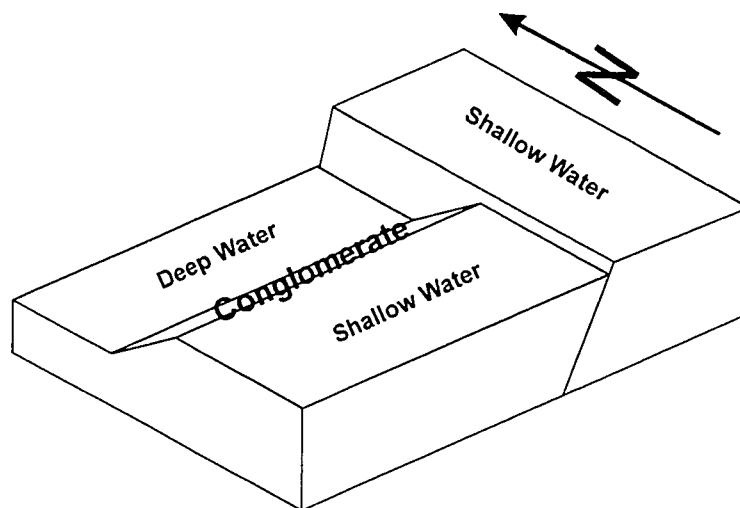
Geomorphologic Considerations

A brief review of two coastal geomorphological principles will be undertaken in order to fully support the reasoning behind our depositional models. They are the concepts of null point and dynamic equilibrium of a coastal profile.

Null Point Theory

The net shore-normal force imparted on a particle on the shoreface is the summation of swash and backwash wave forces and the gravitational force

Figure 3.13: Block diagram of pre-F3 depositional basin topography inferred from structural residual and isopach maps.



acting on the particle (King, 1972, Cowell et al., 1999). On the steep profile of the upper shoreface, gravitational and backwash forces exerted on a fine-grained sand particle will exceed swash forces and the particle will be transported seaward. Conversely, on a shallower slope, such as the lower shoreface, swash forces on a gravel-sized particle will exceed backwash and gravitational forces and the particle will move landward. Consequently, at a given point on the shoreface a clast of a given grain size will experience no net shore-normal force and will rest at that location (Fig. 3.14a). Shoreward directed gravelly dunes on the shoreface of Chesil Beach, England (Hart and Plint, 1989) provide evidence for shoreward-directed transport of gravels in a modern system.

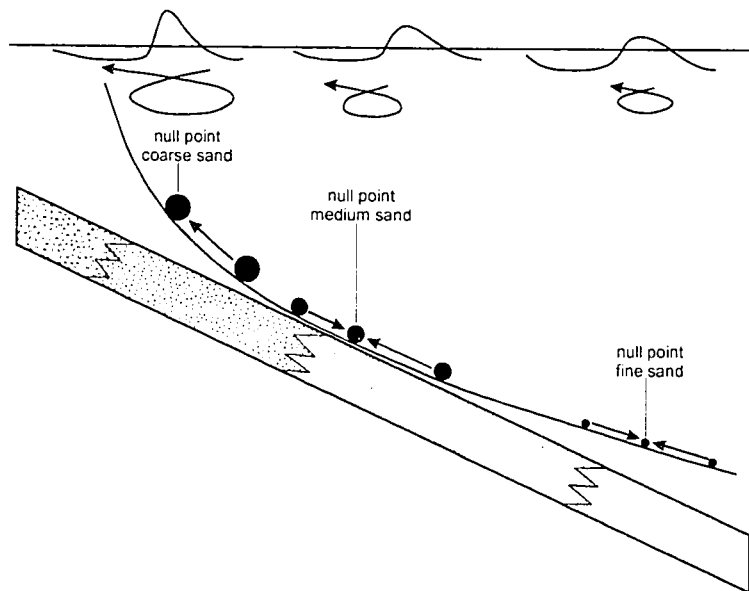
This phenomenon results in shore-normal sorting of grain sizes (Fig. 3.14a). On a coast with a steeper profile, swash energy is dissipated over a smaller area and the energy released is proportionally larger (King, 1972; Swift, 1975). This exaggerates the net imbalance of forces imparted on particles on the shoreface, thus enhancing the sorting process. Given the natural variability of wave heights, the null point of a particle will actually cover a range of depths and distances from shore. On a steeper coast the width of the null-point range of a given particle will be smaller, reducing the mixing of particle sizes and enhancing sorting.

Coastal Profile Equilibrium

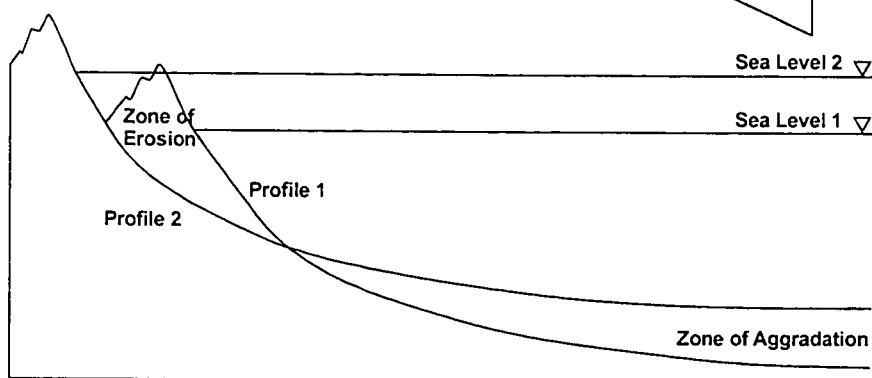
For given wave conditions, sediment size and volume of sediment input a shoreface seeks to develop a profile that is in equilibrium with these conditions

Figure 3.14: a) Null point theory. Wave force asymmetries force larger particles to the upper shoreface and smaller particle to the lower shoreface. Modified from Cowell et al. (1999). b) Landward translation of a shoreface during transgression. The invariant nature of the profile indicates that erosion will occur in the upper shoreface while aggradation will occur in the lower shoreface during transgression. Modified from Swift (1975). c) Seaward translation of a shoreface due to sediment input at the upper shoreface. The upper shoreface oversteepens becoming unstable. Sediment is driven from the upper to lower shoreface in an attempt to establish an equilibrium profile.

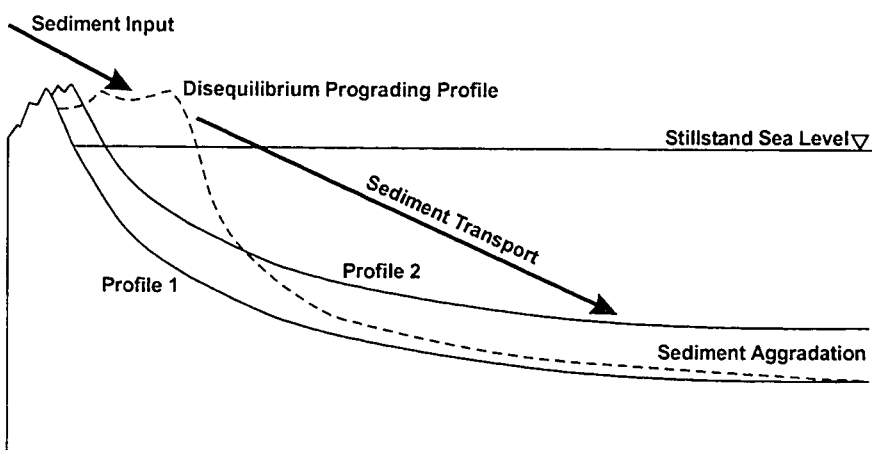
a)



b)



c)



(Swift, 1975; Cowell et al., 1999). High-energy coasts and fine-grained coasts have relatively shallow shoreface profiles whereas lower energy coasts and coarse-grained coasts have relatively steep profiles (King, 1972; Swift, 1975). Assuming that this profile remains invariant, a landward translation of shoreline (transgression) will result in erosion in the upper shoreface and foreshore and aggradation in the lower shoreface and offshore (Fig. 3.14b). Conversely as sediment is supplied to the upper shoreface of a prograding coast, shore-normal forces will transport sediment to the lower shoreface in order to maintain its equilibrium profile (Cowell et al., 1999) (Fig. 3.14c). Pilkey et al. (1993) pointed out that an abrupt change in bathymetry may seriously affect the ability of a shoreface to re-assert its equilibrium profile during progradation. To regain equilibrium, the shoreface must transport additional quantities of sediment in a shore-normal direction in order to eliminate the bathymetric irregularities.

As a shoreface works to re-establish its equilibrium profile, null-point principles and sediment supply dictate that larger particles will be driven to the upper shoreface and smaller particles will be driven to the lower shoreface and offshore.

These two coastal processes, acting together, are capable of creating a pebble accumulation well over 15m thick on the upper shoreface and foreshore . In coastal studies of the British Isles, waves were able to cause movement on pebbles at water depths of up to 9 meters (King, 1972) and modern pebbly beaches can be as much as four to six metres above mean sea level (Carter and Orford, 1981, 1984; Forbes and Taylor, 1987). Concentration of pebbles along

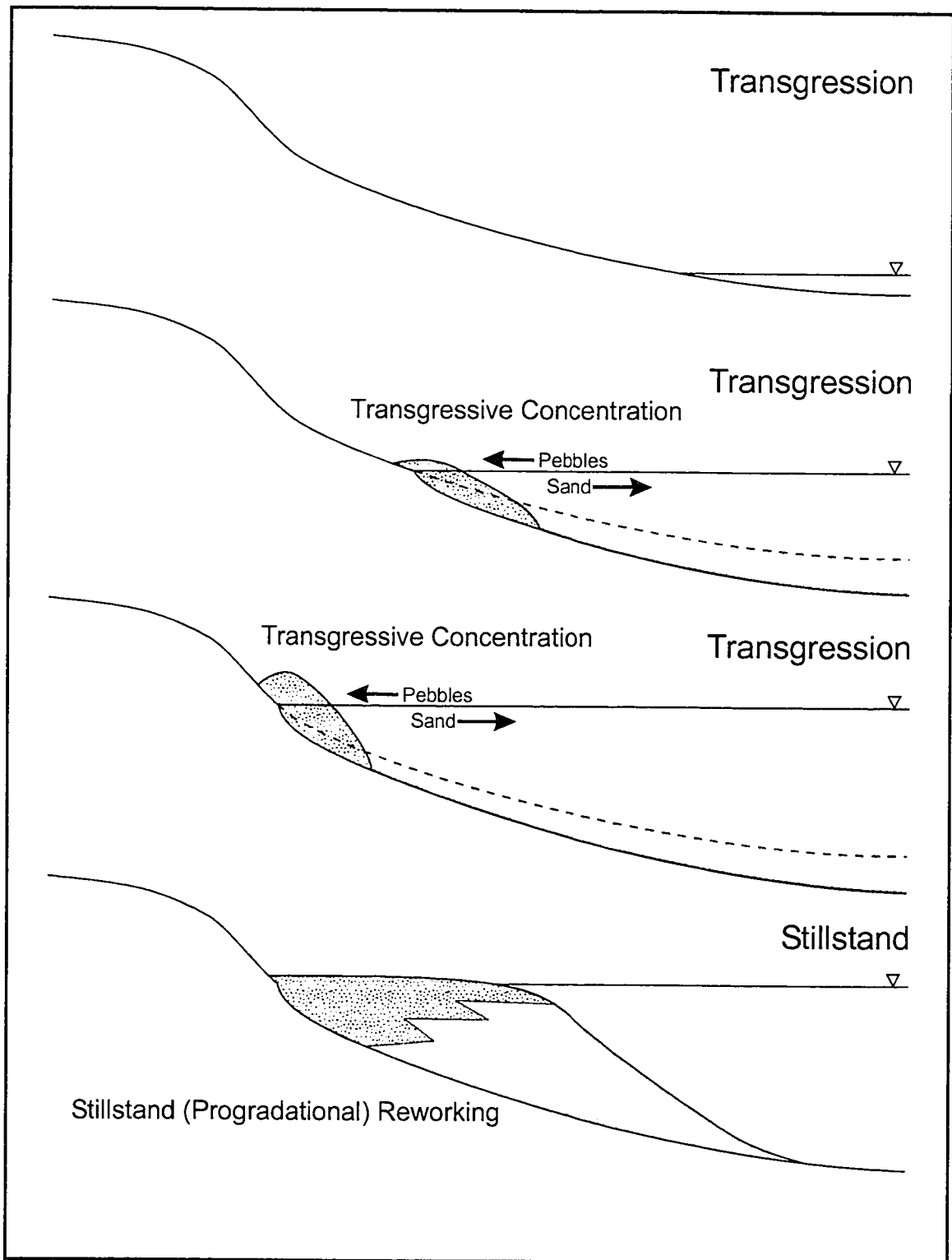
the reef-induced step could occur under transgressive or regressive conditions. These two possibilities are discussed below.

Transgressive Concentration

Cant (1995) suggested that linear Falher conglomerate bodies were deposited as transgressive barriers. This section describes the transgressive barrier depositional model and shows that it is incompatible with the evidence available for the Falher F conglomerate trend.

In the transgressive depositional model, transgressive ravinement during post-F2 relative sea-level rise eroded through the uppermost few meters of parasequence F2 (as suggested in cross-section; Fig. 3.6) and shore-normal sorting accumulated pebbles in the uppermost shoreface and foreshore. This movement generated a pebbly transgressive barrier while driving sand to the lower shoreface (Fig. 3.15). A similar model was proposed for the conglomerate trends in both the Falher A and B (Cant, 1995). The sorting process was enhanced in the deep-water zone of the study area where the shoreface profile was steeper (Fig. 3.13). Relative uplift in the northeast of the study area (Fig. 3.13) prevented pebbles from being transported longshore to that area. This pebbly barrier was then pushed landward (south) by rising relative sea level until it reached the linear reef-induced topographic step where its southward progress was stopped (Fig. 3.15). It should be noted that the absence of a transgressive surface of erosion at the base of the conglomerate body necessitates the

Figure 3.15: Transgressive model. Transgressive erosion and concentration of pebbles in the upper shoreface and foreshore creates a pebbly barrier. The barrier's landward (southward) progress is stopped by topography. Stillstand wave re-working of the barrier yields final "progradational" configuration of the conglomerate body.



placement of a transgressive erosion surface at the underlying F2/F3 contact. The presence of pebbles in the thin fining-upwards succession above F2 is consistent with this interpretation as they suggest that a pebbly shoreline was being eroded during transgression.

During the following (F3) highstand the deep portion of the basin was filled by sand sourced to the shoreface through the channels incised into the barrier. As the deep basin filled with sand, wave breakpoints shifted seaward drawing pebbles into a progradational configuration as a series of breakpoint bars (Fig. 3.15) (King, 1972).

Several practical and theoretical considerations appear to make the transgressive model unlikely. They are: 1) volumetric considerations; 2) observations of modern pebbly barriers and 3) practical considerations on the shifting breakpoint method of moving pebbles.

The F3 conglomerate body is made up of approximately 90% pebbles, and is 3.5 km wide and 5 m thick on average. In the transgressive model, the pebbles that make up the barrier were reworked exclusively from the underlying F2 parasequence. Assuming an approximate concentration of 20% pebbles in the sediments of the uppermost F2 parasequence and approximately 3m of transgressive erosion (Fig. 3.6), 26km of erosive transgression would have been required to account for the volume of pebbles in the F3 barrier. However, the F2 parasequence thins rapidly in the northern part of the study area, due to downlap of the shoreline sediments (well within 26km of the F3 conglomerate body) making this explanation unlikely. Longshore drift (from the southwest) may have

contributed pebbles, but we feel that this explanation only pushes the problem out of our study area without actually resolving the volumetric discrepancy.

A second volumetric discrepancy arises when considering the volume of the F2/F3 transgressive barrier that would be required at the end of transgression in order to account for the final size of the conglomerate body. If, prior to progradational re-configuration, all pebbles were accumulated into a 500m wide barrier (based on modern analogs; Forbes and Taylor, 1987) this barrier would have to be, on average, 35m thick in order to contain all of the pebbles required to create the final F3 conglomerate body. We consider this situation to be unachievable.

Observations of modern pebbly barriers on the East coast of Canada have shown that the composition of a barrier is very similar to the material across which it has transgressed (Forbes and Taylor, 1987). Shorelines transgressing pebbly drumlins resulted in pebbly barriers and transgressions through sandy-pebbly glaciofluvial sediments resulted in sandy-pebbly barriers. Uniformitarian principles suggest that a sandy barrier would have been produced as the transgressive F3 shoreline eroded through sandy material with some pebbles (as observed in core and logs; Fig. 3.6). Casas and Walker (1997) interpreted that sandy barriers were formed during transgressions of the Falher C and D.

Even if the obstacles listed above can be overcome the resulting pebble barrier would have to have been reworked into a progradational configuration as seen in core, logs and cross-section (Fig. 3.6). Seaward shifting wave breakpoints could create a pebbly breakpoint bar seaward of the transgressive

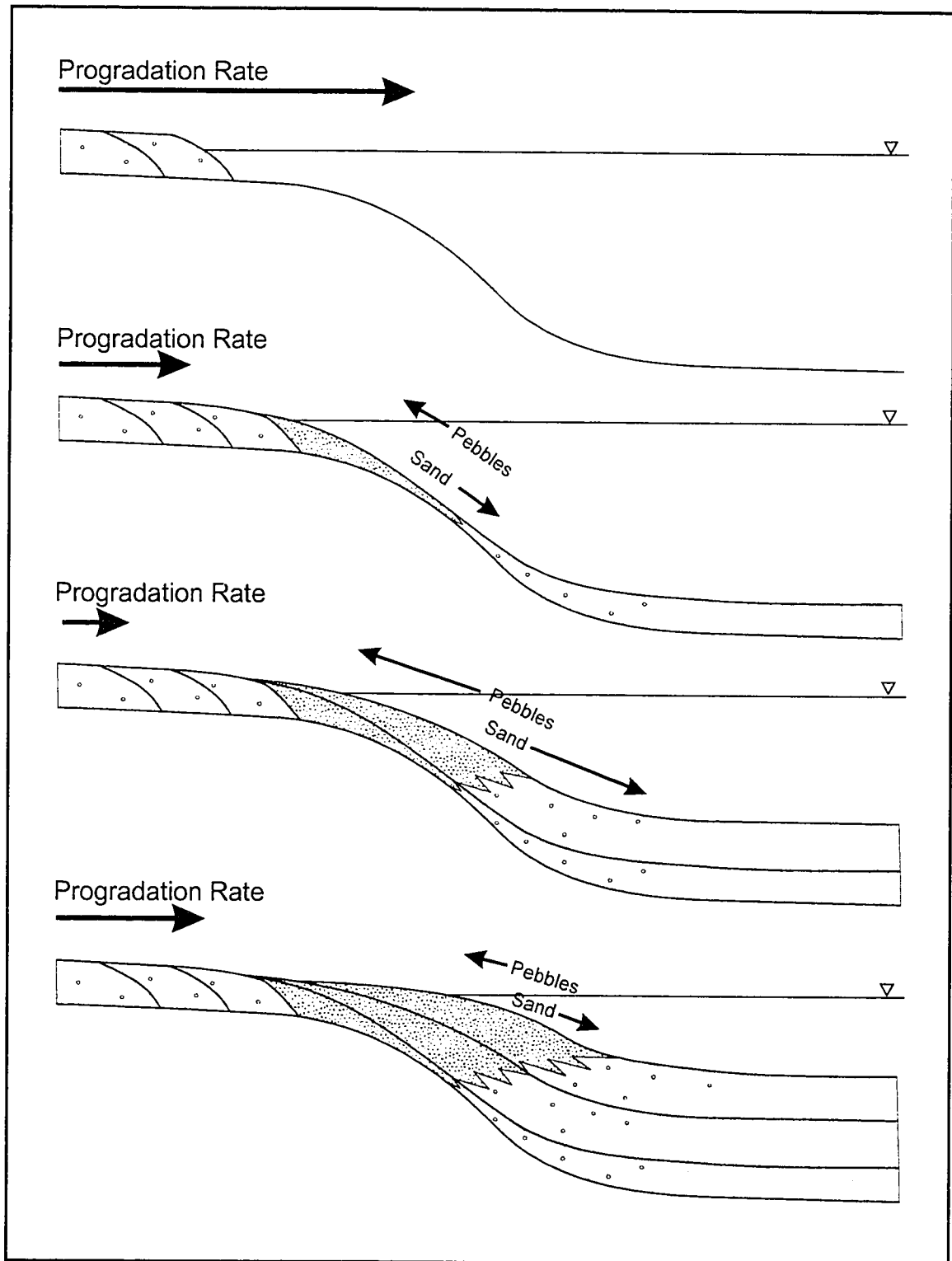
barrier. However, this initial bar would serve to protect the main barrier from further wave attack thus preventing further pebbles from being transported to the shoreface. Therefore only a small volume of pebbles could be moved by this method and will almost certainly not result in the 4 km wide accumulation of pebbles seen in the F3 parasequence.

Regressive Concentration

A more plausible possibility is that after transgression at the end of F2 time, progradation of the mixed sandy-pebbly F3 parasequence began from a highstand shoreline location south of the study area. Prograding sediments were mostly sandy foreshore and upper shoreface deposits due to the shallow water depth (e.g. core 6-32-65-7W6, Fig. 3.6a; Fig. 3.16). When the F3 shoreline arrived at the reef-induced step, progradation slowed down significantly due to the deeper water north of the step (Fig. 3.16). It is during this slowdown in progradation that pebbles accumulated along the F3 shoreline.

The taller sub-aqueous profile of the shoreface at the reef-induced step was no longer in equilibrium with normal Falher sediment input and wave energy. Given the dominantly sandy sediment input and high wave energies (Leckie and Walker, 1982), Falher shorelines would have been in equilibrium with relatively shallow slopes. Therefore during deposition of the F3 parasequence along the topographic step, normal shoreface processes worked to re-establish an equilibrium slope by driving fine-grained sediment from the upper shoreface to

Figure 3.16: Regressive model. Rapid sandy progradation is slowed by topography. Shore-normal sorting traps pebbles at the upper shoreface and foreshore while driving sand to lower shoreface. As the shoreface profile re-establishes equilibrium the progradation rate increases and the pebble concentration diminishes until sandy progradation resumes.



the lower shoreface (Fig. 3.14a) while pebbles and very coarse sands were concentrated on the uppermost shoreface and foreshore (Fig. 3.16). A thick package of sandstone, offshore from the pebble body (e.g. well 8-22-66-8W6, Fig. 3.6b; Fig. 3.8) suggests that such a mechanism was probably at work.

A large amount of sediment was required in order to fill the high accommodation region in the northwest portion of the study area and re-establish a Falher shoreface equilibrium slope. Assuming that the volume of sediment input did not change significantly through the deposition of the F3 parasequence, a significant amount of time would be required for the shoreface to re-establish equilibrium. This time allowed for the segregation and accumulation of a large amount of pebbles in the upper shoreface of the F3 parasequence. The concentration of pebbles in the upper shoreface and foreshore resulted in pebbles being transported to the lower shoreface via rip currents or avalanching (Hart and Plint, 1995, 2003; Arnott, 2002) (Fig. 3.6) resulting in the thin pebble beds observed in the lower shoreface of the F3 parasequence.

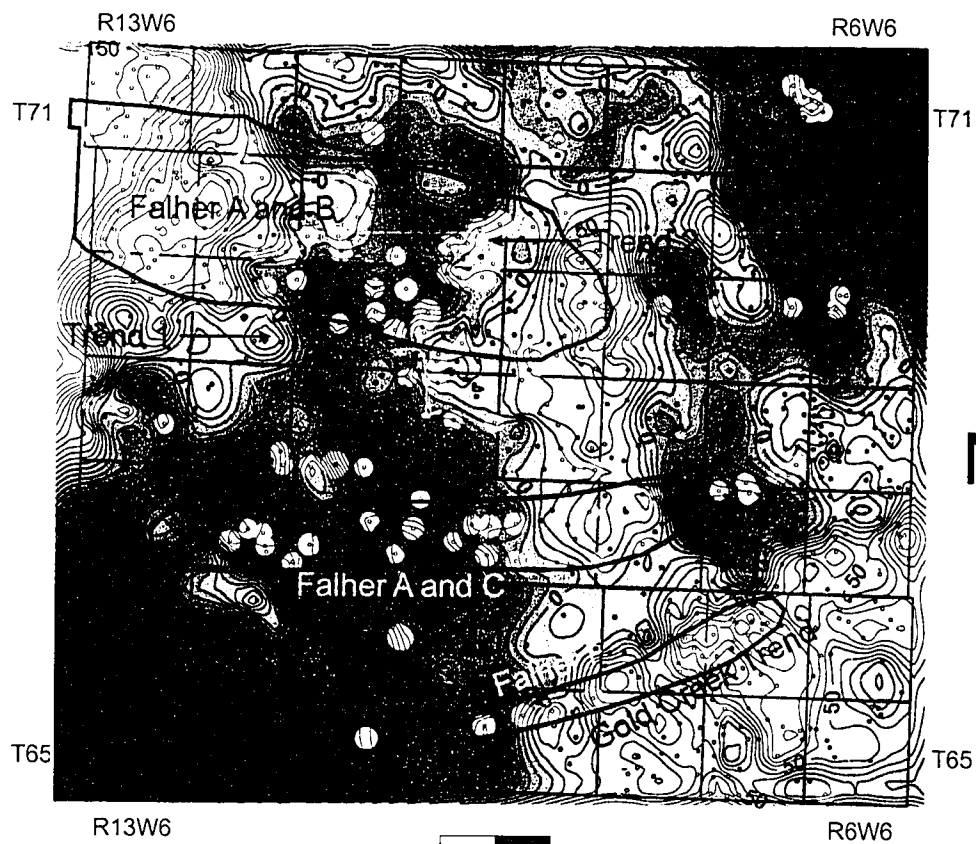
As the equilibrium profile of the F3 shoreline re-asserted itself the pebble concentrating effect was reduced through time until eventually the F3 parasequence continued to prograde as a dominantly sandy shoreline (Fig. 3.16). Arnott (1993) proposed that northward progradation of a Falher D conglomerate body was terminated by an abrupt sea-level drop resulting in a sequence boundary. We propose that a sequence boundary, similar to the one invoked by Arnott (1993), is not required in the Falher F.

Regional Applicability

The observed relationship between the location of the Falher F conglomerate and underlying structures led us to inquire as to whether similar relationships might be present for other linear conglomerate bodies. To that end structural residual maps were generated on the middle Cretaceous Base of Fish Scales zone marker over an area covering much of the Deep Basin (Figs. 3.3 and 3.17) and in the area of the upper Cretaceous Cardium conglomerate oil reservoirs at Carrot Creek (Figs. 3.4 and 3.18). Although the Base of Fish Scales marker overlies the Falher, it was felt that it could be used as a reasonable marker for imaging Falher topographic features in the Deep Basin (Fig. 3.1). This marker underlies the Cardium and so its use to define pre-Cardium tectonic controls is less ambiguous. Residual maps in both areas could be affected by post-depositional structural movements.

The linear trend of the edge of the Gold Creek reef is clearly visible underlying the trend of Falher F producers (used as proxy for conglomerate) on the structural residual map from the Deep Basin. Two other major Falher production trends exist in the mapped area. They are the vertical stacking of conglomeratic Falher A and C shorelines in Township 67 and the multiple conglomeratic Falher A and B shorelines in Townships 69 and 70. Although no obvious residual trends exist in Township 67 there are two faint E-W trending residual highs running through Townships 69 and 70 (Fig. 3.17).

Figure 3.17: Deep Basin base of Fish Scale zone structural residual map. Note the clear linear trend of Gold Creek reef underlying the Falher F production trend. No apparent linear trend exists below the Falher A and C production trend. Two faint linear trends are indicated below the Falher A and B production trend. Production bubbles as in Figure 3.3.



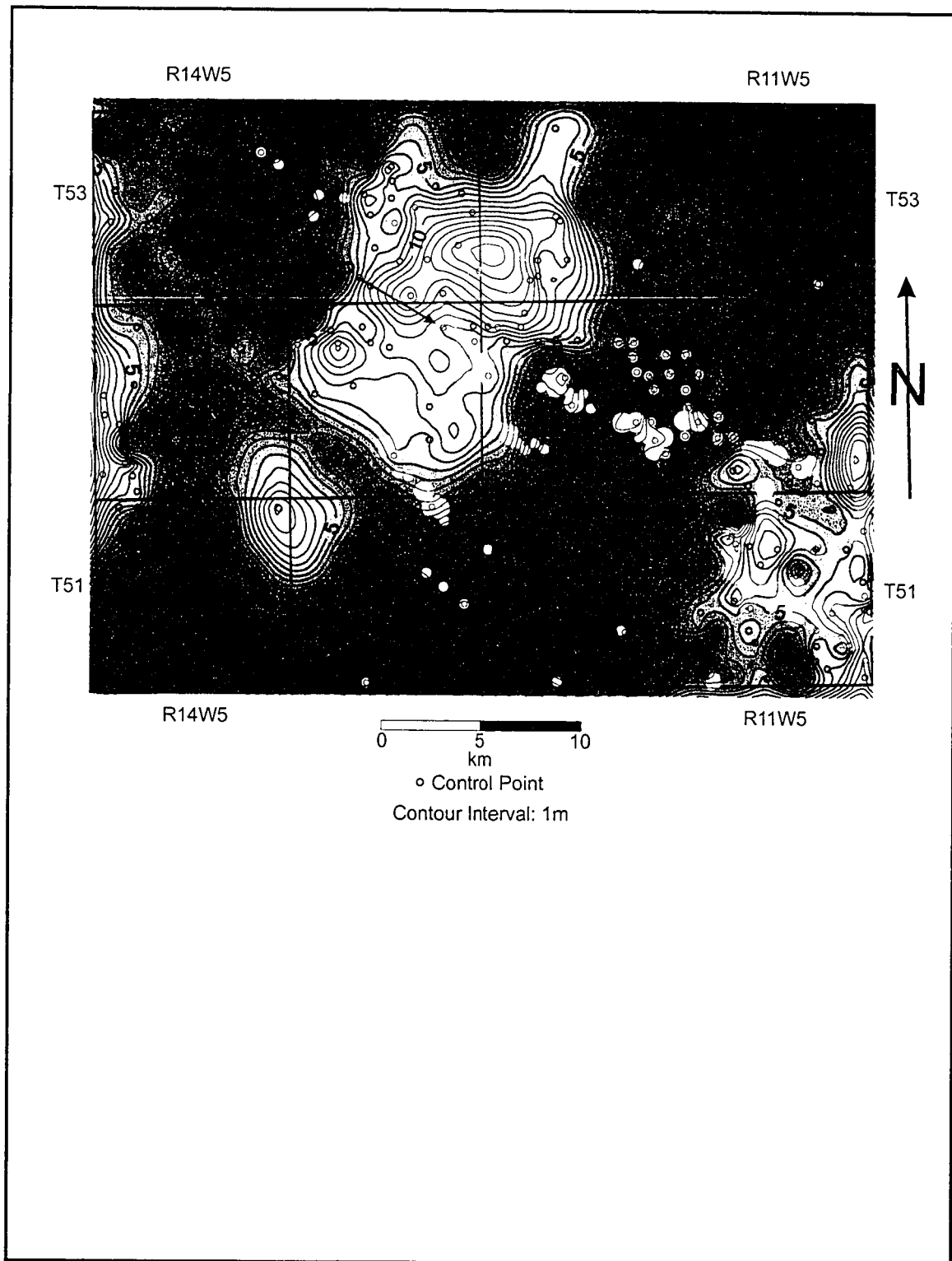
0 5 10
km
○ Control Point
Contour Interval: 10m

Stacking of conglomeratic Falher shorelines has previously been explained by structural control (Cant, 1984; Leckie, 1986a). Movement on normal faults, which made up the southern margin of the actively subsiding Peace River Arch (O'Connell, 1990), controlled the southern limit to transgressions and hence stacked multiple shorelines on top of one another. It is our assertion that not only did these faults control the geographic location of the Falher shorelines, but also controlled the lithologic make-up of the shorelines therefore stacking multiple productive, pebbly shorelines.

The exact pre-Falher topographic layout of the Deep Basin is difficult to image without more detailed mapping. Topographic features in the lower Cretaceous have been obscured due to the complex history of the PRA (O'Connell, 1990), an upper Devonian fringing reef surrounding the PRA (Fig. 3.2) and possible upper Cretaceous movement on NW-SE trending faults (Hart and Plint, 1993b). Detailed structural re-constructions of the lower Cretaceous will be required in order to define lower Cretaceous topography. This work was outside of the scope of this paper.

Two residual low features trending NW-SE are visible underlying two of the main Cardium conglomerate production trends on the structural residual map of the Carrot Creek field (Fig. 3.18). Previous studies suggested that the Cardium conglomerate bodies were deposited along shorelines during a lowstand in the upper Cretaceous (Bergman and Walker, 1987, Arnott, 1991). Stillstand erosion created topographic bevels, bumps and hollows along and into which the Carrot Creek conglomerates were deposited (Bergman and Walker, 1987). Pebbles

Figure 3.18: Carrot Creek base of Fish Scale zone structural residual map. Note the two linear low trends underlying two productive Cardium conglomerate trends. Production bubbles as in Figure 3.4.



were interpreted to be fluvially sourced and reworked into linear bodies by longshore drift (Bergman and Walker, 1987). It is our assertion that the location of these erosional stillstands was influenced by topography which existed during Cardium time. We propose that these linear topographic lows represented step features in Cardium time and that concentration of pebbles along these steps resulted in the Carrot Creek Cardium trends.

Although both the Deep Basin and Carrot Creek maps are suggestive of underlying structural controls detailed mapping, ideally using 3-D seismic data, will be necessary to fully test the hypotheses presented in this paper.

Conclusions

- 1) The Falher F conglomerate body forms a linear body, 2-12m thick and 3.5-4km wide that occurs in only one of four progradational, sandy Falher parasequences present in the Wapiti Field area.
- 2) Vertical lithologic successions through the conglomerate body suggest that it formed during progradation of the Falher shoreline as part of a continuous shoaling-up/drying-up succession.
- 3) Detailed mapping suggest that the longshore extent of the conglomerate body was controlled by syn-depositional accommodation development and that the geographical location of the linear conglomerate trend was probably topographically controlled.

- 4) Topography not only controlled geographic location of the linear conglomerate body but also influenced the lithologic composition of the rocks by enhancing shore-normal sorting processes.
- 5) Topographic control on the distribution of other linear shoreface conglomerate bodies is suggested by our preliminary mapping. Further work is required to test this hypothesis.

Acknowledgments

We wish to thank our collaborative partners who provided financial and/or technical support: EOG Resources Inc., BP Canada, Devon Energy Corporation and Talisman Energy Inc. who provided well log data as well as constructive discussions about our ideas. Millennium Seismic donated the 3-D seismic volume used in this study. We would also like to thank Ivan Marroquin for his assistance in interpreting the 3-D seismic volume, Bob Dalrymple, Bill Arnott, Mike Johnson, Dave O'Neill and Shona Ness for providing critical discussion and feedback. Mapping, cross-section construction and seismic interpretation were conducted using *GeoGraphix* software supplied by Landmark Graphics Corporation.

Chapter 4 Conclusions

The primary objective of this study was to explain the presence of a linear shoreface conglomerate body within a package of prograding sandy shorelines. To that end a sequence stratigraphic framework of the Falher F was developed and detailed mapping of key surfaces and intervals was undertaken. The results demonstrate that depositional relief associated with underlying structures may have played a significant role in the development of linear shoreface conglomerate bodies. In examples presented in this thesis, it appears that the relief was not caused by erosional stillstands but rather predate deposition of the conglomerates. Furthermore, it appears that topography not only controlled the location of a potentially conglomeratic shoreline but also influenced the lithology (i.e. pebbles content) of that shoreline.

Within the Western Canadian Sedimentary Basin (WCSB), conglomeratic reservoirs are among the most prolific hydrocarbon reservoirs. Their excellent reservoir qualities (high permeability and porosity) allow for high recovery factors in oil reservoirs and rapid extraction rates in natural gas reservoirs. However, these characteristics can also hamper reservoir pressure maintenance programs by serving as a conduit for flood fluids to pass easily from injection well to production well without flushing additional reserves from the reservoir. Therefore predictions of conglomerate distribution based on subsurface data can be useful as both an exploration and an exploitation tool.

Although this is not the first study to suggest that tectonically driven depositional relief controls the location of the Falher conglomeratic shorelines, it is the first to demonstrate the phenomenon in more than general terms. Past associations between topography and Falher conglomerates used vague references to basement faulting associated with the underlying Peace River Arch (Leckie, 1986a; Cant, 1995). This study maps out the location of the reef-induced topography and accommodation development associated with possible basement faulting and demonstrates a link between these features and the location of the Falher F conglomerate fairway.

Our introduction of coastal geomorphological principles into this study (not previously discussed in other linear conglomerate studies) has allowed for a thorough analysis of possible depositional processes that likely affected the Falher F shoreline as it prograded through the study area.

The techniques used in this study can be easily applied to exploration and exploitation efforts to predict the distribution of conglomeratic shorefaces in the subsurface. A broad understanding of tectonics affecting a basin will allow for a focusing of efforts towards regions with structural elements similar to those in the study areas presented. 3-D seismic can then be shot in order to get more detailed images of structural elements in the subsurface. The application of these techniques can reduce seismic budgets while enhancing the chances of drilling success.

Bibliography

- Armstrong, J. 1979. Regional considerations of the Elmworth field and the Deep Basin: Discussion. *Bulletin of Canadian Petroleum Geology*, v. 27, No. 4, p. 525-527.
- Arnott, R.W.C. 1991. The Carrot Creek "K" pool, Cardium Formation, Alberta: a conglomeratic reservoir related to a wave-reworked distributary mouth-bar complex. *Bulletin of Canadian Petroleum Geology*, v. 39, No. 1, p. 43-53.
- Arnott, R.W.C. 1993. Sedimentological and sequence stratigraphic model of the Falher "D" Pool, Lower Cretaceous, northwestern Alberta. *Bulletin of Canadian Petroleum Geology*, v. 41, no. 4, p. 453-463.
- Arnott, R.W.C. 2002. The role of fluid- and sediment-gravity flow processes during deposition of the (subsurface) Carrot Creek conglomerates (Cardium Formation, Upper Cretaceous), west-central Alberta. CSPG convention abstract, 7p.
- Benton, M.J. and Harper, D.A.T. 1997. *Basic Paleontology*. Addison Wesley Longman, Essex, England, 342p.
- Bergman, K.M. and Walker, R.G. 1987. The importance of sea-level fluctuations in the formation of linear conglomerate bodies; Carrot Creek member of the Cardium Formation, Cretaceous Western Interior Seaway, Alberta, Canada. *Journal of Sedimentary Petrology*, vol. 57, No. 4, p. 651-665.

- Caddel, E.M. 2000. Sedimentology and stratigraphy of the Falher C Member, Spirit River Formation, northeastern British Columbia. Unpublished M.Sc. thesis, University of Calgary, Calgary, Canada, 242p.
- Cant, D.J. 1983. Spirit River Formation – A stratigraphic-diagenetic gas trap in the Deep Basin of Alberta. The American Association of Petroleum Geologists Bulletin, v. 67, no. 4, p. 577-587.
- Cant, D.J. 1984. Development of shoreline-shelf sand bodies in a Cretaceous epeiric sea deposit. Journal of Sedimentary Petrology, v. 54, No. 2, p. 541-556.
- Cant, D.J. 1988. Regional structure and development of the Peace River Arch, Alberta: a Paleozoic failed-rift system? Bulletin of Canadian Petroleum Geology, v. 36, No. 3, p. 284-295.
- Cant, D.J. 1995. Sequence stratigraphic analysis of individual depositional successions: Effects of marine/nonmarine sediment partitioning and longitudinal sediment transport, Mannville Group, Alberta foreland basin, Canada. AAPG Bulletin, v. 79, No. 5, p. 749-762.
- Cant, D.J. and Ethier, V.G. 1984. Lithology-dependant diagenetic control of reservoir properties of conglomerates, Falher Member, Elmworth field, Alberta. AAPG Bulletin, v. 68, no. 8, p. 1044-1054.
- Carter, R.W.G. and Orford, J.D. 1981. Overwash processes along a gravel beach in South-East Ireland. Earth Surface Processes and Landforms, v. 6, p. 413-426.

- Carter, R.W.G. and Orford, J.D. 1984. Coarse clastic barrier beaches: a discussion of the distinctive dynamic and morphosedimentary characteristics. *Marine Geology*, v. 60, p. 377-389.
- Casas, J.E. and Walker, R.G. 1997. Sedimentology and depositional history of Units C and D of the Falher Member, Spirit River Formation, west-central Alberta. *Bulletin of Canadian Petroleum Geology*, v. 45, no. 2, p. 218-238.
- Cowell, P.J., Hanslow, D.J., and Meleo, J.F. 1999. The shoreface. *In*: Short, A.D. (ed.), *Handbook of Beach and Shoreface Morphodynamics*. John Wiley and Sons, Toronto, 379p.
- Demarest, J.M. and Kraft, J.C. 1987. Stratigraphic record of Quaternary sea levels: Implications for more ancient strata. *In*: Nummedal, D., Pilkey, O.H. and Howard, J.D. (eds.), *Sea level fluctuation and coastal evolution: SEPM Special Publication 41*, p. 223-239.
- Ekdale, A.A., Bromley, R.G., and Pemberton, S.G. 1984. Ichnology – The use of trace fossils in sedimentology and stratigraphy. *Society of Economic Paleontologists and Mineralogists*, Tulsa, 317p.
- Forbes, D.L. and Taylor, R.B. 1987. Coarse-grained beach sedimentation under paraglacial conditions, Canadian Atlantic coast. *In*: Fitzgerald, D. and Rosen, P. (eds.), *Glaciated coasts*. Academic Press, New York, 364p.
- Hart, B.S. and Plint, A.G. 1989. Gravelly shoreface deposits: a comparison of modern and ancient facies sequences. *Sedimentology*, v. 36, p. 551-557.
- Hart, B.S. and Plint, A.G. 1993a. Origin of an erosion surface in shoreface sandstones of the Kakwa Member (Upper Cretaceous Cardium Formation,

- Canada): importance for reconstruction of stratal geometry and depositional history. *In*: Posamentier, H.W., Summerhayes, C.P., Haq, B.U. and Allen, G.P. (eds.), Sequence stratigraphy and facies associations. Special Publication, International Association of Sedimentologists, v. 18, p. 451-467.
- Hart, B.S. and Plint, A.G. 1993b. Tectonic influence on deposition and erosion in a ramp setting: Upper Cretaceous Cardium Formation, Alberta foreland basin. AAPG Bulletin, v. 77, No. 12, p. 2092-2107.
- Hart, B.S. and Plint, A.G. 1995. Gravelly shoreface and beachface deposits. *In*: Plint, A.G. (ed.) Sedimentary facies analysis; a tribute to the research and teaching of Harold G. Reading. Special Publications of the International Association of Sedimentologists, v. 22, p. 75-99.
- Hart, B.S. and Plint, A.G. 2003. Stratigraphy and reservoir character of shoreface conglomerates: insights from exposures of the Cardium Formation. Bulletin of Canadian Petroleum Geology. V. 51, No. 4, p. 437-464.
- Jackson, P.C. 1984. Paleogeography of the Lower Cretaceous Mannville Group of western Canada. *In*: Masters, J.A. (Ed.), Elsworth – Case study of a deep basin gas field. American Association of Petroleum Geologists, Memoir, No. 38, p. 49-78.
- Kamola, D.L. and Van Wagoner, J.C. 1995. Stratigraphy and facies architecture of parasequences with examples from the Spring Canyon member, Blackhawk Formation, Utah. *In*: Van Wagoner, J.C. and Bertram, G.T. (Eds.), Sequence stratigraphy of foreland basin deposits – Outcrop and subsurface

examples from the Cretaceous of North America. AAPG Memoir, No. 64, p. 27-54.

King, C.A.M. 1972. Beaches and Coasts. Second Edition. Edward Arnold, London, 570p.

Kleinspehn, K.L., Steel, R.J., Johannessen, E. and Netland, A. 1984.

Conglomeratic fan-delta sequences, Late Carboniferous – Early Permian, western Spitsbergen. *In*: Koster, E.H. and Steel, R.J. (Eds.), Sedimentology of Gravels and Conglomerates. Canadian Society of Petroleum Geologists, Memoir 10 (1984), p. 279-294.

Leckie, D.A. 1986a. Rates, Controls and sand-body geometries of transgressive-regressive cycles: Cretaceous Moosebar and Gates Formations, British Columbia. AAPG Bulletin, v. 70, No. 5, p. 516-535.

Leckie, D.A. 1986b. Petrology and tectonic significance of Gates Formation (early, Cretaceous) sediments in northeast British Columbia. Canadian Journal of Earth Science, v. 23, p. 129-141.

Leckie, D.A. and Walker, R.G. 1982. Storm- and tide-dominated shorelines in Cretaceous Moosebar – Lower Gates interval – outcrop equivalents of Deep Basin gas trap in western Canada. American Association of Petroleum Geologists, Bulletin, v. 66, p. 138-157.

Massari, F. and Parea, G.C. 1988. Progradational gravel beach sequences in a moderate- to high-energy, microtidal marine environment. Sedimentology, v. 35, p. 881-913.

- Masters, J.A. 1984. Lower Cretaceous oil and gas in Western Canada. *In*: Masters, J.A. (Ed.), Elmworth – Case study of a deep basin gas field. American Association of Petroleum Geologists, Memoir, No. 38, p. 1-33.
- McLean, R.J. 1979. Regional considerations of the Elmworth field and the Deep Basin. *Bulletin of Canadian Petroleum Geology*, v. 27, No. 1, p. 53-62.
- Miall, A.D. 2000. Principles of sedimentary basin analysis, 3rd Edition. Springer-Verlag, Berlin Heidelberg, 616p.
- Moore, P.F. 1989. Devonian geohistory of the western interior of Canada. *In*: McMillan, N.J., Embry, A.F. and Glass, D.J. (Eds.), Devonian of the world (vol. I). Canadian Society of Petroleum Geologists, Calgary, p. 67-83.
- O'Connell, S.C., Dix, G.R. and Barclay, J.E. 1990. The origin, history, and regional structural development of the Peace River Arch, Western Canada. *Bulletin of Canadian Petroleum Geology*, v. 38A, p. 4-24.
- Pemberton, S.G., Spila, M., Pulham, A.J., Saunders, T., MacEachern, J.A., Robbins, D. and Sinclair, I.K. 2001. Ichnology and sedimentology of shallow to marginal marine systems. Ben Nevis and Avalon reservoirs, Jeanne d'Arc basin. *Geological Association of Canada Short Course Notes*, v. 15, 343p.
- Pilkey, O.H., Young, R.S., Riggs, S.R., Smith, A.W.S., Wu, H. and Pilkey, W.D. 1993. The concept of shoreface profile of equilibrium: a critical review. *Journal of Coastal Research*, v. 9, No. 1, p. 255-278.
- Rahmani, R.A. 1984. Facies control of gas trapping, Lower Cretaceous Falher A cycle, Elmworth area, northwestern Alberta. *In*: Masters, J.A. (Ed.), Elmworth

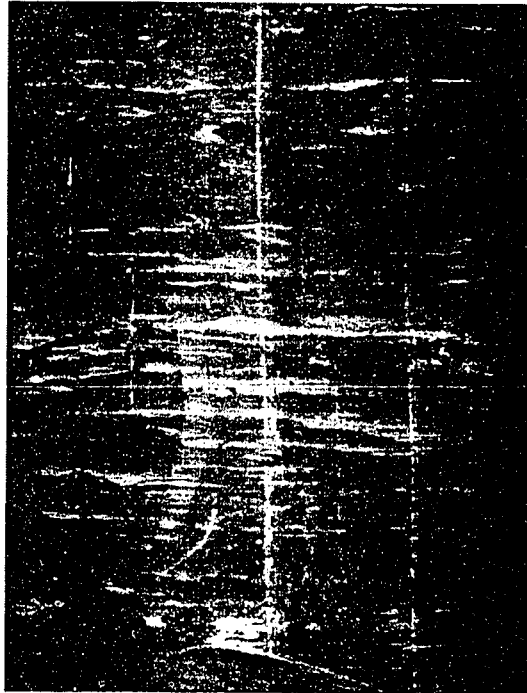
- Case study of a deep basin gas field. American Association of Petroleum Geologists, Memoir, No. 38, p. 141-152.
- Retallack, G.J. 1990. Soils of the Past. Unwin Hyman, Boston, 520p.
- Roberts, A., 1998. Curvature analysis: 'new' attributes for the delineation of faults, map lineaments and surface shape. American Association of Petroleum Geologists, Convention Program with Abstracts (CD-ROM), Salt Lake City, May 17-28.
- Rouble, R., and Walker, R.G. 1997. Sedimentology, high-resolution allostratigraphy, and key stratigraphic surfaces in Falher members A and B, Spirit River Formation, West-central Alberta. *In*: Pemberton, S.G., and James, D.P. (Eds.), Petroleum geology of the Cretaceous Mannville group, Western Canada. Canadian Society of Petroleum Geologists, Memoir 18, p. 1-29.
- Smith, D.G., Zorn, C.E., Stoessinger, W. and Radke, M. 1984. The paleogeography of the Lower Cretaceous of western Alberta and northeastern British Columbia in and adjacent to the Deep Basin of the Elmworth area. *In*: Masters, J.A. (Ed.), Elmworth – Case study of a deep basin gas field. American Association of Petroleum Geologists, Memoir, No. 38, p. 79-114.
- Stephenson, E.A. 1968. Estimation of natural gas reserves. *In*: Beebe, W.B. and Curtis, B.F. (Eds.), Natural gases of North America. American Association of Petroleum Geologists, Memoir, No. 9, p. 2046-2103.
- Swift, D.J.P. 1975. Barrier-island genesis: Evidence from the central Atlantic Shelf, Eastern U.S.A. Sedimentary Geology, v. 14, p. 1-43.

- Swinchatt, J.P. 1967. Formation of large-scale cross-bedding in a carbonate unit. *Sedimentology*, v. 8, No. 2, p. 93-120.
- Van Wagoner, J.C., Mitchum, R.M., Campion, K.M. and Rahmanian, V.D. 1990. Siliciclastic sequence stratigraphy in well logs, cores, and outcrops: concepts for high-resolution correlation of time and facies. *AAPG Methods in Exploration Series*, v. 7, 55p.
- Wadsworth, J., Boyd, R., Diessel, C. and Leckie, D. 2003. Stratigraphic style of coal and non-marine strata in a high accommodation setting: Falher Member and Gates Formation (Lower Cretaceous), western Canada. *Bulletin of Canadian Petroleum Geology*, v. 51, No. 3, p. 275-303.
- Walker, R.G. and Plint, A.G. 1992. Wave- and Storm-dominated shallow marine systems. *In*: Walker, R.G. and James, N.P. (Eds.), *Facies models – Response to sea level change*. Geological Association of Canada, St. John's, p. 219-238.

Appendices

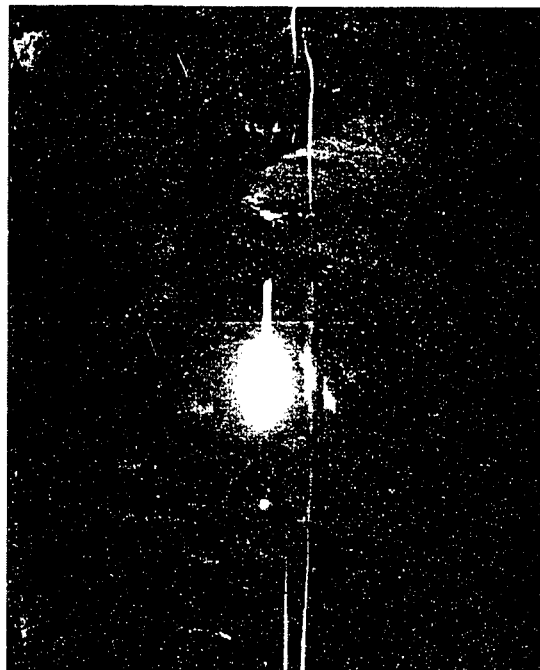
Appendix 1: Representative photographs of lithofacies discussed in Chapter 2.

Refer to text for further discussion of sedimentological features in each facies.



10
cm 5
0

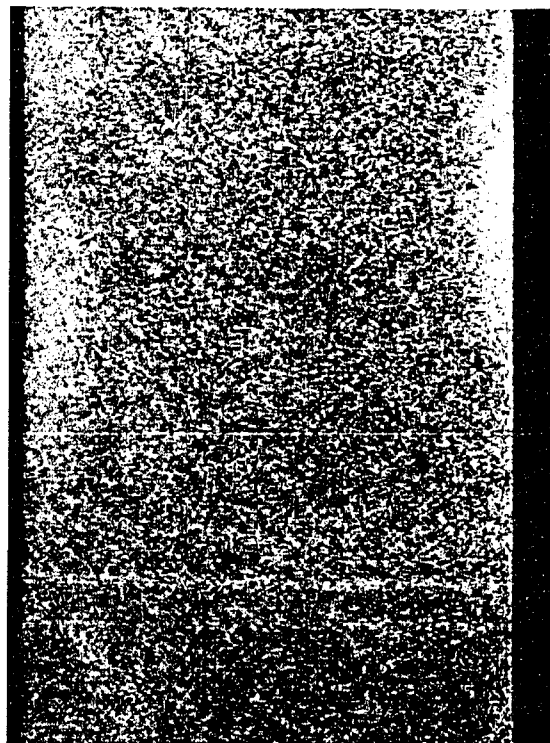
2393m, core 7-27-66-7W6



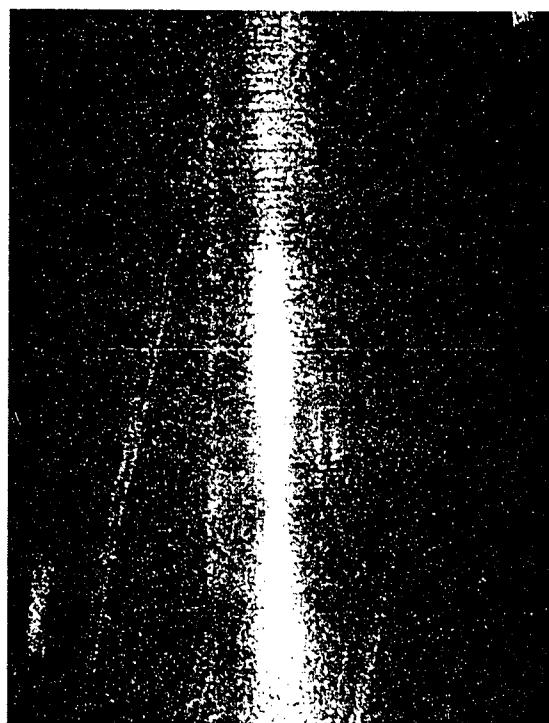
2912m, core 5-32-65-9W6

Facies 1: Sandy mudstones

10
cm
5
0



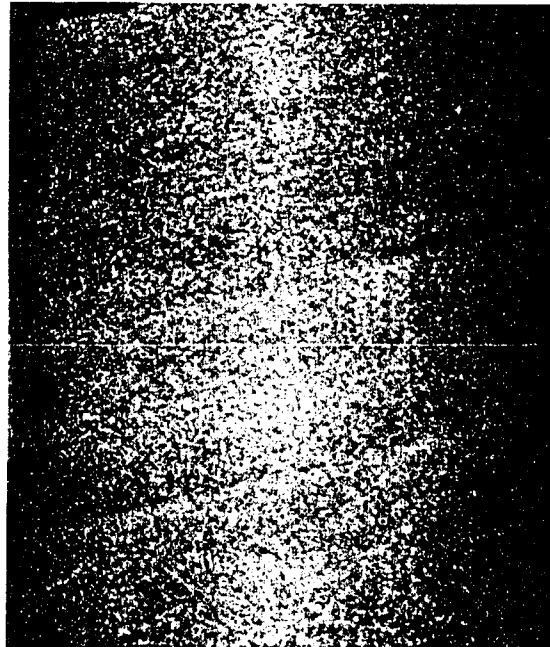
2214m, core 2-32-66-6W6



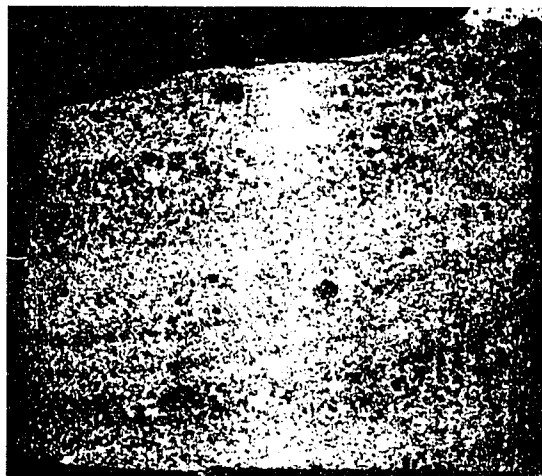
2739m, core 3-33-65-9W6

Facies 2: HCS sandstone

cm
10
5
0

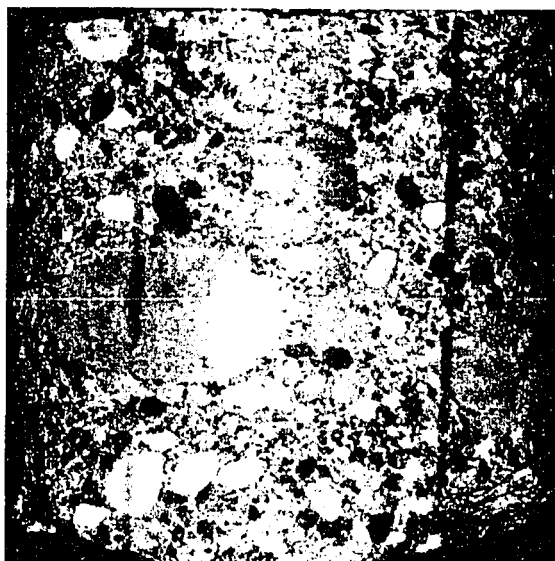


2744m, core 3-33-65-9W6



2904m, core 5-32-65-9W6

Facies 3: Cross-bedded sandstones



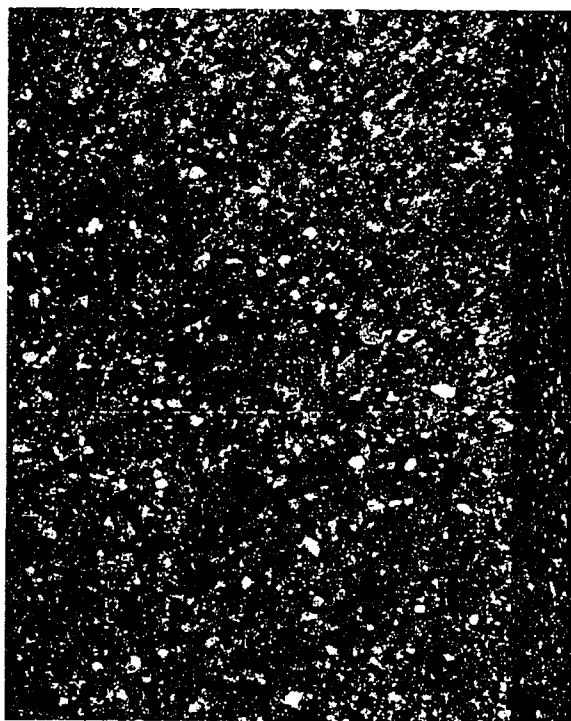
10
cm 5
0

2730m, core 3-33-65-9W6



2642m, core 13-27-65-9W6

Facies 4a: Poorly-sorted conglomerate



10
cm — 5
0

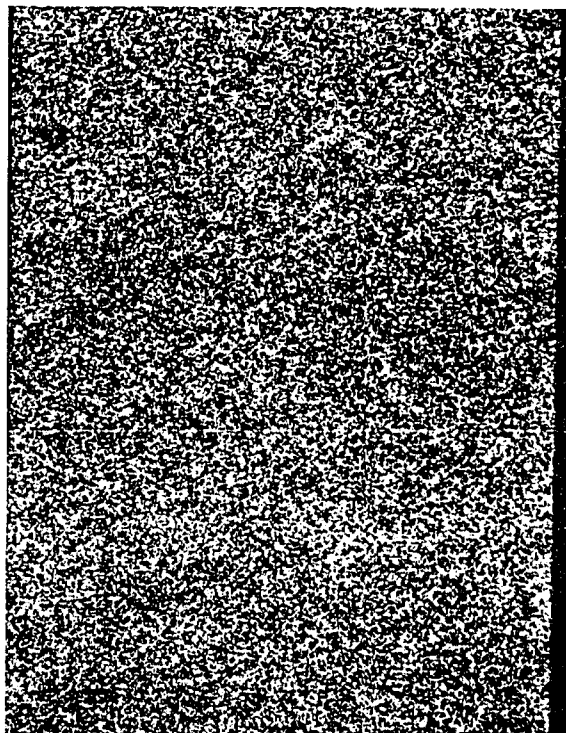
2637m, core 13-27-65-9W6



2639m, core 13-27-65-9W6

Facies 4b: Well-sorted conglomerate

10
cm 5
0



2466m, core 2-8-66-7W6



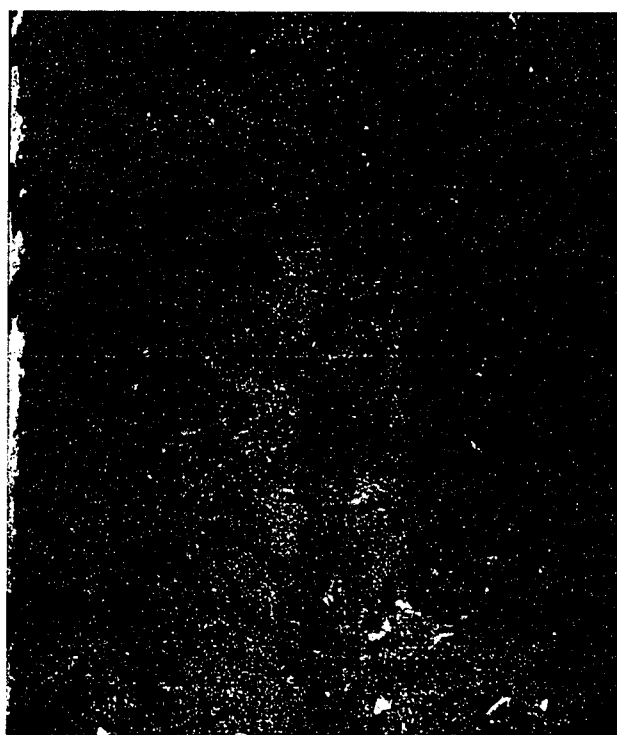
2201m, core 2-32-66-6W6

Facies 5: Planar bedded sandstones

10
cm 5
0

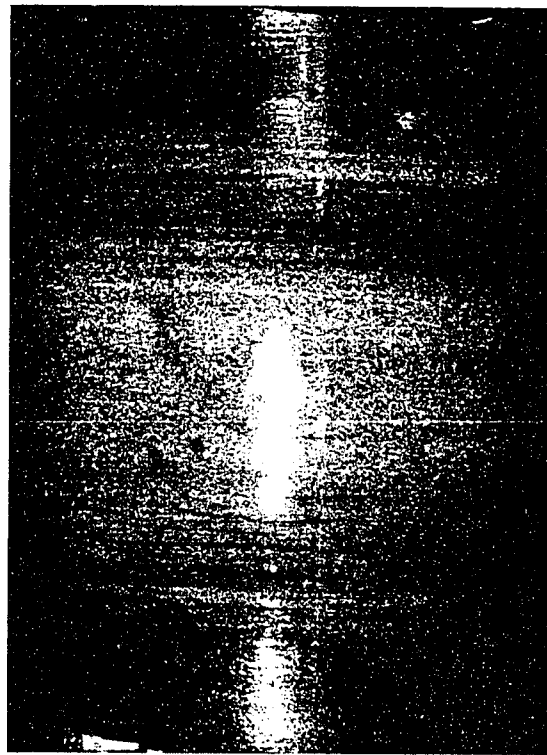


2622m, core 6-32-65-7W6



2622.5m, core 6-32-65-7W6

Facies 6: Carbonaceous mudstones



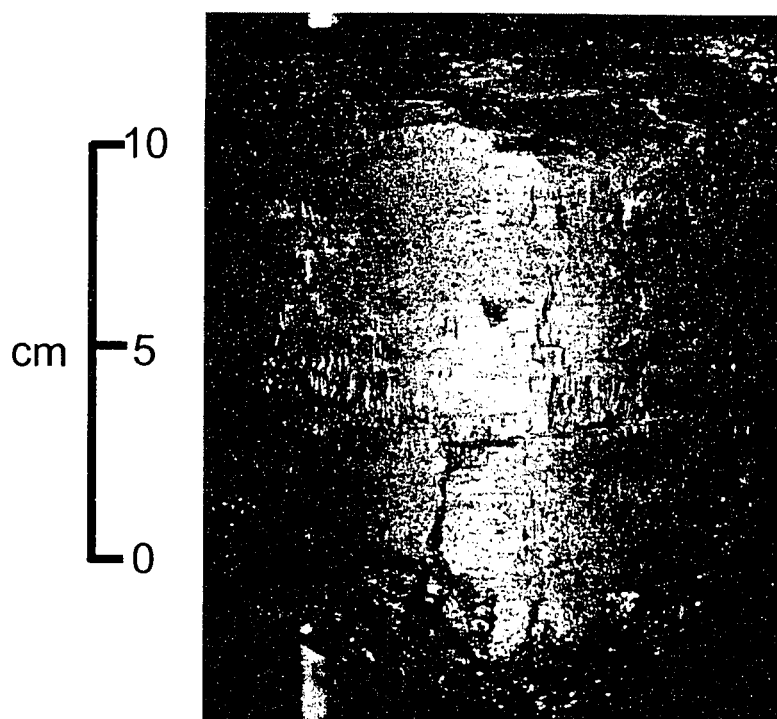
10
cm 5
0

2567m, core 8-2-66-9W6



2462m, core 2-8-66-7W6

Facies 7: Carbonaceous sandstones



2568m, core 8-2-66-9W6

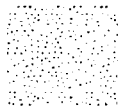
Facies 8: Coal

Appendix 2: Core logs alongside their respective logged interval. Well logs included are: Gamma-ray, resistivity, and neutron porosity.

Core Symbol Legend



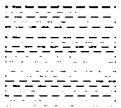
Conglomerate with sand matrix



Conglomerate without matrix



Massive Sand



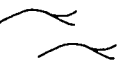
Shale



Coal



Trough Crossbedding



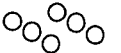
SCS Bedding



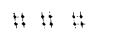
Faint SCS Bedding



Ripples



Pebbles and Pebbly Horizons



Calcareous Horizons



Root Traces



Convolute Shale Layers



Trace Fossils

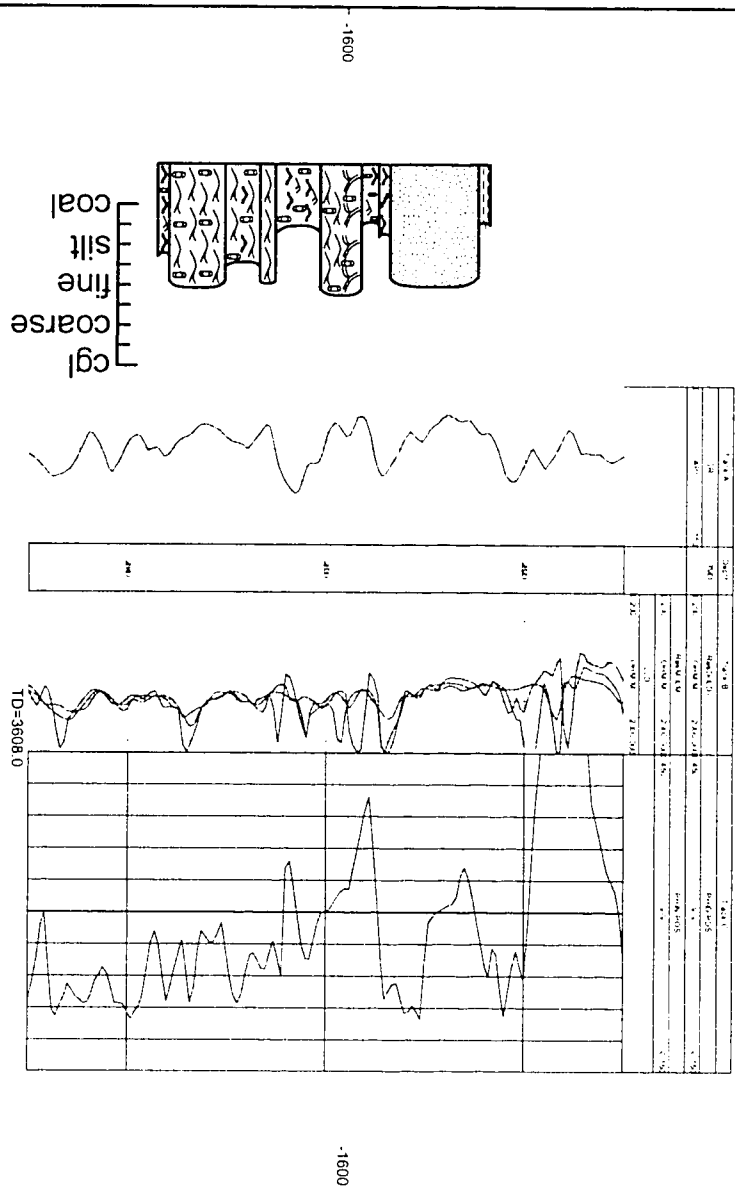


Shell Layer

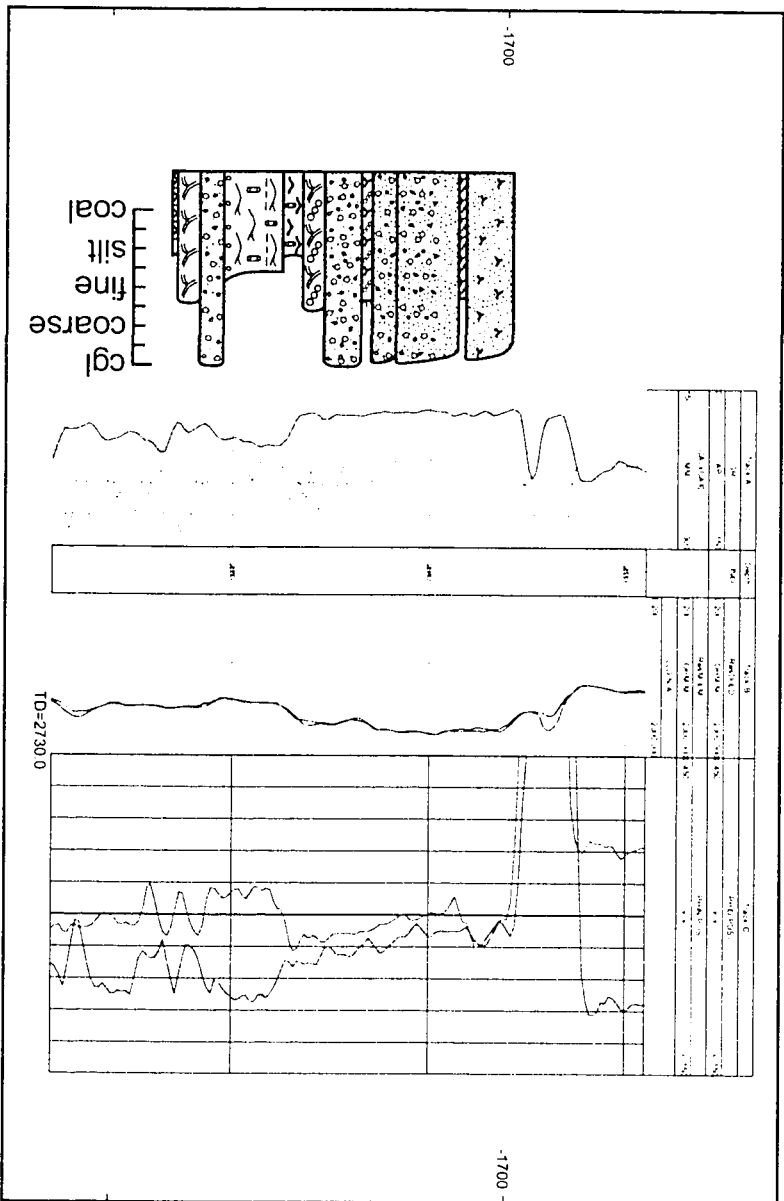


Coal Fragments

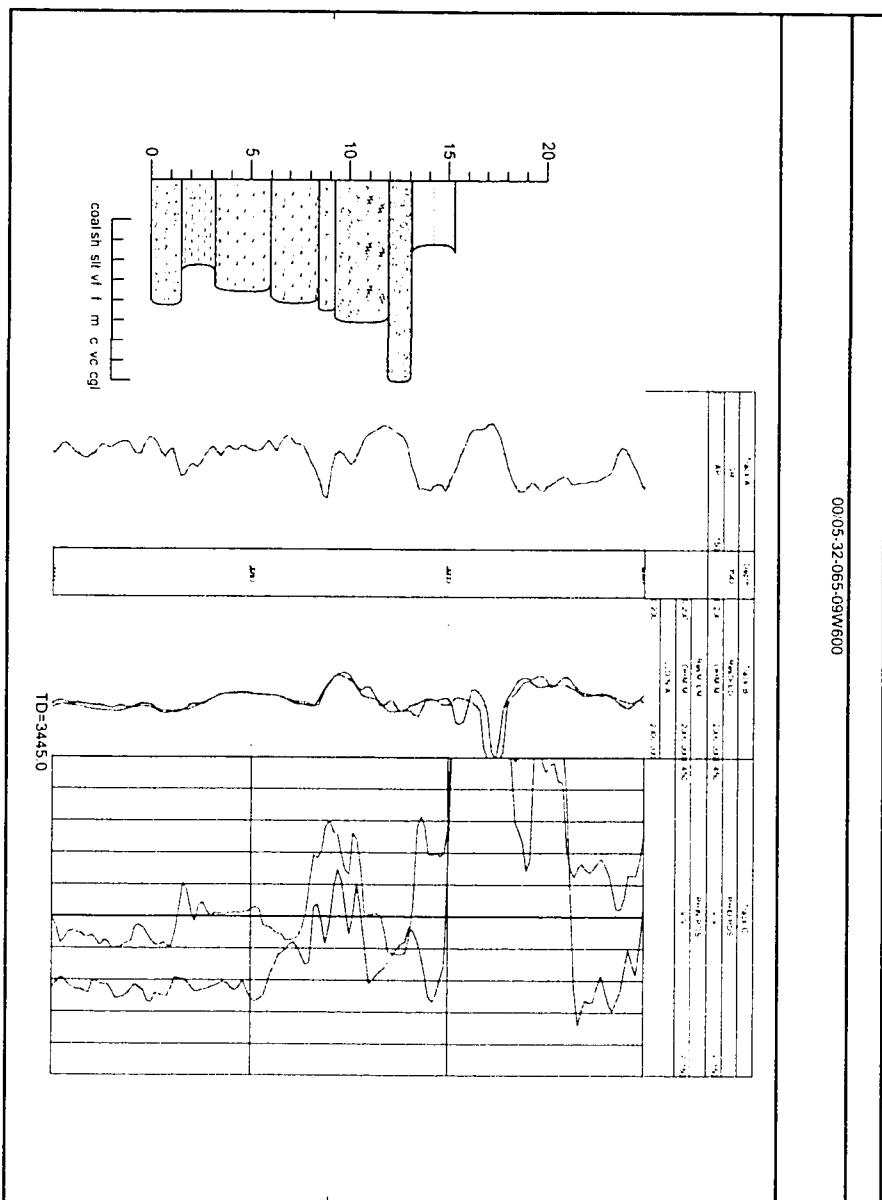
00/06-32-065-07W600



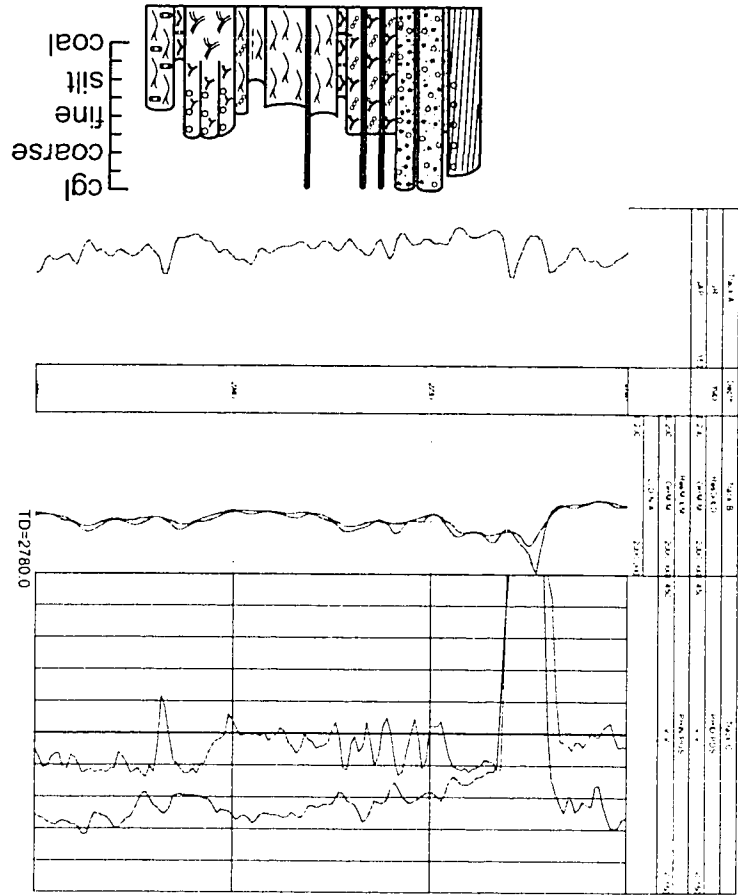
00.13.27.065.09W600



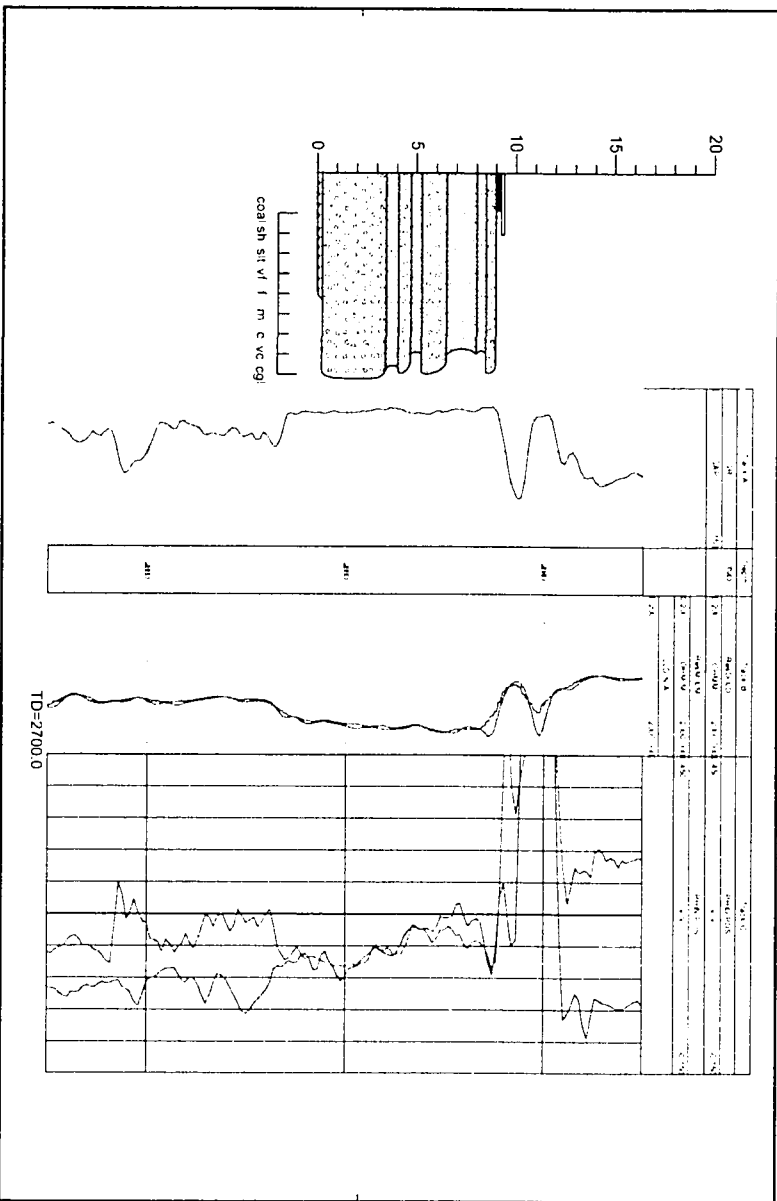
00:05:32-065-09W600

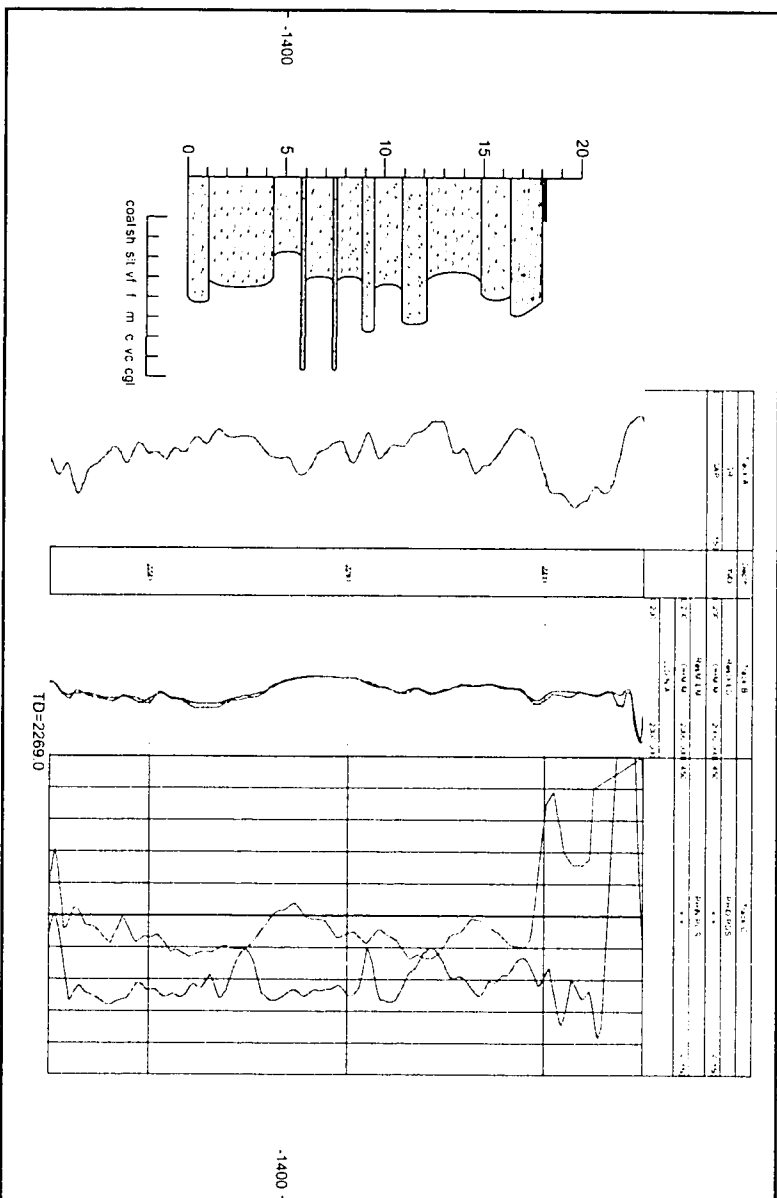


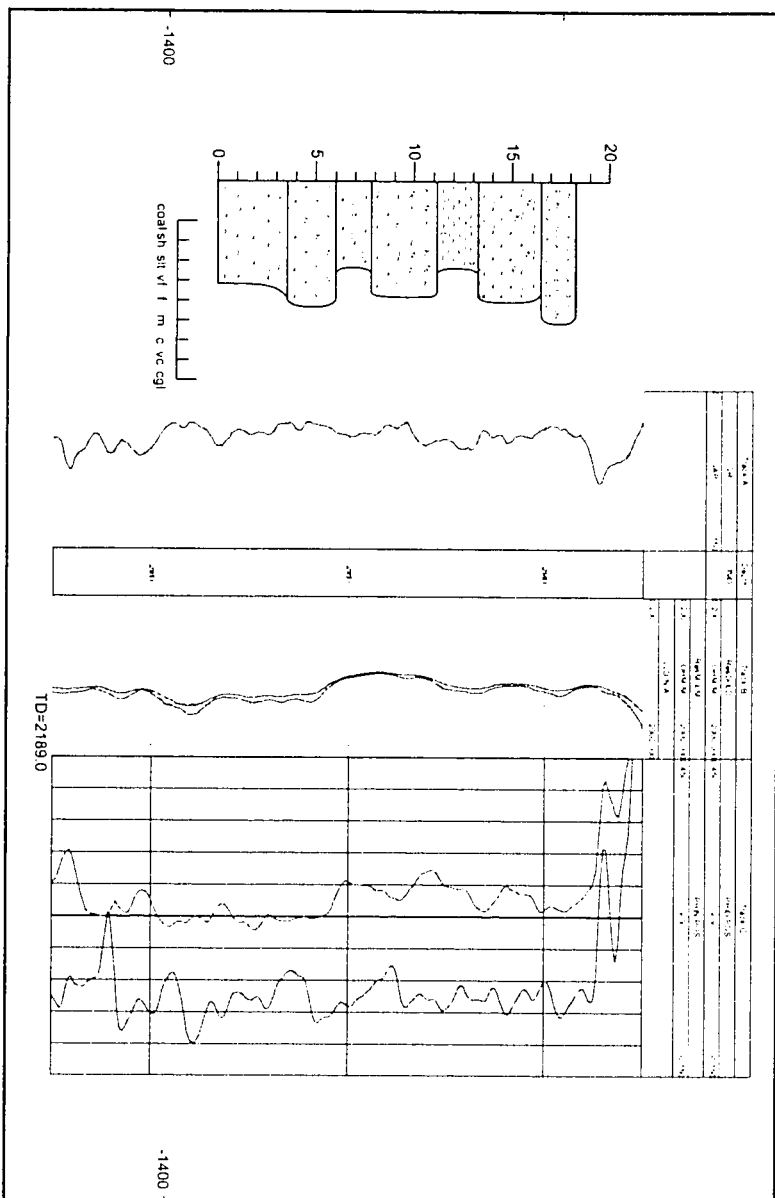
00:03:33-065-09W600



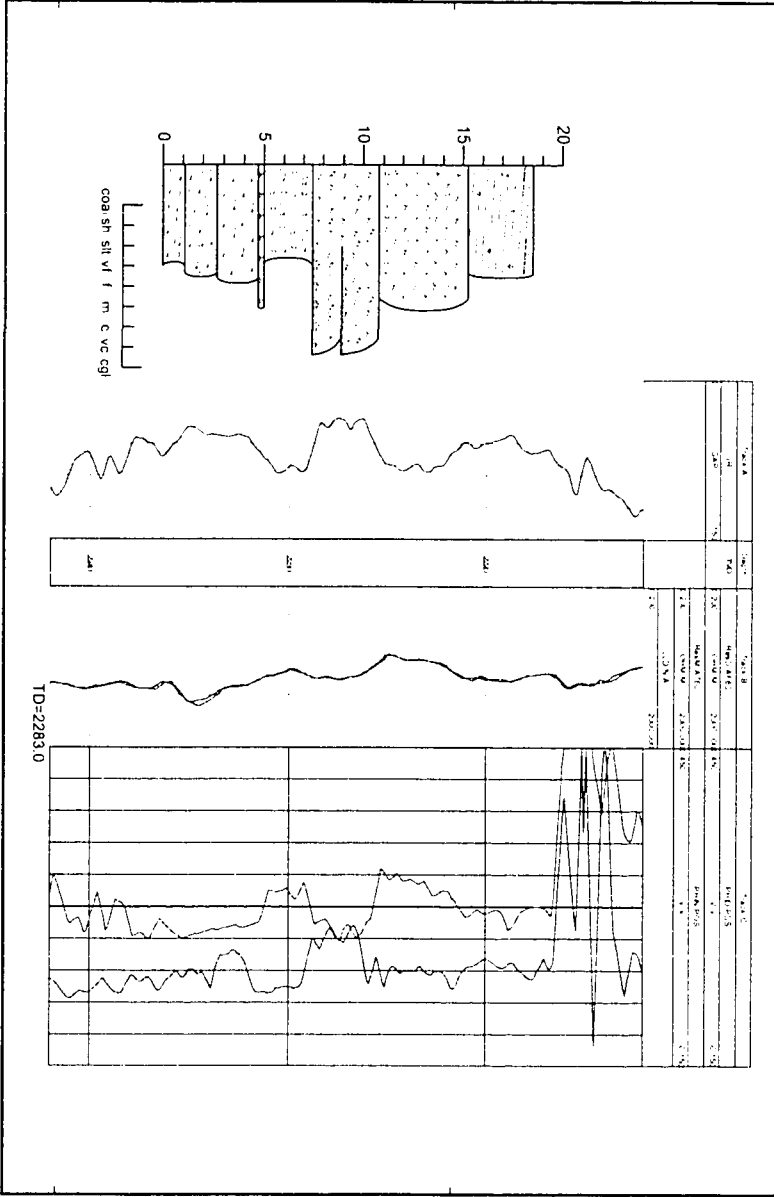
00/10-36-065-09W600



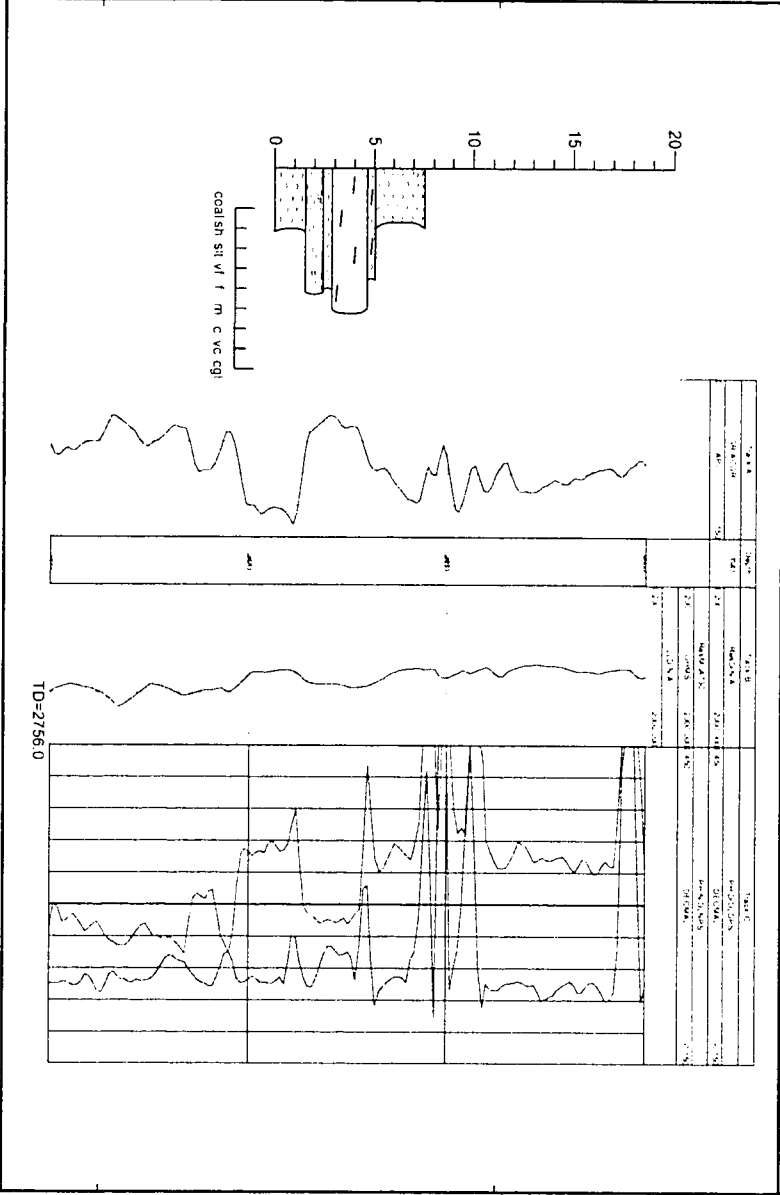




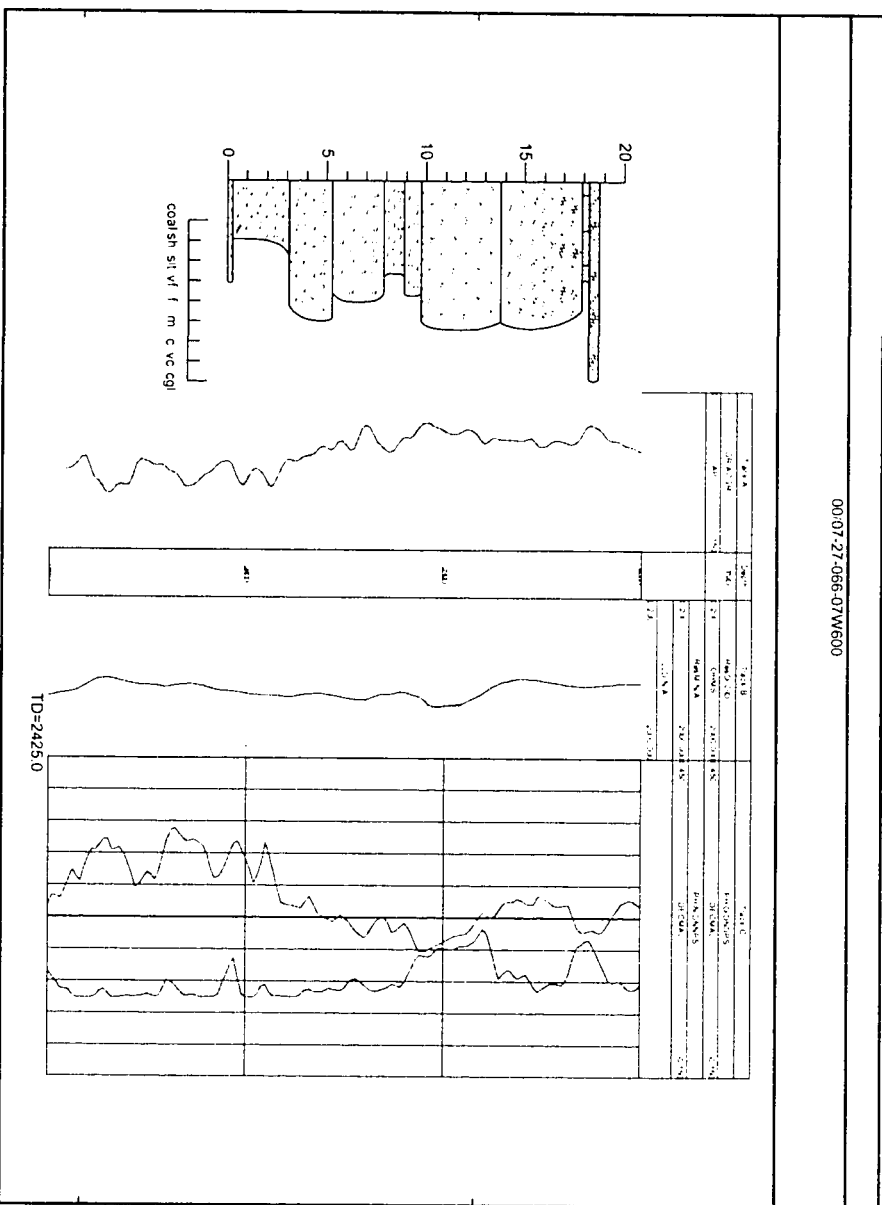
00 09-34-066-06W600



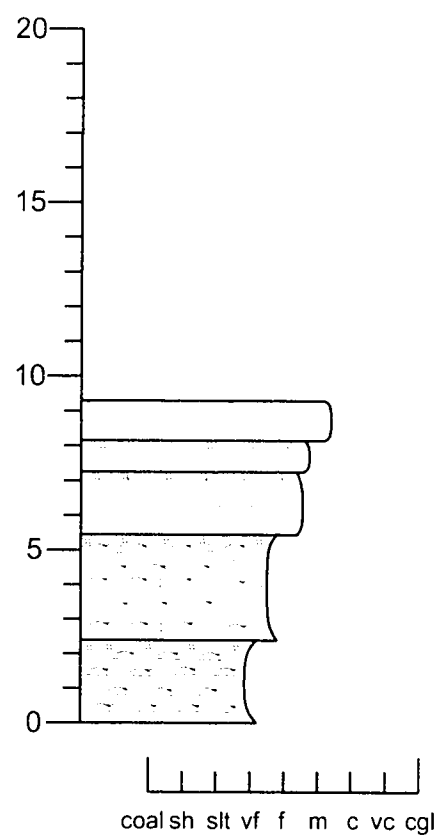
00:02:08-066-07W600



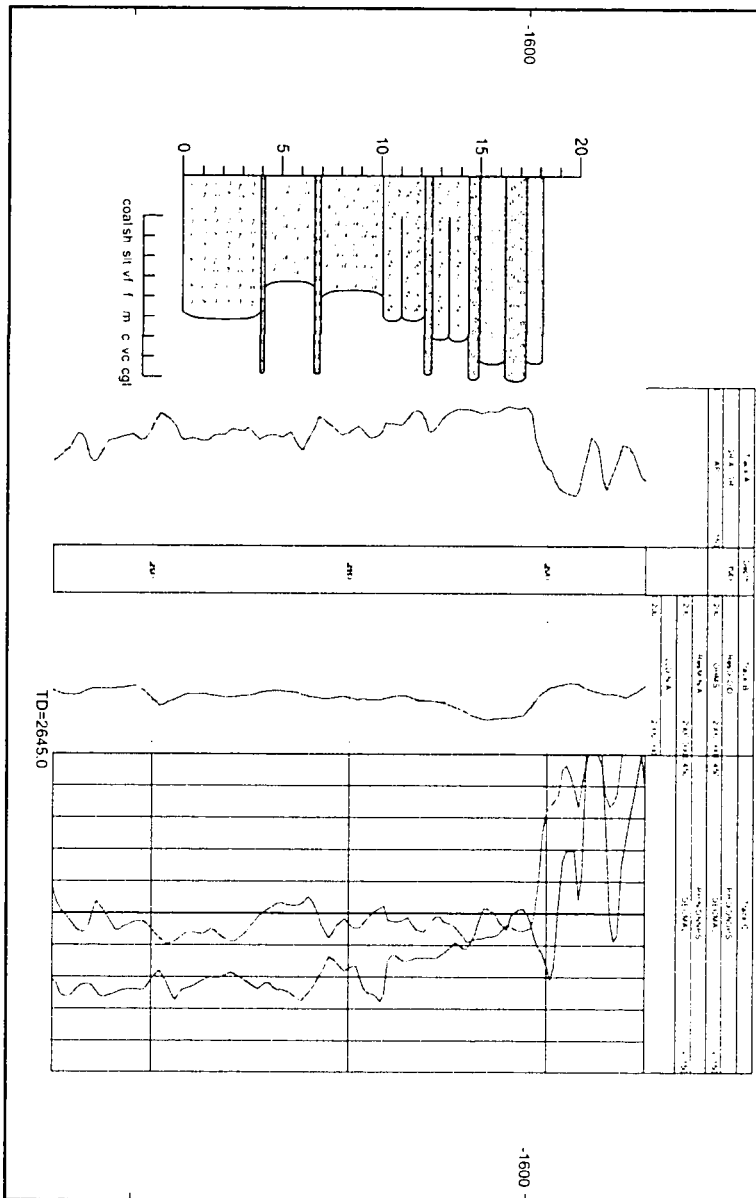
00:07-27-066-07W600



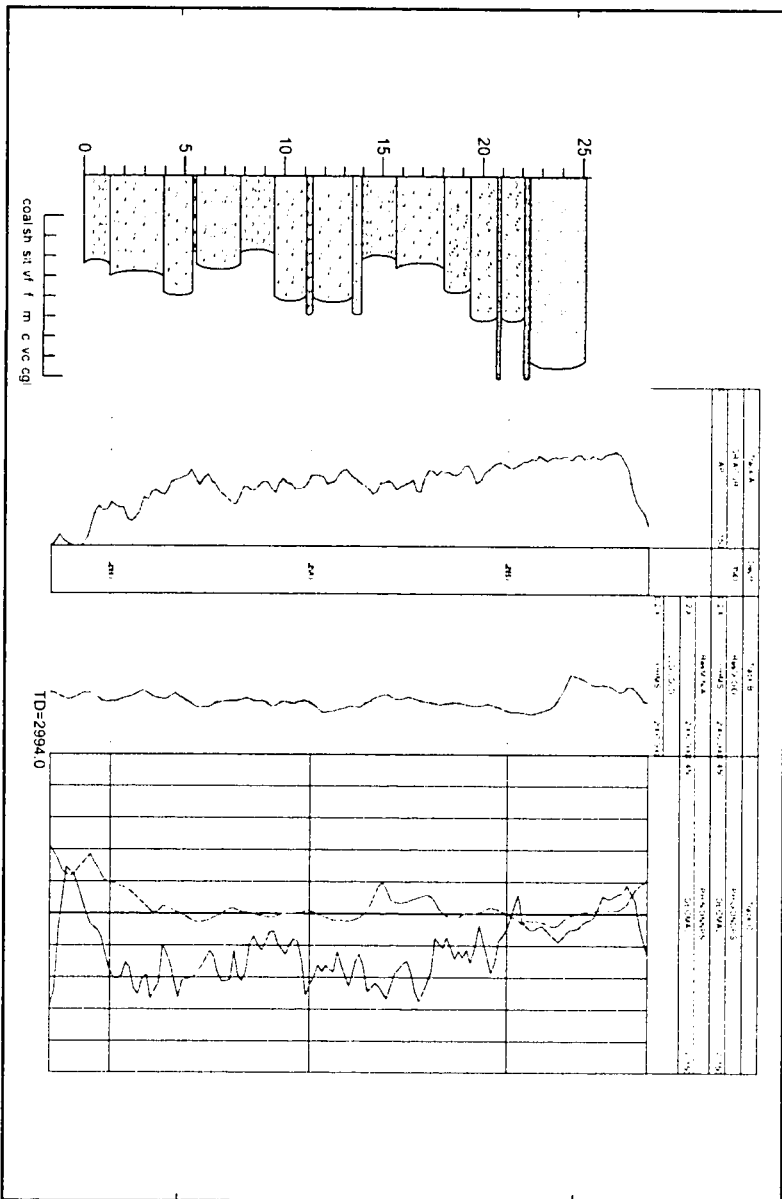
5-7-66-8W6



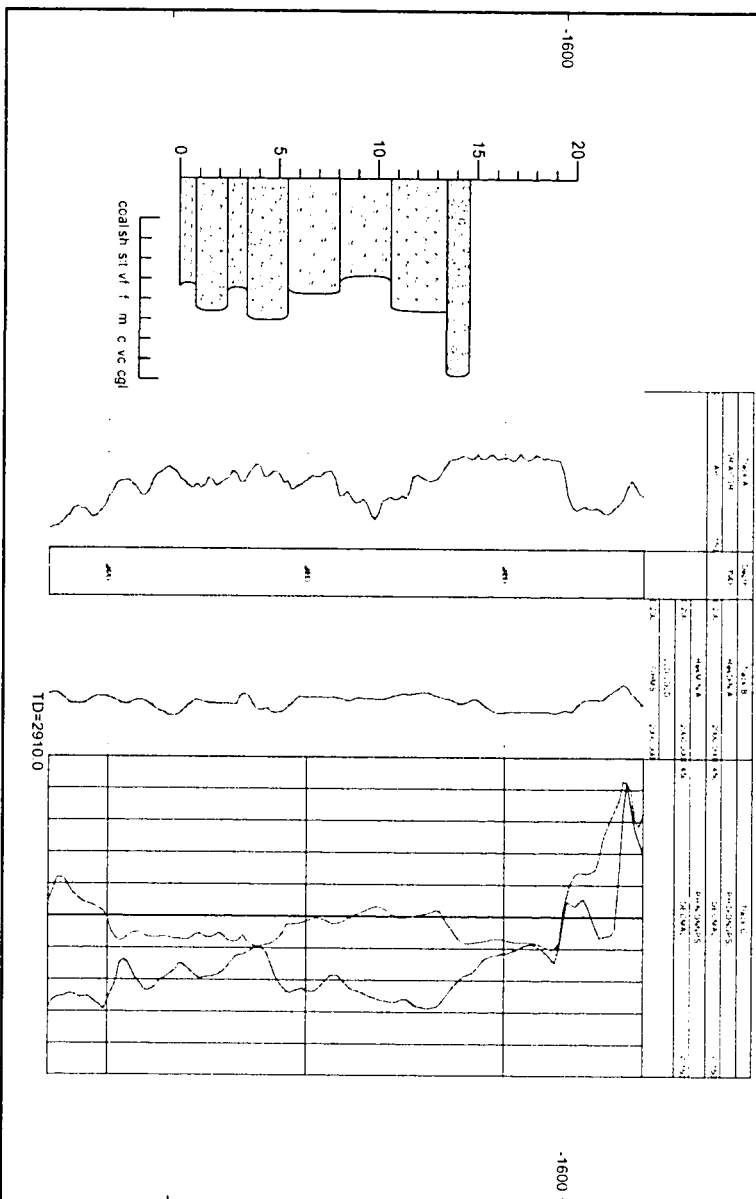
0001-08-066-08W600



0011-13-066-08W600



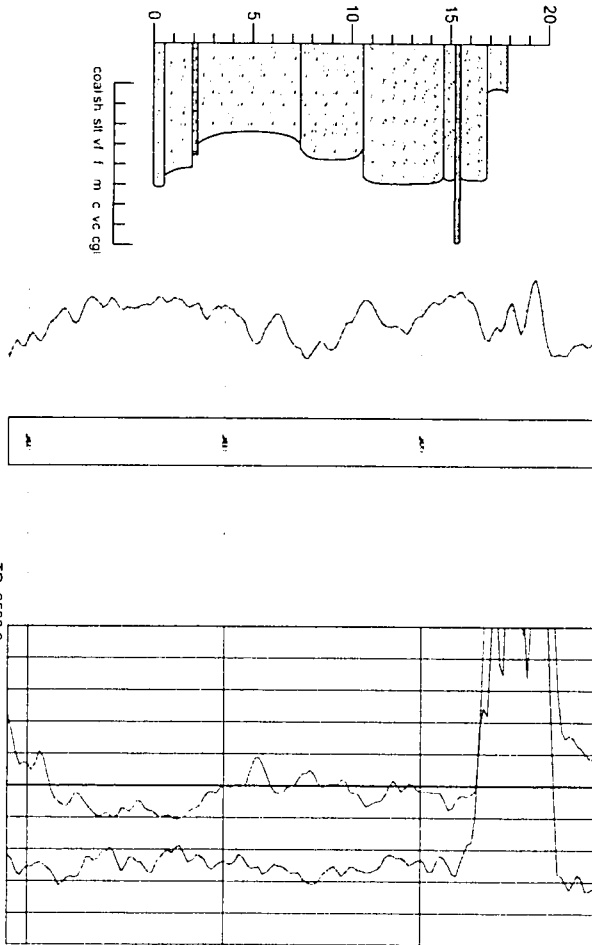
00:06:17-066-08W600



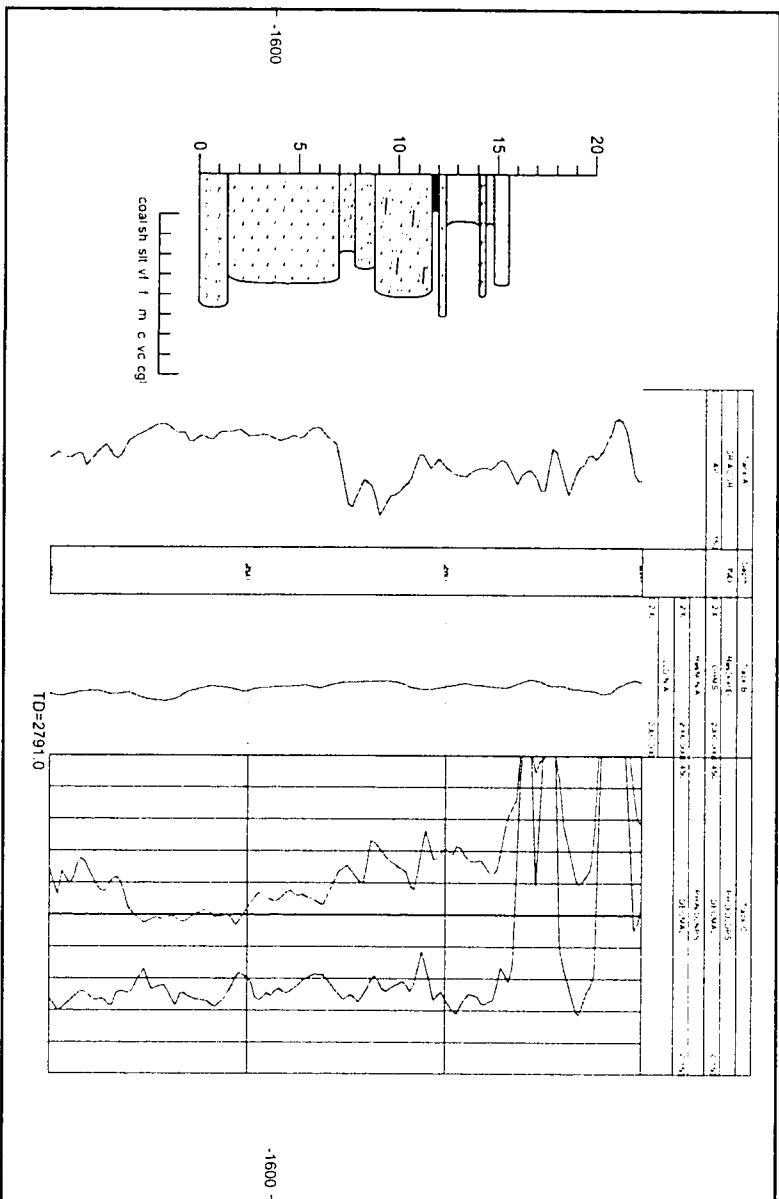
00-03-18-066-08W600



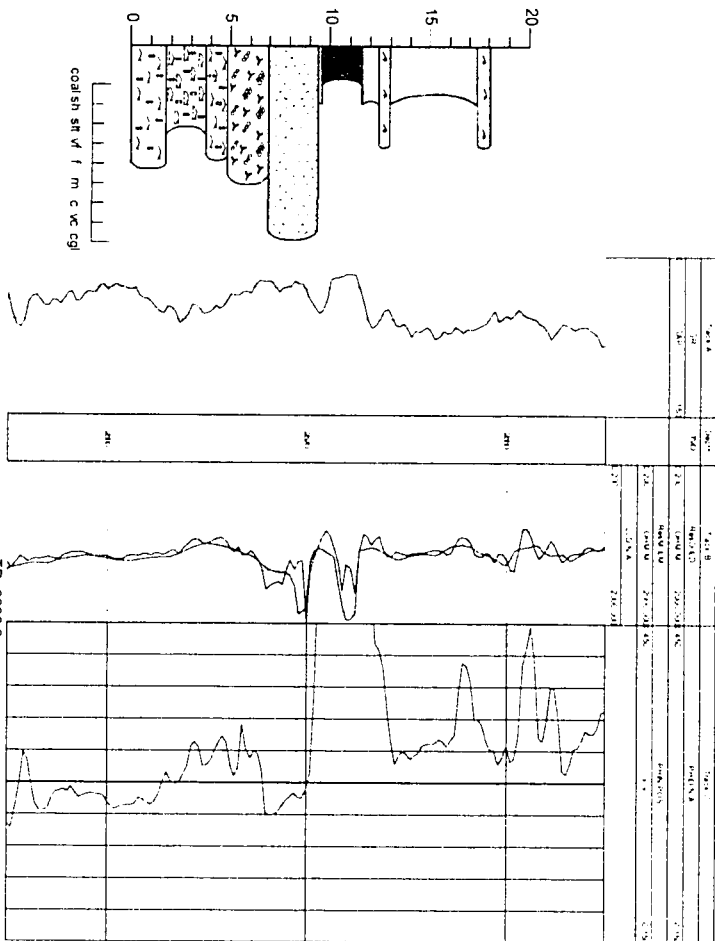
T.A. 1		T.A. 2	
DATE	01/11/18	DATE	01/11/18
TIME	14:00	TIME	14:00
LOCATION	00-03-18-066-08W600	LOCATION	00-03-18-066-08W600
WELL	00-03-18-066-08W600	WELL	00-03-18-066-08W600
DEPTH	200	DEPTH	200
TIME	14:00	TIME	14:00
LOCATION	00-03-18-066-08W600	LOCATION	00-03-18-066-08W600
WELL	00-03-18-066-08W600	WELL	00-03-18-066-08W600
DEPTH	200	DEPTH	200



00:02:21-066-08W600

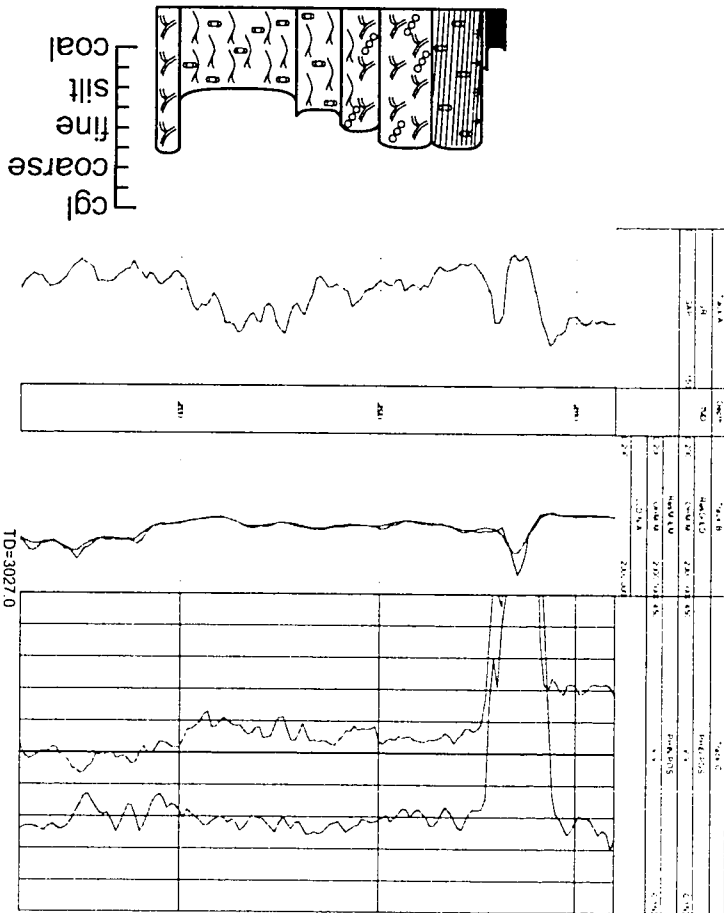


00-08-02-066-09W600

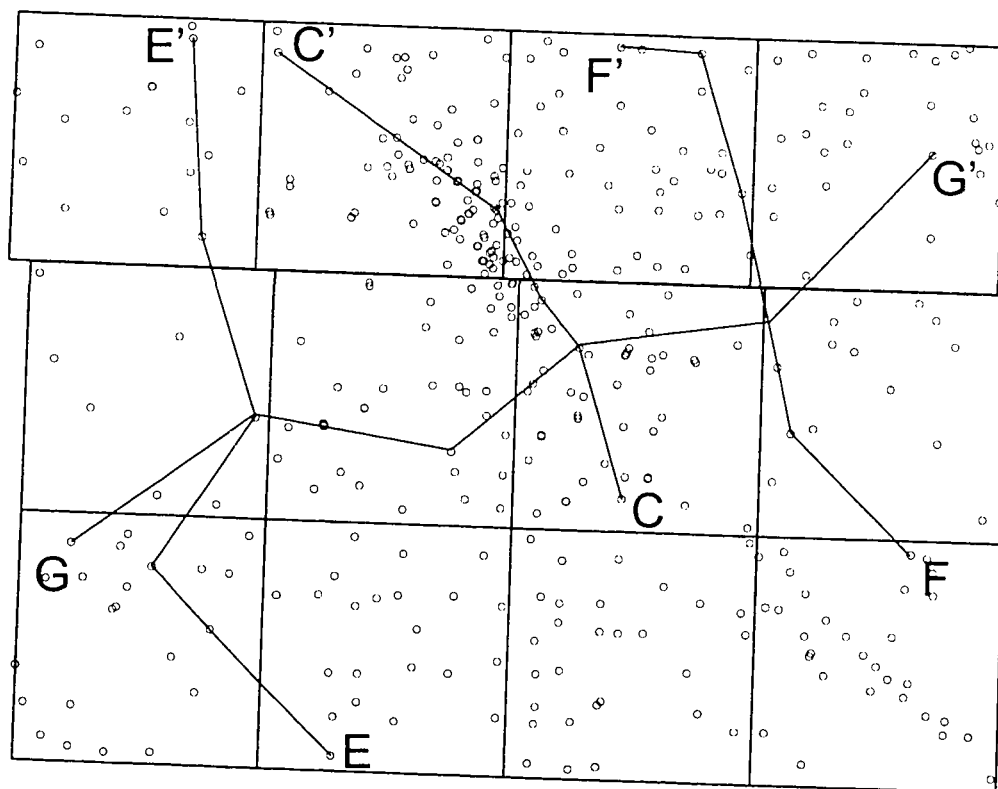


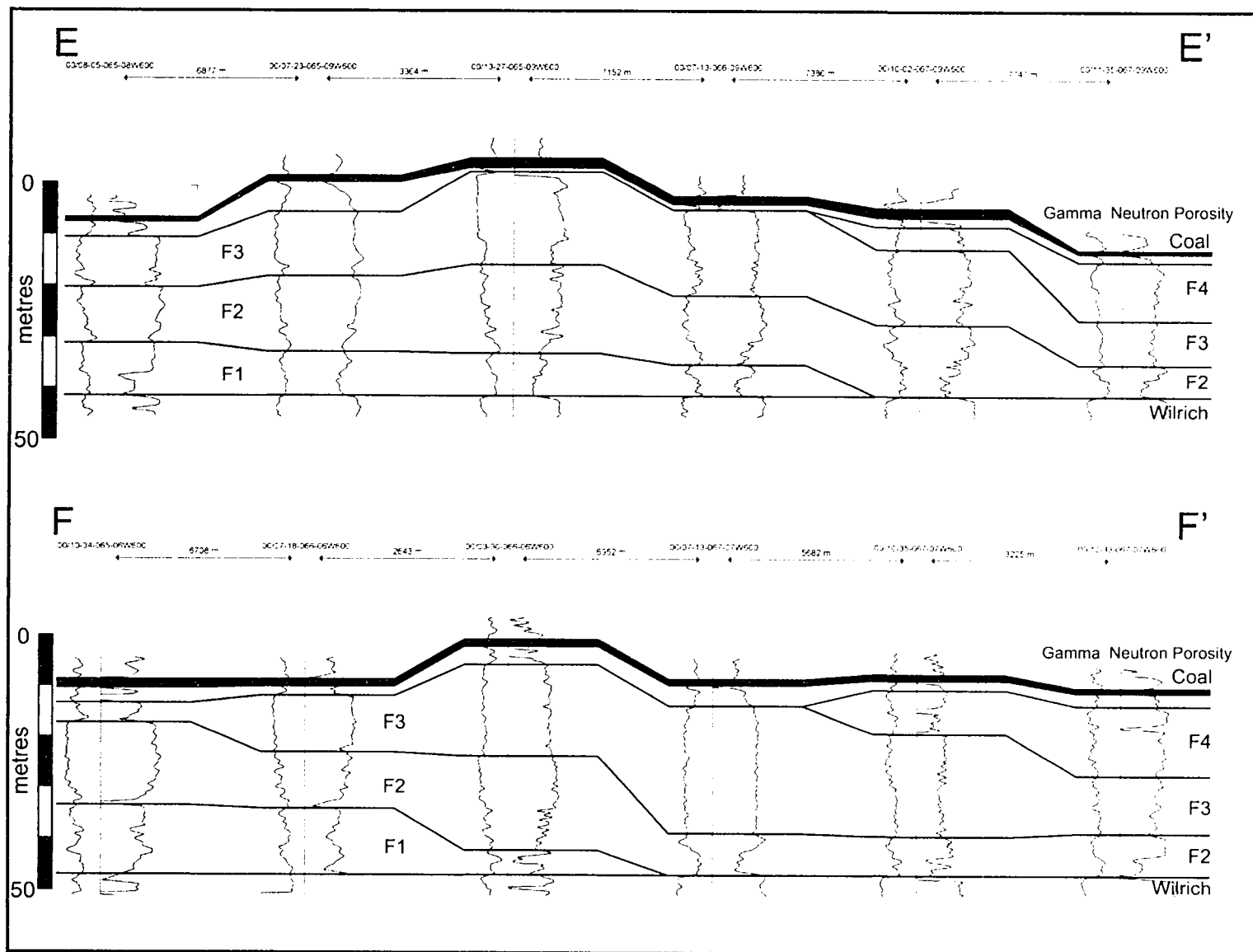
00-07-13-066-03W600

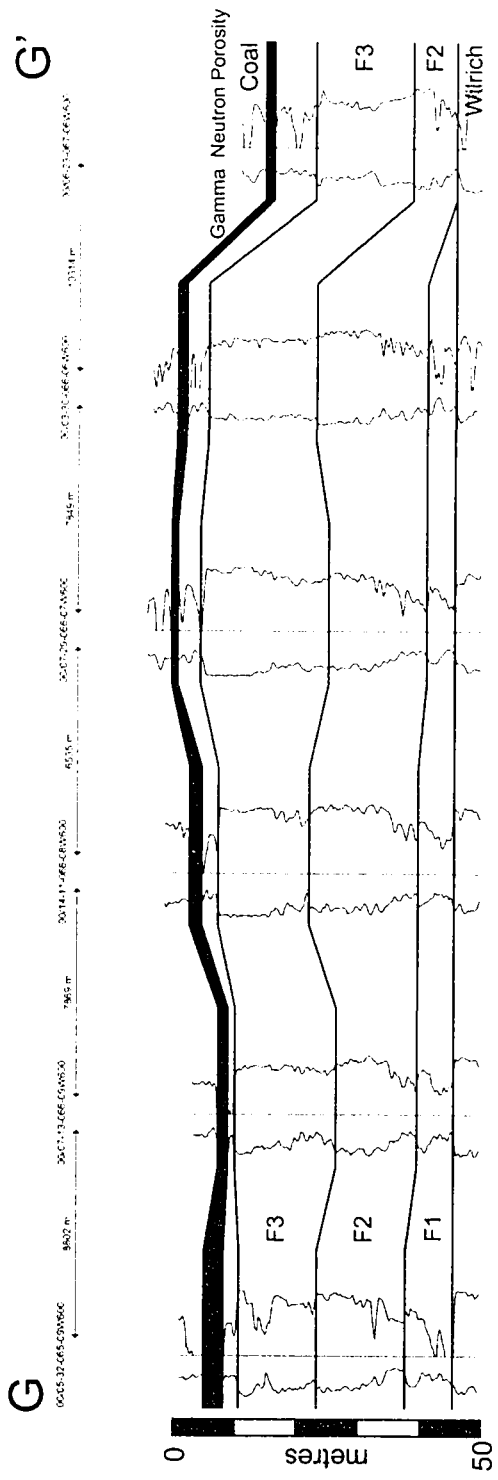
○



Appendix 3: Two dip-oriented cross-sections illustrating the progradational nature of the Falher F interval within the study area. One strike-oriented cross-section is included to illustrate consistency of picks across the study area. Note that the regional cross-section C-C' is located in Figure 3.8.







Appendix 4: Volumetric calculation of the reserves of the mapped Falher F pool.

This is compared to the actual recovered reserves of the pool in order to assess the accuracy of the mapping. The close correspondence of the reserve calculation to the actual cumulative production of the pool suggests that the mapping is accurate.

Reserve Calculation

$$\text{GIP} = 10000 * \Phi * (1-S_w) * h * A * (288.72/101.4) * P/(T*Z) \text{ (Stephenson, 1968)}$$

Where:

GIP = gas in place (m^3)

10000: area correction (m^2/ha)

Φ = average porosity (fraction)

S_w = water saturation (fraction)

h = average reservoir thickness (m)

A = reservoir area (ha)

288.72/101.4: temperature correction

P = reservoir pressure (kPa)

T = reservoir temperature (K)

Z = gas compressibility (fraction)

Falher F reservoir

$\Phi = 0.15$ (from logs)

$S_w = 0.25$ (estimate)


$h = 3.5$ m (from mapping)

$A = 9728$ ha (from mapping)

$P = 31000$ kPa (from well pressure data)

$T = 340$ K (from well information)

$Z = 0.93$ (estimate)


$$\text{GIP} = 1.07 * 10^{10} \text{ m}^3$$

Recovery factor: 0.8 (estimate)

$$\text{Recoverable reserves} = 8.55 * 10^9 \text{ m}^3$$

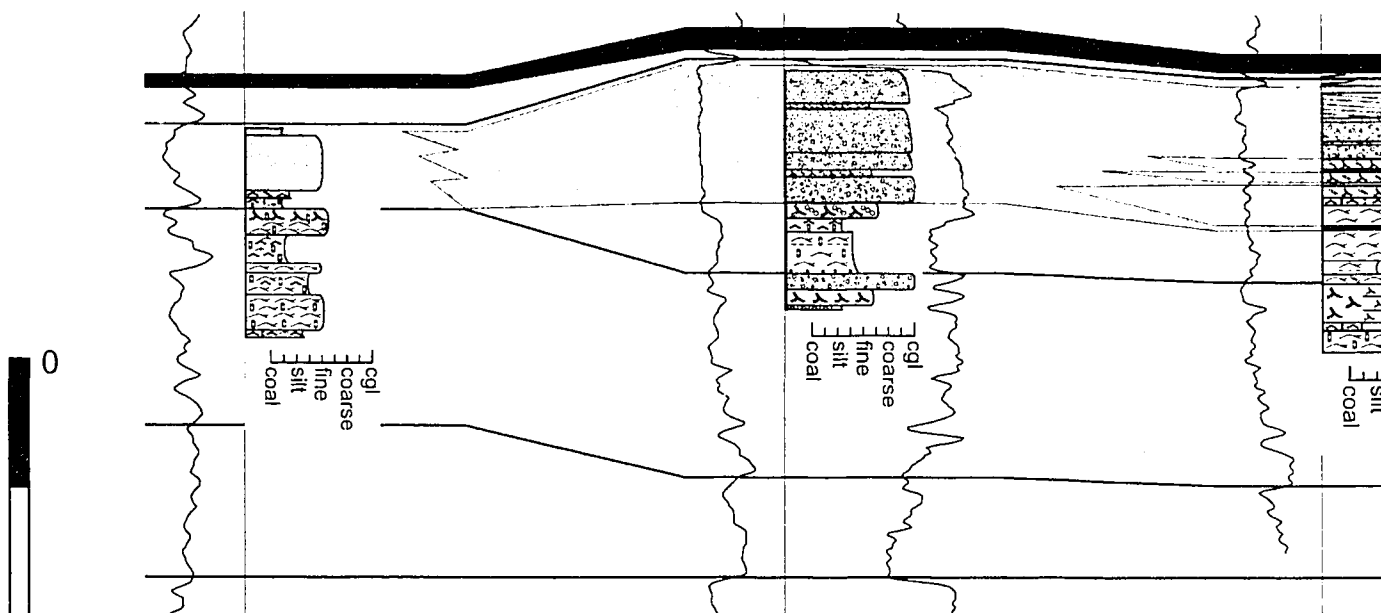
$$\text{Cumulative production} = 9.01 * 10^9 \text{ m}^3 \text{ (production data)}$$

A Landward

00/06-32-065-07W600

00/13-27-065-09W600

00/03-33-065-09



B Landward

00/07-01-066-08W600

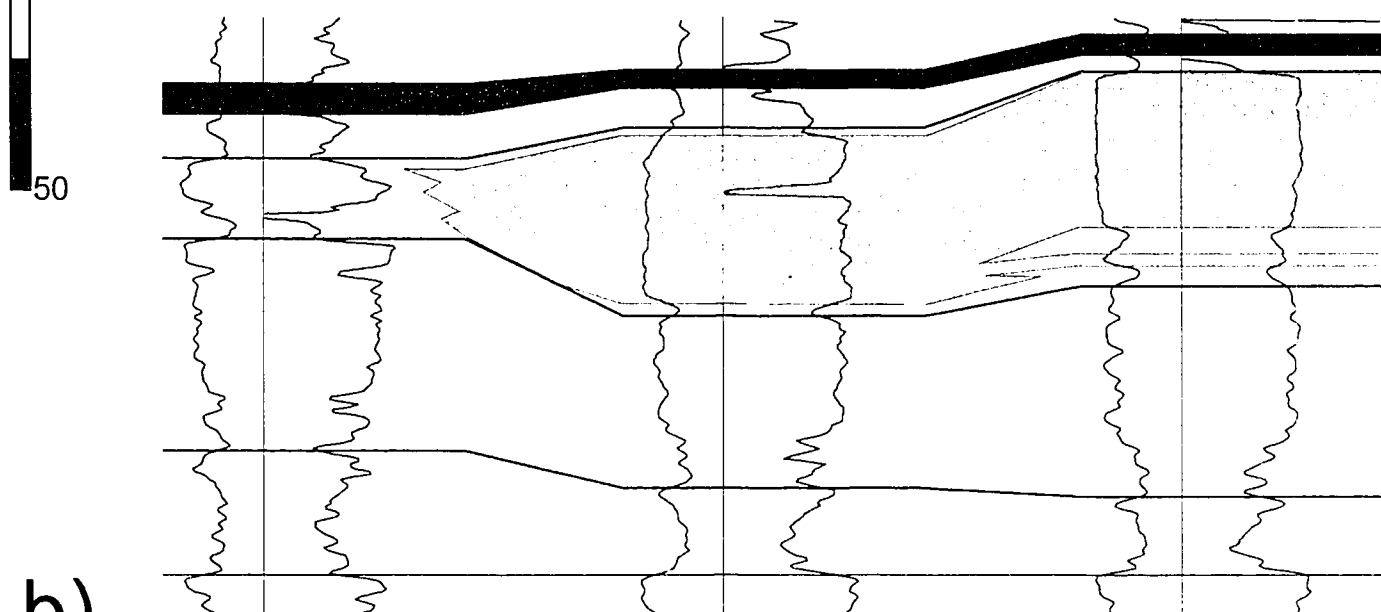
1296 m

00/07-12-066-08W600

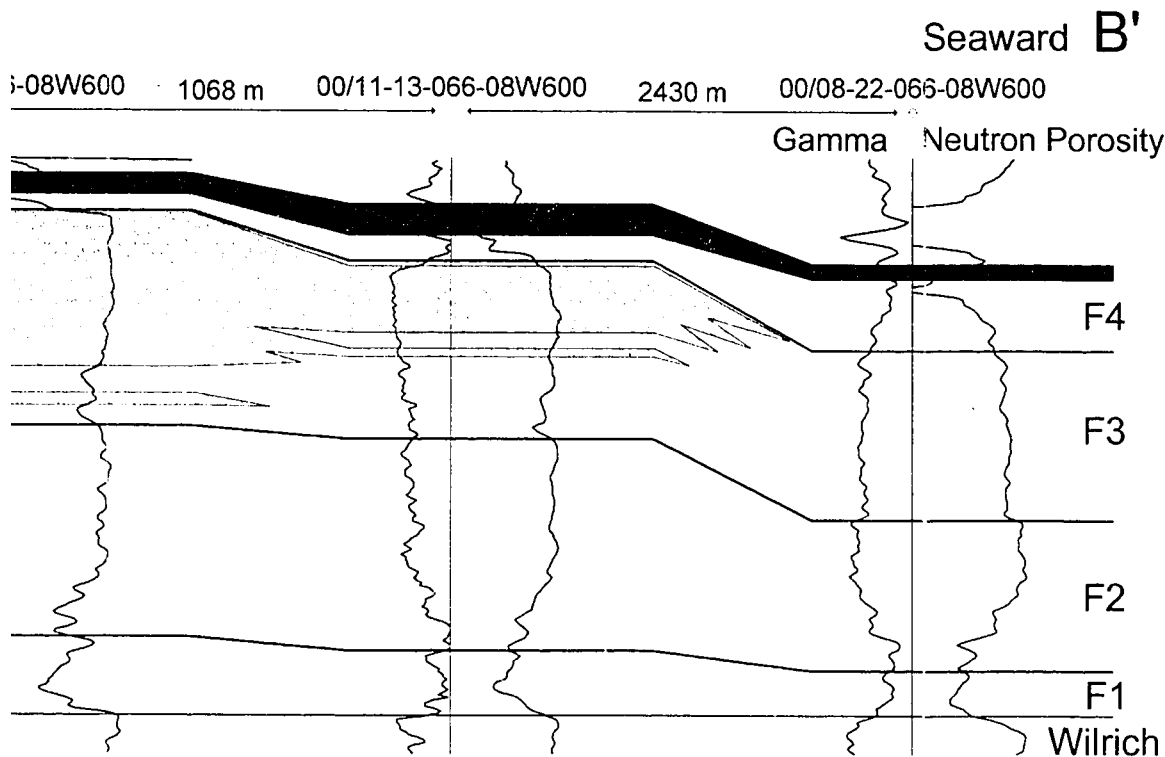
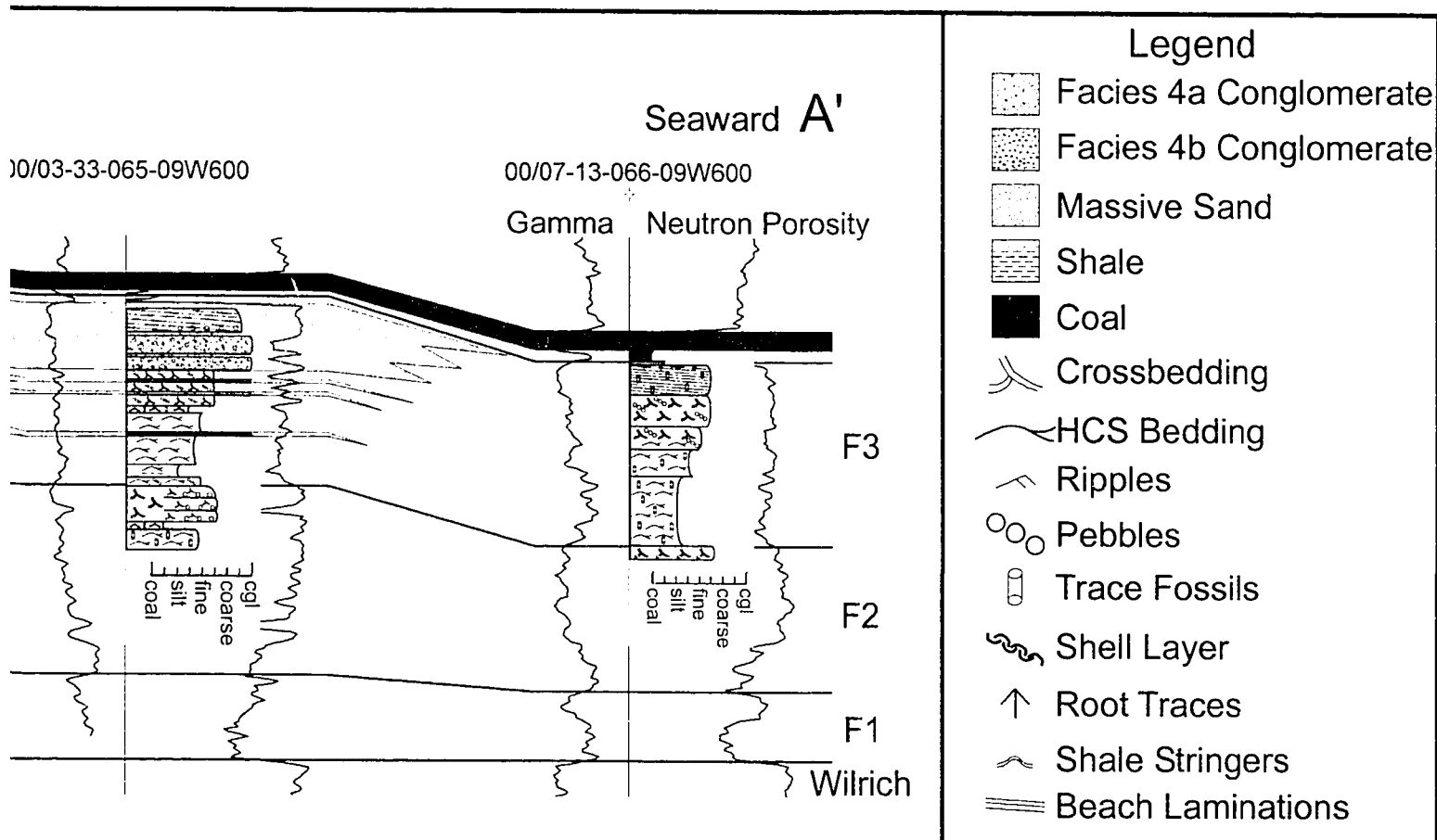
1573 m

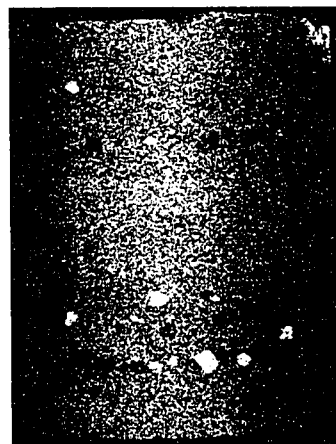
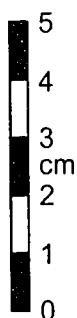
00/01-13-066-08W600

1



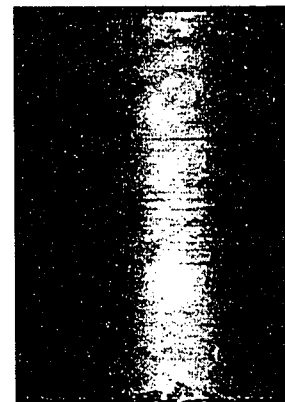
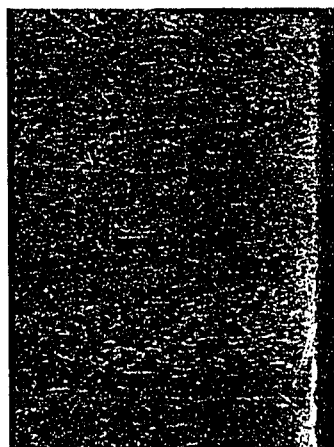
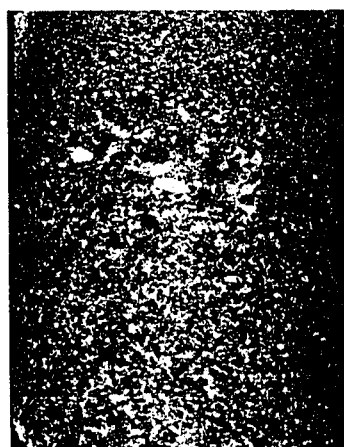
b)





Facies 1
Sandy Shales
Nereites Ichnofacies
Offshore
2393m, core 7-27-66-7W6

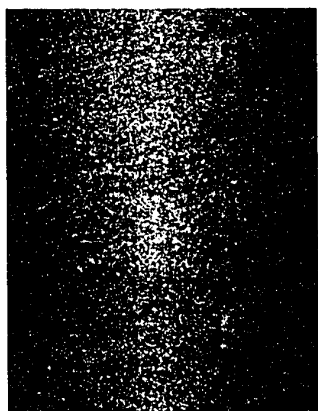
Facies 2
HCS Sandstones
Cruziana Ichnofacies
Lower Shoreface
2908m, core 5-32-65-9W6



Facies 4b
Well Sorted Conglomerate
Open Framework
Foreshore
2727m, core 3-33-65-9W6

Facies 5
Planar Bedded Sandstones
Skolithos Ichnofacies
(*Macaronichnus*)
Foreshore
2220m, core 9-34-66-6W6

Facies 6
Carbonaceous Shales
Abundant Plant Material
Coastal Plain
2901m, core 5-32-65-9W6



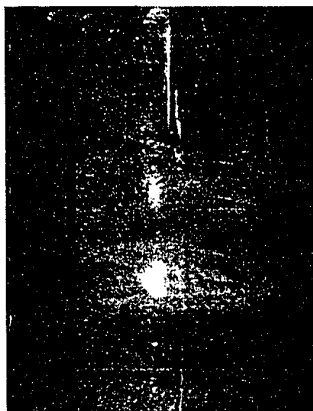
Facies 3
Cross-bedded Sandstones
Skolithos/Cruziana Ichnofacies
Upper Shoreface
2743m, core 3-33-65-9W6



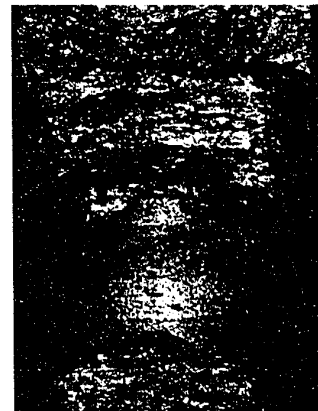
Facies 4a
Poorly Sorted Conglomerate
Closed Framework
Upper Shoreface
2641m, core 13-27-65-9W6



Facies 6
Carbonaceous Shale
Abundant Plant Material
Coastal Plain
2501m, core 5-32-65-9W6



Facies 7
Current Rippled Sandstone
Carbonaceous Shale Partings
Coastal Plain Fluvial
2567m, core 8-2-66-9W6



Facies 8
Coal
Coastal Plain
2569m, core 8-2-66-9W6

